National Institute of BUILDING SCIENCES

# Natural Hazard Mitigation Saves: Utilities and Transportation Infrastructure

*An Authoritative Source of Innovative Solutions for the Built Environment*

**Cover Photo:** Greenville, North Carolina — This power substation is surrounded by the flooding Tar River floodwaters. Utility companies have managed to set up a route around this and the main facility. Photo by Dave Gatley, FEMA News Photo (September 21, 1999)

**Suggested Citation:** Multihazard Mitigation Council (2018). *Natural Hazard Mitigation Saves: Utilities and Transportation Infrastructure.* Principal Investigator Porter, K.; co-Principal Investigators Scawthorn, C.; Huyck, C.; Investigators: Eguchi, R., Hu, Z.; Schneider, P., Director, MMC. National Institute of Building Sciences, Washington.

National Institute of
BUILDING SCIENCES

# Natural Hazard Mitigation Saves: Utilities and Transportation Infrastructure

Premier Plus Sposor

Premier Sponsors

Lead Sponsor

Sponsors

Supporter

Prepared by the
National Institute of Building Sciences
Multihazard Mitigation Council

October 2018

National Institute of BUILDING SCIENCES

# Mitigation Saves:

# Utilities and Transportation Infrastructure Investments Can Provide Significant Returns

## Introduction

Natural hazards present significant risks to many communities across the United States. Fortunately, there are measures governments, building owners, developers, tenants and others can take to reduce the impacts of such events. These measures—commonly called mitigation—can result in significant savings in terms of safety, and prevent property loss and disruption of day-to-day life.

The National Institute of Building Sciences (Institute) began a study in 2017 to update and expand upon its well-known 2005 study, *Natural Hazard Mitigation Saves: An Independent Study to Assess the Future Savings from Mitigation Activities,* which looked at the value of mitigation. In October 2018, the Institute released the second in a series of interim results. This latest report, *Natural Hazard Mitigation Saves: Utilities and Transportation Infrastructure,* examines the potential benefits associated with mitigation investments made on select utility and transportation infrastructure.

## Utility and Transportation Infrastructure Mitigation

The project team sought to use Economic Development Administration (EDA) grants to look at how the agency's mitigation efforts to address four potential perils and four categories of utilities and infrastructure might benefit communities. Of the 859 EDA grants the project team reviewed, only 16 related to natural-hazard mitigation of utilities and transportation lifelines. Of these, the team acquired sufficient data to estimate benefit cost ratios (BCRs) for 12 mitigation investments.

Because too few EDA grants were available to provide statistical value, the project team modified its objectives to analyze the grants as case studies. Since the grants did not represent all common retrofit measures (particularly in regard to earthquakes), the project team also analyzed potential mitigation measures to address the gaps.

The EDA grants studied by the project team included:

- Flood mitigation for roads and railroads (five grants), with BCRs ranging between 2.0 and 11.0 for four grants, and one grant exhibiting a BCR of 0.2.
- Flood mitigation for water and wastewater facilities (four grants), which produced BCRs between 1.3 and 31.0.
- Wind mitigation for electric and telecommunications (two grants). These grants were estimated to produce BCRs of approximately 8.5.
- Flood mitigation for electric and telecommunications (one grant). This grant produced an estimated BCR of 9.4.

Note: While not statistically valid, these grants, when viewed as case studies, offer anecdotal evidence of the potential value of such types of mitigation.

# Mitigation Saves: Utilities and Transportation Infrastructure Investments Can Provide Significant Returns

In light of the unexpectedly limited grant data, the project team supplemented the analysis of grants by studying a few leading options for natural-hazard mitigation of utilities and transportation infrastructure. These included:

- Replace specific water supply pipeline segments to create a "resilient water-supply grid" that better resists earthquakes. (At least two West Coast water utilities are designing a resilient grid.) The project team estimated this measure would save up to $8 per $1 spent, depending on local seismic hazard.
- Strengthen electric substation equipment to better resist earthquake loads and to create a "resilient electric grid." (At least three West Coast electric utilities have been developing a resilient electric grid.) The project team estimated this measure would save up to $8 per $1 spent, depending on local seismic hazard.
- Strengthen highway bridges to better resist earthquake loads. The project team estimated this measure would produce a benefit of $3 per $1 spent.
- Perform prescribed burns in the watershed of water utilities to reduce wildfire and inhibit soil-carrying runoff that can cause turbidity in reservoirs. The project team found that this measure is unlikely to be cost effective, and that water utilities have less-expensive options available to address turbidity resulting from runoff after wildfires.

In addition to the specific projects examined, the study provides new analysis methods that can be readily applied to other projects to support consistent means for determining BCRs.

| HAZARD | PROJECT DESCRIPTION | BCR |
|---|---|---|
| **Flood** (from actual EDA grants) | Elevate rail, Iowa | 2:1 |
| | Elevate rail, Missouri | 2:1 |
| | Elevate road, Nebraska | 7:1 |
| | Elevate road and reconstruct bridge, Iowa | 11:1 |
| | Reconstruct bridge, New Mexico | 0.2:1 |
| | Elevate water treatment plant equipment, Virginia | 10:1 |
| | Relocate water treatment plant, Iowa | 1:1 |
| | Relocate wastewater treatment plant, Iowa | 4:1 |
| | Protect water and wastewater treatment plants, North Carolina | 31:1 |
| | Mitigate electric and telecommunications substation, Wisconsin | 9:1 |
| **Wind** (from actual EDA grants) | Replace aboveground power lines, Vermont | 6:1 |
| | Improve electric power lines, Texas | 6:1 |
| **Earthquake** (based on project team analysis) | Implement resilient water distribution grid, San Francisco, CA | 8:1 |
| | Implement resilient water distribution grid, Los Angeles, CA | 6:1 |
| | Implement resilient water distribution grid, Portland, OR | 0.6:1 |
| | Implement resilient water distribution grid, Seattle, WA | 2:1 |
| | Retrofit electric substations, San Francisco, CA | 8:1 |
| | Retrofit electric substations, Los Angeles, CA | 8:1 |
| | Retrofit electric substations, Portland, OR | 6:1 |
| | Retrofit electric substations, Seattle, WA | 2:1 |
| | Improve columns and footings of highway bridges, California | 3:1 |

**Table 1.** *BCRs for select infrastructure mitigation measures (based on actual EDA grants and project team analysis for potential resilience initiatives).*

# Table of Contents

# Index of Figures

# Index of Tables

# Natural Hazard Mitigation Saves: Utilities and Transportation Infrastructure

## 1 Introduction

### 1.1 Background

More than a decade ago, the National Institute of Building Sciences released a study, *Natural Hazard Mitigation Saves: An Independent Study to Assess the Future Savings from Mitigation Activities,* which found society saves $4 for every $1 spent on mitigation by the Federal Emergency Management Agency (FEMA).

In the years since, the United States has experienced some of the most devastating disasters in the country's history. Just four of the major disasters that occurred in 2017—Hurricanes Harvey, Irma, and Maria and the extensive wildfires in California—will likely represent some of the highest collective losses from natural disasters in any year since the founding of the nation. Disasters in 2017 caused $306 billion in damages (NOAA 2018), which, is coincidentally the approximate amount spent annually on new construction in the United States. This means that 2017 may be the first time in U.S. history in which natural disasters effectively wiped out the value of all new construction in the same year: the tipping point of unsustainability.

Future disasters are inevitable, yet their growing frequency and magnitude of destruction are substantially exacerbated by the decisions Americans make in where and how they build. The populations of cities and communities continue to grow in hazard-prone areas. Unless something is done to change the course of destruction, future events will affect more lives, more businesses, and the U.S. economy as a whole.

Despite the widely publicized impacts of disasters such as Hurricanes Katrina and Sandy, the funding for mitigation has declined over the years, even if the risks clearly have not. Just as financial advisors tell anyone planning their financial future (whether preparing for their kids' college education, buying a house, or saving for retirement) to start saving long in advance, the nation must also prepare and plan for future events. U.S. communities and individuals need to be ready for potential hazardous events that, though they might not arrive until long into the future, will be all too real when they strike, and have the potential to impact lives for months and possibly years.

Pre-disaster mitigation—preparing in advance for future disasters—better assures that hazardous events will have short-lived and more manageable outcomes. Mitigation saves lives, preserves homes and belongings, reduces the need for temporary shelter, helps economies to spring back faster, and lowers recovery costs. At the same time, investing in mitigation invigorates the economy through increased construction—whether the funding comes through federal or state programs, or through privately financed retrofits and new construction.

In January 2018, building on the goals of its *2005 Mitigation Saves* study, the National Institute of Building Sciences released the *Natural Hazard Mitigation Saves: 2017 Interim Report* to share the results from the first stage of a multi-year project. The purpose of this new study is to help decision-makers to build a mitigation strategy so they can protect lives, property, and assets. The findings are intended to inform future code changes to make communities more resilient, help jurisdictions make decisions on what codes to adopt and enforce, and assist policymakers in developing effective federal programs that support pre-disaster mitigation. *The 2017 Interim Report* measured the benefits and costs of two categories of natural-hazard mitigation: efforts supported by federal grants to reduce risk to existing, mostly public-sector property, and options to design new buildings to exceed key design requirements of the *2015 International Building Code* (IBC) and *2015 International Residential Code* (IRC), and to adopt requirements of the *2015 International Wildland-Urban Interface Code* (IWUIC).

The *2017 Interim Report* expanded on the 2005 study by examining an additional peril (fire at the wildland-urban interface), by including grants from additional federal programs and agencies, and by examining the benefits and costs of designing new buildings to exceed key requirements of the 2015 IBC and 2015 IRC and to comply with the 2015 IWUIC. However, several other mitigation options remained to be examined:

- Remediation of utilities and transportation lifelines, the subject of this report.
- The impact of the adoption and application of modern building codes to be released in early 2019.
- Retrofit of existing private-sector buildings. The Institute expects to publish benefit-cost ratios (BCRs) for this option in early 2019.
- Miscellaneous other options, such as zoning to avoid development in hazard-prone geographic areas and design of certain classes of buildings to exceed I-Code requirements, that were not previously examined in the *2017 Interim Report*. The Institute expects to publish BCRs for some of these options in early 2019.
- Mitigation activities by federal agencies, such as flood control measures by the U.S. Army Corps of Engineers (USACE), or weather and earth-science warning and prediction activities by the National Oceanic and Atmospheric Administration (NOAA) and the U.S. Geological Survey (USGS). The Institute has not yet secured funding to explore this option.
- Business continuity planning (BCP) and disaster recovery (DR). Many large businesses and a few small businesses use BCP/DR in addition to or instead of strengthening infrastructure. BCP/DR is probably highly cost effective. The Institute has not yet secured funding to explore this option.

## 1.2 Objectives

In 2018, a team of experts that contributed to the 2005 study undertook new research to update and expand the earlier study to include estimated BCRs for natural-hazard mitigation of utilities and transportation lifelines.

The project team studied a number of benefits, including property loss reduction, reduced deaths and nonfatal injuries, reduced incidence of post-traumatic stress disorder (PTSD), reduced direct and indirect business-interruption losses, and reduced losses associated with environmental impacts. The team acknowledged benefits for a reasonable lifespan of the mitigation measure: 75 to 100 years, depending on the infrastructure being mitigated. The team discounted monetary benefits at three discount rates: the cost of borrowing, 3%, and 7% per year, but did not discount death or injury benefits. However, costs do include up-front and long-term maintenance costs.

Methodologies reflect those presented in the *2017 Interim Report* or well-established models of hazard (the occurrence frequency with various levels of environmental excitation such as flood depth) and vulnerability (the relationship between loss and degree of environmental excitation). In some cases, new methodological elements were required, in which case the project team thoroughly documented the new methodologies in this report. In no case were proprietary models used. All new methodologies were vetted by an independent oversight committee of experts—independent in the sense that they are empaneled by the National Institute of Building Sciences and not by the subcontractor charged with carrying out the analysis.

The project team set out to estimate BCRs for four categories of infrastructure: water and wastewater; electricity and telecommunications; ports; and roads and railroads, across four perils: earthquake, flooding, wind, and fire at the wildland-urban interface. The project team sought to use Economic Development Administration (EDA) grants to represent the population of mitigation measures for each combination of peril and infrastructure with any significant mitigation activity. During the progress of its research, the project team found that, although EDA had issued 859 grants as of early 2017, only 16 appeared to fund natural-hazard mitigation of utilities and transportation lifelines. Of these, the team was able to acquire sufficient data to estimate BCRs for 12 mitigation investments.Because too few EDA grants were available to provide statistical value, the project team modified its objectives. In light of these limited data, the team instead decided to analyze the grants as case studies to show the degree to which mitigation of utilities and transportation lifelines can be cost effective. In some cases, new analytical procedures were developed and documented to provide other analysts with new tools to use in benefit-cost analysis (BCA).

The 12 summarized grants do not capture all common, practical retrofit measures for utilities and transportation lifelines (particularly in regards to making water supply systems, electric utility infrastructure, and highway bridges better resistant to earthquakes). The project team undertook analysis of additional mitigation measures to address these gaps.

Finally, the project team speculated that prescribed burns to reduce turbidity in water-supply reservoirs might represent a cost-effective mitigation measure to reduce impacts on water supply from fire at the wildland-urban interface. The thought was that wildfires would burn off the vegetation that stabilizes soil, and that later storm runoff could carry soil and bacteria downhill into reservoirs, producing turbidity and additional biochemical oxygen demand. Following consultation with several water agencies, the project team found that turbidity in reservoirs after wildfires could be readily addressed much less expensively without performing prescribed burns. Prescribed burns would almost certainly produce very small BCRs, at least when benefits are compared to lower cost strategies to deal with reservoir turbidity.

## 1.3 Findings

The EDA grants studied by the project team included:

- Flood mitigation for roads and railroads (five grants), with BCRs between 2.0 and 11.0 for four grants, and one grant with a BCR of 0.2. The number of grants is too small to provide statistical value, but they do provide case studies showing that flood mitigation of roads and railroads can be highly cost effective, especially elevation of easily flooded roads that incur heavy traffic. In addition, the analysis offers a relatively simple new way to estimate drownings in vehicles, which is not currently covered in Hazus.
- Flood mitigation for water and wastewater facilities (four grants), which produced BCRs between 1.3 and 31.0. Again, too few grants were available to provide statistical value, but they do show that such measures can be highly cost effective, and the analyses provide new, relatively simple methods to account for business-interruption and environmental losses not currently available in Hazus.
- Wind mitigation for electric and telecommunications (two grants). These grants were estimated to produce BCRs of approximately 8.5, providing similar anecdotal evidence of the potential value of this category of mitigation measure.
- Flood mitigation for electric and telecommunications (one grant). This grant produced an estimated BCR of 9.4. Again, one grant only serves as anecdotal evidence of the potential benefit of this kind of mitigation, not statistical information. However, the analysis offers a new, simple method to estimate business-interruption losses for this category of effort.

In light of the unexpectedly limited grant data, the project team supplemented the analysis of grants by studying a few leading options for natural-hazard mitigation of utilities and transportation infrastructure, in particular:

- Replace selected water supply pipeline segments to create a "resilient water-supply grid" that better resists earthquakes. At least two West Coast water utilities are designing a resilient grid: The Los Angeles Department of Water and Power (LADWP) and East Bay Municipal Utility District (EBMUD). The project team estimated this measure would save up to $8 per $1 spent, depending on local seismic hazard.
- Strengthen electric substation equipment to better resist earthquake loads and to create a "resilient electric grid." At least three West Coast electric utilities have been developing a resilient electric grid: LADWP, Southern California Edison (SCE), and Pacific Gas and Electric (PG&E). The project team estimated this measure would save up to $8 per $1 spent, depending on local seismic hazard.
- Strengthen highway bridges to better resist earthquake loads. The California Department of Transportation (Caltrans) has been strengthening its highway bridges since the 1971 San Fernando Earthquake, and particularly since the 1989 Loma Prieta Earthquake. The project team estimated this measure would produce a benefit of $3 per $1 spent.
- Perform prescribed burns in the watershed of water utilities to reduce wildfire and inhibit soil-carrying runoff that can cause turbidity in reservoirs. This measure is not commonly performed, at least not for the purposes of reducing turbidity in drinking water reservoirs. The project team found that it is unlikely to be cost effective, and that water utilities have less-expensive options available to address turbidity resulting from runoff after wildfires.

| Hazard | Infrastructure Type | Project Description | Benefit ($mil) | Cost ($mil) | BCR |
|---|---|---|---|---|---|
| **Flood** (from actual EDA grants) | Rail | Elevate rail, Coralville, IA | 17 | 8.3 | 2:1 |
| | Rail | Elevate rail near SEMO Port, MO | 3 | 1.5 | 2:1 |
| | Road | Elevate road, Seward, NE | 9.4 | 1.3 | 7:1 |
| | Road and Bridge | Elevate road and reconstruct bridge, Iowa City, IA | 456 | 40.5 | 11:1 |
| | Bridge | Reconstruct bridge, Ruidoso, NM | 0.27 | 1.3 | 0.2:1 |
| | Water Treatment Plant | Elevate water treatment plant equipment, Portsmouth, VA | 112 | 11.6 | 10:1 |
| | Water Treatment Plant | Relocate water treatment plant, Columbus Junction, IA | 5.9 | 4.6 | 1:1 |
| | Wastewater Treatment Plant | Relocate wastewater treatment plant, Iowa City, IA | 195 | 54 | 4:1 |
| | Water and Wastewater Treatment Plants | Protect water and wastewater treatment plants, Greenville, NC | 212 | 6.8 | 31:1 |
| | Electric and Telecommunications | Mitigate electric and telecommunications substation, Reedsburg, WI | 2.2 | 0.235 | 9:1 |
| **Wind** (from actual EDA grants) | Electric Power Lines | Replace aboveground power lines from Derby to West Charleston and Bloomfield to Canaan, VT | 111.5 | 17.2 | 6:1 |
| | Electric Power Lines | Improve electric power lines, Seabrook, TX | 6.4 | 3.7 | 6.1 |
| **Earthquake** (based on project team analysis) | Resilient Water Supply Grid | Implement resilient water distribution grid ( 6-inch diameter pipe/16-inch ERDIP[1] trunk line grid/located every 10th distribution pipe), San Francisco, CA | 3,340 | 403 | 8:1 |
| | Resilient Water Supply Grid | Implement resilient water distribution grid (6-inch diameter pipe/16-inch ERDIP trunk line grid/located every 10th distribution pipe), Los Angeles, CA | 2,534 | 403 | 6:1 |
| | Resilient Water Supply Grid | Implement resilient water distribution grid (6-inch diameter pipe/ 16-inch ERDIP trunk line grid/located every 10th distribution pipe), Portland, OR | 238 | 403 | 0.6:1 |
| | Resilient Water Supply Grid | Implement resilient water distribution grid (6-inch diameter pipe/ 16-inch ERDIP trunk line grid/located every 10th distribution pipe), Seattle, WA | 696 | 403 | 2:1 |
| | Resilient Electric Grid | Retrofit electric substations (for peak ground acceleration of 0.47g), San Francisco, CA | 38 | 5 | 8:1 |
| | Resilient Electric Grid | Retrofit electric substations (for peak ground acceleration of 0.47g), Los Angeles, CA | 40 | 5 | 8:1 |
| | Resilient Electric Grid | Retrofit electric substations (for peak ground acceleration of 0.47g), Portland, OR | 31 | 5 | 6:1 |
| | Resilient Electric Grid | Retrofit electric substations (for peak ground acceleration of 0.47g), Seattle, WA | 10 | 5 | 2:1 |
| | Highway Bridges | Improve columns and footings based on Caltrans Seismic Retrofit Program | 1,344 | 441 | 3:1 |

**Table 1.** BCRs for select infrastructure mitigation measures (based on actual EDA grants and project team analysis for potential resilience initiatives).

[1] Earthquake-Resistant Ductile Iron Pipe (ERDIP).

## 1.4 Organization of this Report

Sections 2 through 5 summarize the benefit-cost analyses of 12 EDA grants. Section 6 summarizes the BCA of a resilient water supply grid. Section 7 summarizes the BCA of a resilient electric grid. Section 8 summarizes the BCA of the Caltrans highway bridge mitigation program. Bibliographic references are provided in Section 9.

# 2 Flood Mitigation for Roads and Railroads

## 2.1 Elevate Rail in Coralville, Iowa

***Summary of the grant.*** EDA, under its Economic Adjustment Assistance program, provided a grant of $7.8 million in 2010 U.S. dollars (USD) (approximately $8.3 million in 2018) to the city of Coralville, Iowa, to elevate rail next to the Iowa River and to elevate nearby trails. The elevated rail bed would protect rail traffic along the line: approximately two trains per day, according to a crossing inventory report filed with the U.S. Federal Railroad Administration (FRA) and available through its online geographic information system (GIS) tool, the FRA GIS Web Application.[2] The elevated rail bed and elevated trails were also intended to act as levees to protect buildings along the city's Iowa River shoreline near the rail bed. Figure 1 shows the locations of the elevated rail bed. The stretch of rail north of the yellow pushpin in the figure runs just east of First Avenue. The stretch south and east of the yellow pushpin runs just north of Second Street. A creek flows into the Iowa River near the pushpin. Satellite imagery shows elevated trails adjacent to the creek; these appear to be the ones mentioned in grant data.

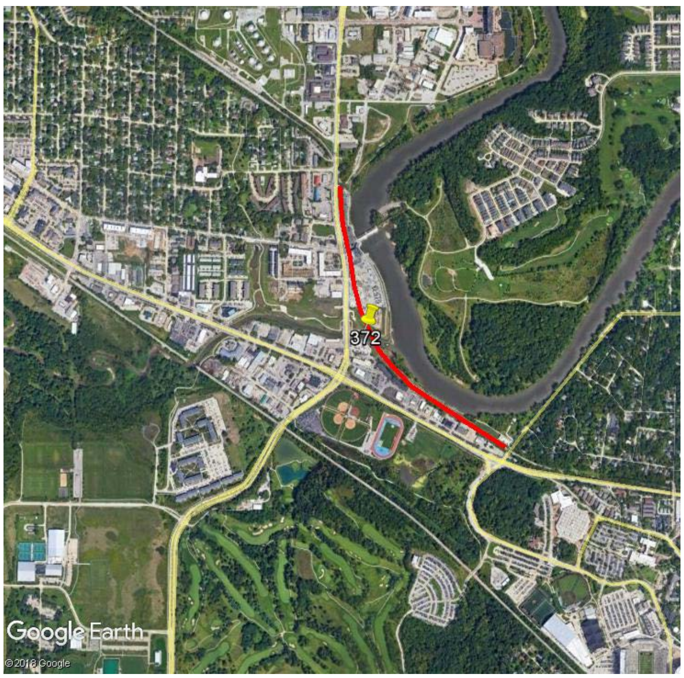


**Figure 1.** Elevated rail in Coralville, Iowa.

The original rail bed appears to have had a lowest elevation of approximately 645 ft above sea level (ASL), which was raised to approximately 651 ft ASL. Reviews of FEMA FIRMettes[3] suggest that the 100-year and 500-year floodplains near the rail have upper edges at approximately 645 ft ASL and 647 ft ASL, respectively. (Elevations are calculated here using the datum in Google Earth, as opposed to that of the FEMA FIRMettes.) A conservative estimate from satellite imagery of buildings just west of First Avenue and south of Second Street suggests

[2] See http://fragis.fra.dot.gov/GISFRASafety/.
[3] A FIRMette is a full-scale section of a Flood Insurance Rate Map (FIRM).

1.5 million $ft^2$ of buildings, in approximately equal proportions of dwellings and workplaces. Using a replacement cost of $\$200/ft^2$, plus 50% added for content value, the project team conservatively estimated $460 million in protected property. Satellite imagery of First Avenue and Second Street suggest traffic flow of 25,000 trips per day.

***Flood hazard.*** Using the elevations and exceedance frequencies associated with a 0.2% and 1% annual chance of flooding, the researchers estimated a relationship between elevation and exceedance frequency (a flood hazard curve) by assuming that the natural logarithm of exceedance frequency varies linearly with elevation.

***Direct damage to buildings.*** The Hazus Flood Model provides a vulnerability function for a variety of building types. The analysis for this project uses a vulnerability function for 2-story buildings without basements.

***Loss of use duration and costs.*** The project team conservatively estimated that delayed use of rail would cost $264/train-hour in 2018 USD (Schlake et al. 2011). The figure considers cost of cars, locomotives, fuel, and labor, considering both actual and opportunity costs for an "average" train of 69 cars and 2.7 locomotives per train. The project team assumed that restoring function to a rail line requires one day per foot of flooding for floodwater to recede (as assumed elsewhere in this study) plus one day to inspect the line and clear debris.

If the flood-protection measure affects roadway access to residential property but does not affect actual damage to the property, then it is assumed that residents must stay in hotels and eat out, at a cost (or equivalent value) of the General Services Administration (GSA) local per-diem rate for meals and incidental expenses and accommodations. The project team assumed that one hotel room accommodates a typical family averaging 2.5 people. If the flood-protection measure affects roadway access to workplaces, the resulting direct business interruption cost is taken to be the state daily per-capita gross domestic product (GDP). Indirect business interruption losses are taken as 0.5 times the total of additional living expenses and direct business interruption losses, as shown previously in this study.

If the flood-protection measure actually did protect homes and workplaces, then for convenience, the project team estimated additional living expenses, direct business interruption losses, and indirect business interruption losses as a factor of property losses taken from those estimated for federal grants for flood protection examined earlier in the study: a total of 30%.

***Casualties.*** Hazus does not calculate flood-related deaths and injuries. However, for this grant, an estimate seemed practical, using the following methodology: in flooding, the primary causes of death is due to people drowning when they try to drive through flooded areas. Fatality statistics from four Texas floods between 1990 and 2001 show approximately 80 drownings (Table 2). The project team tabulated the population in the counties experiencing the greatest rainfall intensities (at least 12 inches of rain in 2 days) in each flood using U.S. Census data, and found that 8.9 million people were affected by the floods. The ratio of 80 deaths to 8.9 million people suggests a fatality rate of 0.90 per 100,000 population. Approximately half of drownings in floods are attributed to people trying to drive through floodwaters, so the project team estimated 0.45 deaths per 100,000 people who would normally use a road that, in the analysis, is flooded or protected by a flood-mitigation measure. Counts of people were estimated one of three ways: (1) An engineer associated with the EDA grant provided an estimate of the number of people using the road; (2) A flood-protection measure protects a route into an otherwise isolated neighborhood, in which case the project team estimated the population of that neighborhood; or (3) the product of vehicle count per mile in satellite imagery, estimated traffic speed in miles per hour, and assuming 18 hours of traffic flow. The project team preferred Method 1 over 2, and 2 over 3. Method 3 is crude, but should provide a reasonable estimate on an order-of-magnitude basis.

| Location | Date | Deaths | Population | Counties |
|---|---|---|---|---|
| **Central Texas** | Oct 1998 | 29 | 1,585,304 | Comal, Bexar, Guadalupe, and Gonzales |
| **Houston** | Jun 2001 | 22 | 3,668,308 | Harris and Jefferson Counties |
| **Dallas** | May 1995 | 15 | 1,954,250 | Dallas County |
| **Central Texas** | Dec 1991 | 14 | 1,699,000 | Bexar and Travis |
| **Total** | | 80 | 8,906,862 | |

Note: Comal, Bexar, Guadalupe and Gonzales Counties identified per https://pubs.usgs.gov/fs/FS-147-99/; Bexar and Travis counties identified per https://pubs.er.usgs.gov/publication/wri954289.

**Table 2.** Casualty modeling for flooded roads.

***Historic losses.*** None seem to apply.

***Environmental losses.*** None seem to apply.

***Benefit-cost ratio.*** Considering the foregoing project-specific information presented here, the general procedures presented here and elsewhere in the study, a 100-year project life, and a cost-of-borrowing discount rate of 2.2%, the project team calculated the project produced $17 million in benefit at a cost of $8.3 million, for an overall BCR of $2.05 saved per $1.00 invested, i.e., 2 to 1. The estimate may be overly conservative because it is unclear from satellite imagery how far the flood protection extends from the rail line. Most of the benefits are from reduced property loss, as shown in Figure 2. Using higher discount rates of 3% and 7%, the BCRs would be lower: 1.7 and 0.9, respectively.

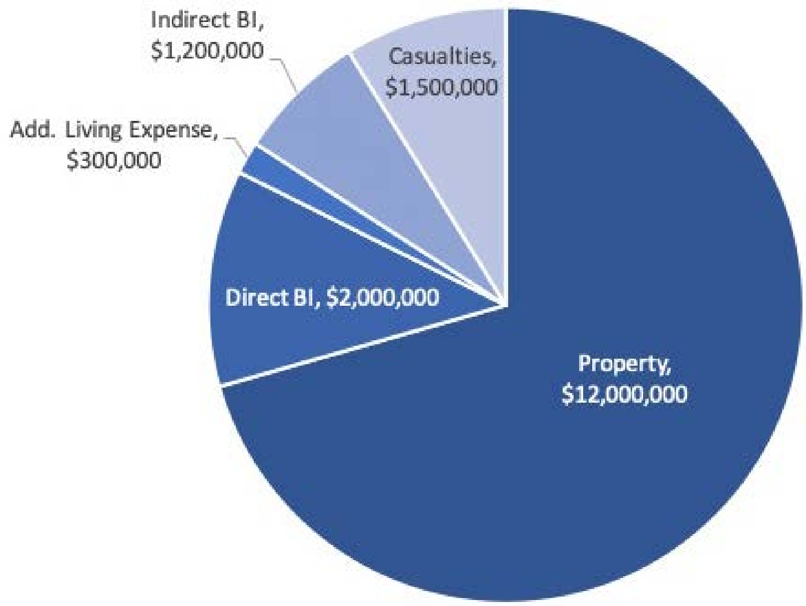


**Figure 2**. Estimated benefits from elevated rail and trails in Coralville, Iowa.

## 2.2 Elevate Rail near SEMO Port, Missouri

***Summary of the grant.*** EDA, under its Economic Adjustment Assistance program, provided a grant of $1.9 million in 2014 USD to the Southeast Missouri (SEMO) Regional Port Authority for various measures to improve rail through the port. A large portion of the grant, approximately $1.5 million in 2018 USD, elevated rail along the Mississippi River, as shown highlighted in green in Figure 3. The work elevated the rail from the base flood elevation (BFE) -9.5 ft (that is, 9.5 feet below BFE) to BFE -4 ft (i.e., 4 feet below BFE); the grantee suggested that it did not seem cost effective to better protect the rail in light of the much greater cost that would have been required. Grant data and FEMA FIRMettes suggest nearby 100-year and 500-year floodplains have upper edges about 352 ft ASL and 355 ft ASL, respectively. The grantee estimated traffic at 8 to 21 trains per week.

***Flood hazard.*** Using the elevations and exceedance frequencies associated with a 0.2% and 1% annual chance of flooding, the project team estimated a relationship between elevation and exceedance frequency (a flood hazard curve) by assuming that the natural logarithm of exceedance frequency varies linearly with elevation.

***Loss of use duration and costs.*** As used elsewhere in this study, delayed use of rail is conservatively estimated to cost $264/train-hour in 2018 USD (Schlake et al. 2011). That figure considers the cost of cars, locomotives, fuel, and labor, considering both actual and opportunity costs for an “average” train of 69 cars and 2.7 locomotives per train. It is assumed that restoring function to a rail line requires one day per foot of flooding for floodwater to recede (as assumed elsewhere in this study) plus one day to inspect the line and clear debris.

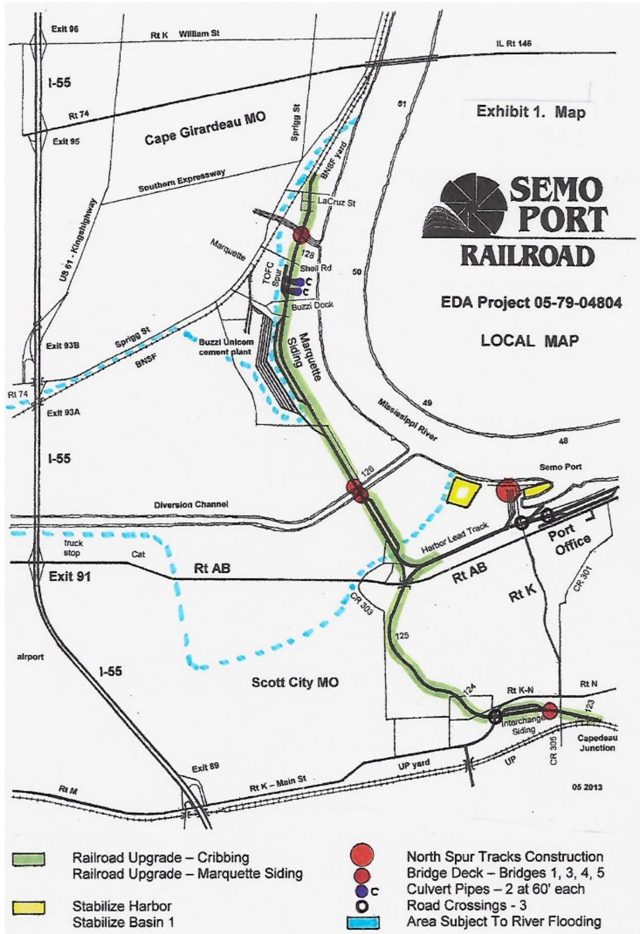


**Figure 3**. Elevated rail (highlighted in green) in the SEMO Port Railroad.

***Casualties.*** None seem to apply.

***Historic losses.*** None seem to apply.

***Environmental losses.*** None seem to apply.

***Benefit-cost ratio.*** Considering the foregoing project-specific information presented here and a conservative traffic estimate of 13 trains per week (the geometric rather than arithmetic mean of the two traffic estimates), the general procedures presented here and elsewhere in the study, a 100-year project life, and a cost-of-borrowing discount rate of 2.2%, the project produced $3.0 million in benefit at a cost of $1.5 million, for an overall BCR of $2.00 saved per $1.00 invested, i.e., 2 to 1. All of the benefits are from reduced business interruption losses, as shown in Figure 4. Using higher discount rates of 3% and 7%, the BCRs would be lower: 1.5 and 0.7, respectively.

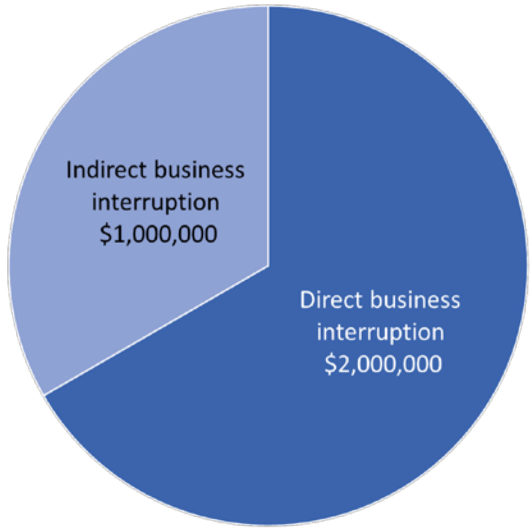


**Figure 4**. Estimated benefits from elevating rail near SEMO Port, Missouri.

## 2.3 Elevate Road in Seward, Nebraska

***Summary of the grant.*** EDA, under its Economic Adjustment Assistance program, provided a grant of $2.2 million in 2010 USD (approximately $2.6 million in 2018) to Seward, Nebraska to elevate and extend a road to an industrial facility. Only the portion of the project cost associated with elevating the road (approximately $1.3 million) is considered here, because the extension constituted an expansion rather than remediation of the roadway. Figure 5 shows the location of the road, just south of the Big Blue River (the green space stretching from the middle top of the image to the middle right). The road does not provide protection to the industrial facility, which is at a slightly higher elevation. The FEMA FIRMettes suggest that the 100-year and 500-year floodplains near the road have upper edges of approximately 1,446 ft and 1,448 ft ASL, respectively. The road appears to have pre- and post-remediation elevations of 1,441 ft and 1,449 ft ASL, respectively. The industrial facility has 500 employees, so the analysis assumed 500 trips.

***Flood hazard.*** Using the elevations and exceedance frequencies associated with a 0.2% and 1% annual chance of flooding, the project team estimated a relationship between elevation and exceedance frequency (a flood hazard curve) by assuming that the natural logarithm of exceedance frequency varies linearly with elevation.

***Direct damage to buildings.*** Not applicable.

***Loss of use duration and costs.*** Loss of access costs $139 per capita daily GDP per day, and the analysis assumed 2.5 people per each of 500 employees. No residences were protected, so no additional living expenses apply.

***Casualties.*** As described elsewhere, the project team estimated 0.45 deaths per 100,000 trips, and 500 trips in this particular case.


Note: The BCA considers only the extension between the midpoint of the road (the middle pushpin) and east end (the right-hand pushpin).

**Figure 5.** Elevated and extended road in Seward, Nebraska.

***Historic losses.*** None seem to apply.

***Environmental losses.*** None seem to apply.

***Benefit-cost ratio.*** Considering the foregoing project-specific information presented here, the general procedures presented here and elsewhere in the study, a 100-year project life, and a cost-of-borrowing discount rate of 2.2%, the project team calculated that the project produced $9.4 million in benefit at a cost of $1.3 million, for an overall BCR of $7.20 saved per $1.00 invested, i.e., 7 to 1. Most of the benefits were from business interruption loss, as shown in Figure 6. Using higher discount rates of 3% and 7%, the BCRs are lower: 6 and 3, respectively.

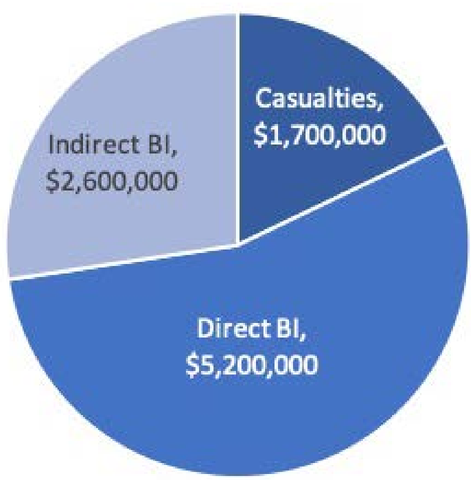


**Figure 6.** Estimated benefits of elevating access road in Seward, Nebraska.

## 2.4 Elevate Road and Reconstruct Bridge in Iowa City, Iowa

***Summary of the grant.*** EDA, under its Economic Adjustment Assistance program, provided a grant for a project that ultimately cost $40.6 million in 2018 USD to Iowa City, Iowa, to elevate 3,500 ft of a road and to reconstruct a bridge to an industrial facility. Figure 7 shows the location of the work: the Park Road Bridge and North Dubuque Street serve as an artery for 25,000 daily trips each way between Iowa City and Interstate 80. The road also provides the only access to a 1,000-bed University of Iowa residence hall, two apartment complexes, and a few other residences. The FEMA FIRMettes and city data suggest that the 100-year and 500-year floodplains near the road have upper edges of approximately 651 ft and 653 ft ASL, respectively, using the same datum as Google Earth. The road appears to have pre- and post-remediation elevations of 644 ft and 652 ft ASL, respectively.

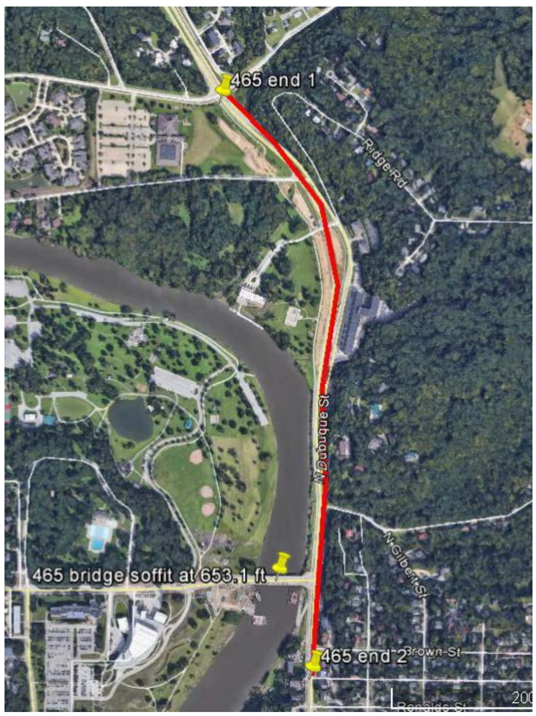


**Figure 7.** Elevated roadway (North Dubuque Street, highlighted by the red line) and elevated bridge (Park Road Bridge over the Iowa River, yellow pushpin) in Iowa City, Iowa.

***Flood hazard.*** Using the elevations and exceedance frequencies associated with a 0.2% and 1% annual chance of flooding, the project team estimated a relationship between elevation and exceedance frequency (a flood hazard curve) by assuming that the natural logarithm of exceedance frequency varies linearly with elevation.

***Direct damage to buildings.*** Not applicable.

***Loss of use duration and costs.*** Loss of access to homes for approximately 1,100 people costs $146 per person per day using local GSA per diem rates and assuming two students per hotel room.

***Casualties.*** As described elsewhere, the project team estimates 0.45 deaths per 100,000 trips, and 25,000 trips in this particular case.

***Historic losses.*** None seem to apply.

***Environmental losses.*** None seem to apply.

***Benefit-cost ratio.*** Considering the foregoing project-specific information presented here, the general procedures presented here and elsewhere in the study, a 100-year project life, and a cost-of-borrowing discount rate of 2.2%, the project team calculated that the project produced $456 million in benefit at a cost of $40.5 million, for an overall BCR of $11 saved per $1.00 invested, i.e., 11 to 1. Most of the benefits are from avoided casualties—people who would drown because they try to drive through the flooded street, as shown in Figure 8. Using higher discount rates of 3% and 7%, the BCRs are essentially the same, 11 to 1, because the analysis does not discount human life.

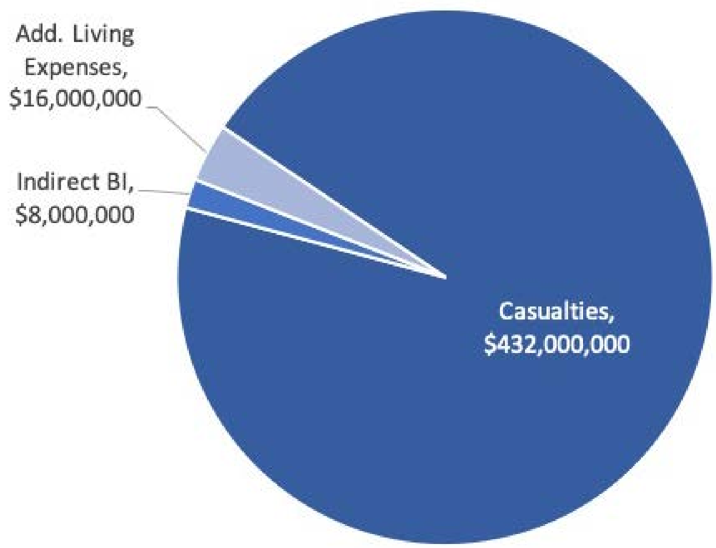


**Figure 8.** Estimated benefits of elevating access road in Seward, Nebraska.

## 2.5 Reconstruct Bridge in Ruidoso, New Mexico

***Summary of the grant.*** EDA, under its Economic Adjustment Assistance program, provided a grant worth $1.3 million in 2018 USD to Ruidoso, New Mexico to reconstruct a bridge that provides access to the homes of 1,000 people. Figure 9 shows the location of the bridge, which spans the Rio Ruidoso. The bridge was raised slightly but greatly widened to double the flow beneath it, remediating the potential for overtopping of the bridge during heavy rainfall. The FEMA FIRMettes suggest that the 100-year and 500-year floodplains near the bridge have upper edges of approximately 6,823 ft and 6,831 ft ASL, respectively, although those elevations reflect the damming effect of the bridge. The road appears to have a pre-remediation elevation of 6,823 ft ASL.

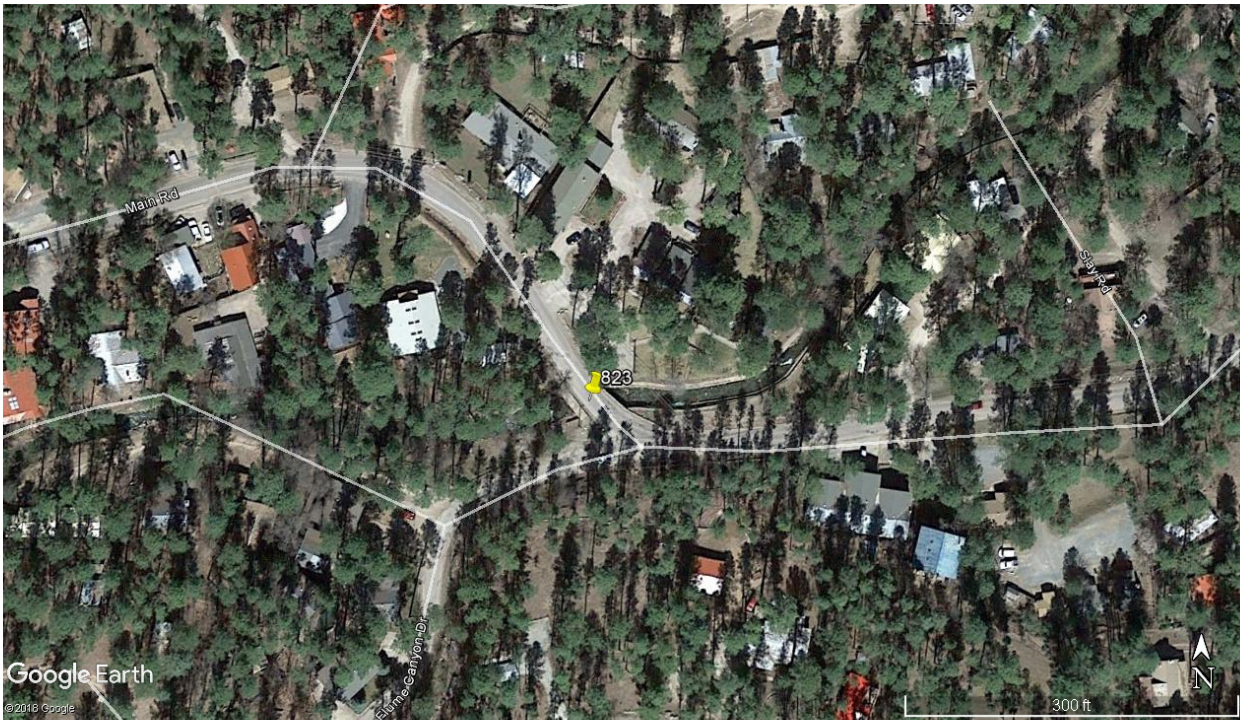

**Figure 9.** Reconstructed bridge (yellow pushpin) over Main Road in Ruidoso, New Mexico.

***Flood hazard.*** Using the elevations and exceedance frequencies associated with a 0.2% and 1% annual chance of flooding, the project team estimated a relationship between elevation and exceedance frequency (a flood hazard curve) by assuming that the natural logarithm of exceedance frequency varies linearly with elevation. To approximate the effect of widening the floodway below the bridge, the project team treated the post-reconstruction elevation as having an elevation of 6,827 ft ASL.

***Direct damage to buildings.*** Not applicable.

***Loss of use duration and costs.*** Loss of access costs $132 per capita for meals and accommodations.

***Casualties.*** As described elsewhere, the project team estimated 0.45 deaths per 100,000 trips, and 1,000 trips in this particular case.

***Historic losses.*** None seem to apply.

***Environmental losses.*** None seem to apply.

***Benefit-cost ratio.*** Considering the foregoing project-specific information presented here, the general procedures presented here and elsewhere in the study, a 100-year project life, and a cost-of-borrowing discount rate of 2.2%, the project team calculated that the project produced $270,000 in benefit at a cost of $1.3 million, for an overall BCR of $0.21 saved per $1.00 invested, i.e., 0.21 to 1, as shown in Figure 10. Using higher discount rates of 3% and 7%, the

BCRs are lower: 0.17 and 0.10, respectively. A BCR below 1to 1 reflects that the grant decision is based on criteria other than the long-term average cost effectiveness of the mitigation measure.

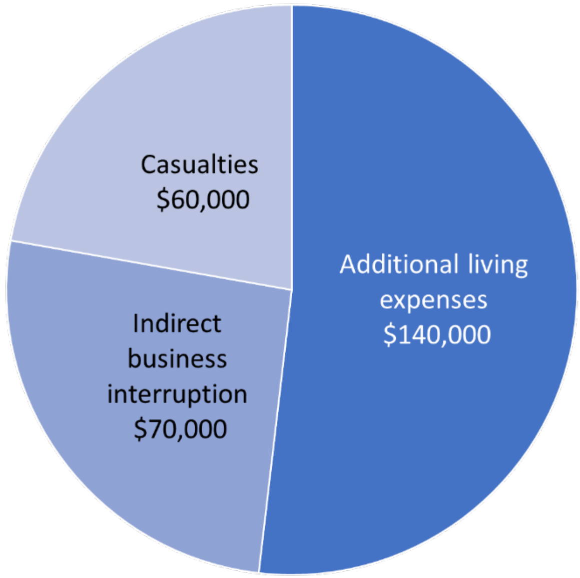


**Figure 10**. Estimated benefits from reconstructing the Main Road Bridge over Rio Ruidoso in Ruidoso, New Mexico.

# 3 Flood Mitigation for Water and Wastewater Infrastructure

This section presents analyses of grants to mitigate natural-hazard risk to water and wastewater facilities. Some of the grants address water facilities, some address wastewater, and one addresses both.

## 3.1 Elevate Water Treatment Plant Electrical Equipment in Portsmouth, Virginia

***Summary of the grant.*** EDA, under its Economic Adjustment Assistance program, provided a grant in the amount of $8.6 million in 2003 USD (approximately $11.6 million in 2018) to Portsmouth, Virginia. The grant relocated the electrical equipment for Portsmouth's Lake Kilby water treatment facility from a location at 21 ft ASL, 1 foot lower than the upper edge of FEMA's Special Flood Hazard Area (SFHA) (the so-called 100-year floodplain, around 22 ft ASL), to a new location at 40 ft ASL (approximately 8 ft higher than the upper edge of the 500-year floodplain). Figure 11 shows the locations of the old and new electrical facility. The effort aimed to maintain water service during floods to the city's population of 96,200 people.

A B
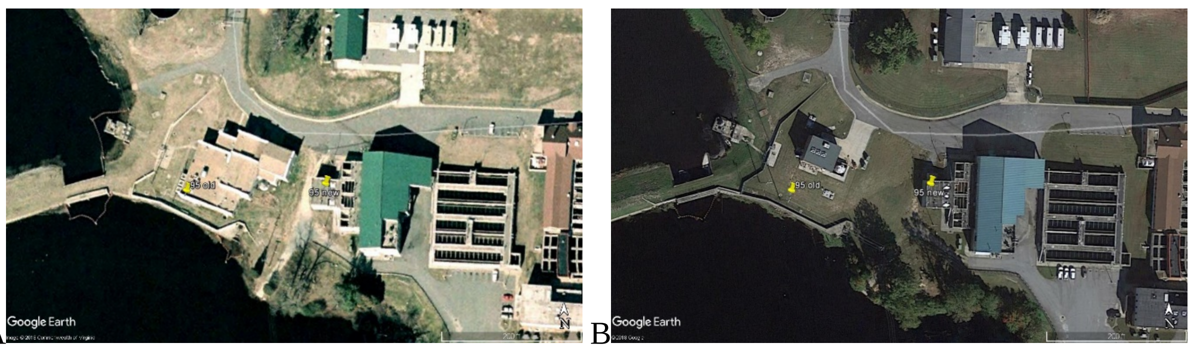


**Figure 11.** Portsmouth's water treatment plant: A) in 2003, and B) in 2015.

***Flood hazard.*** Using the elevations and exceedance frequencies associated with a 0.2% and 1% annual chance of flooding, the project team estimated a relationship between elevation and exceedance frequency (a flood hazard curve) by assuming that the natural logarithm of exceedance frequency varies linearly with elevation.

***Direct damage to control building equipment.*** The Hazus Flood Model provides a vulnerability function for small water treatment plants that operate by pressure.

***Loss of use duration and costs.*** The project team assumed that restoring mechanical equipment at a water treatment plant to function requires one day per foot of flooding for floodwater to recede (as assumed elsewhere in this study) plus one week to disassemble, clean, and dry motors, pumps, and other rotating equipment, and less time to clean and dry electrical equipment. During that time, residences lack water for showers and toilets so residents must relocate temporarily. They might stay in hotels, at a cost of the GSA per diem for lodging (one room for a household of up to three) plus the GSA per diem rate for meals and incidental expenses (one per each person). It may be that people stay with friends or family or in a shelter at little or no cost, but economists see the value lost as worth something. Residents would rather be at home. The measure of that preference, in this case, is taken as the GSA per diem rates.

Businesses cannot operate without functioning bathrooms. If a water treatment plant is inoperative, all businesses are similarly affected. Customers or employees cannot simply go next door. Nor are there likely to be portable toilets available for the entire community at a moment's notice. The analysis therefore estimates the direct business interruption costs resulting from loss of potable water as the state-average per-capita daily GDP. Indirect business interruption is taken as 0.5 times the sum of additional living expenses and direct business interruption loss, as elsewhere in this study.

The local GSA per diem for accommodations, for meals and incidental expenses, and the state per-capita daily GDP are $87, $61, and $141 respectively.

***Casualties.*** As discussed elsewhere in this study, the primary cause of death in flooding is due to people drowning when they try to drive through flooded areas. Casualty losses are therefore assumed to be zero in this case, and there seems to be no reason to suspect that PTSD would occur from temporary loss of potable water service.

***Historic and environmental losses.*** None seem to apply.

***Benefit-cost ratio.*** Considering the project-specific information presented here, general procedures presented elsewhere in the study, a 100-year project life, and a cost-of-borrowing discount rate of 2.2%, the project team calculated that the project produced $112 million in benefit at a cost of $11.6 million, for an overall BCR of $9.70 saved per $1.00 invested, i.e., 10 to 1. Most of the benefits result from reduced business interruption (Figure 12), with a small contribution from reduced property damage (largely building and equipment damage). At discount rates of 3% and 7%, the BCRs are lower: 8 and 3, respectively.

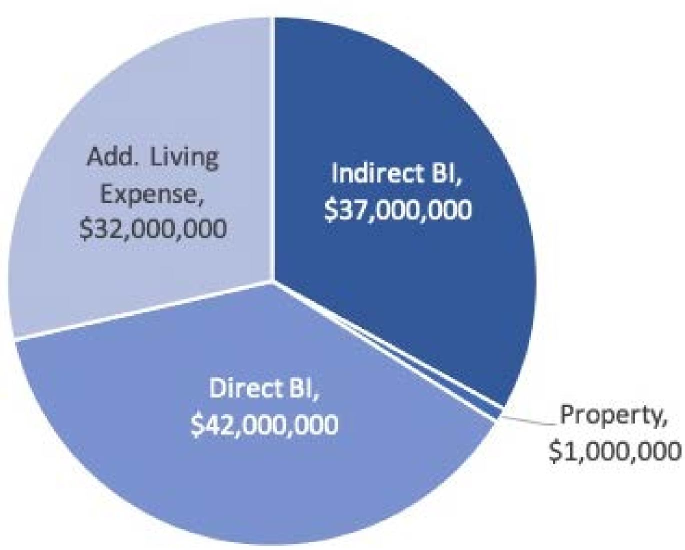


**Figure 12.** Estimated benefits from elevating electrical equipment at the water treatment plant in Portsmouth, Virginia.

## 3.2 Relocate Water Treatment Plant in Columbus Junction, Iowa

***Summary of the grant.*** EDA, under its Economic Adjustment Assistance program, provided a grant of $4.6 million (2010 USD) to Columbus Junction, Iowa. The grant relocated the city's water treatment facility from a location at 587 ft ASL, 2 feet lower than the upper edge of FEMA's SFHA (the so-called 100-year floodplain, around 589 ft ASL), see Figure 13, to a new location at 594 ft ASL (2 ft higher than the upper edge of the 500-year floodplain, around 592 ft ASL, see Figure 14. The goal was to maintain water service to Columbus Junction during floods. The water treatment plant serves 60 commercial customers and 600 residential customers; the total population measures 1,850.


Note: In this FEMA FIRMette, the blue area represents the special flood hazard area, with at least 1% annual chance of flooding. The brown areas have between 0.2% and 1% annual chance of flooding.

**Figure 13**. The old water treatment plant in Columbus Junction, Iowa.


**Figure 14.** The new water treatment plant in Columbus Junction, Iowa.

***Flood hazard.*** Using the elevations and exceedance frequencies associated with a 0.2% and 1% annual chance of flooding, the project team estimated a relationship between elevation and exceedance frequency (a flood hazard curve) by assuming that the natural logarithm of exceedance frequency varies linearly with elevation.

***Direct damage to control building equipment.*** The Hazus Flood Model provides a vulnerability function for small water treatment plants that operate by pressure.

***Loss of use duration and costs.*** It is assumed here that restoring the water treatment plant to function requires one day per foot of flooding for floodwater to recede (as assumed elsewhere in this study) plus one week to disassemble, clean, and dry motors, pumps, and other rotating equipment, and less time to clean and dry electrical equipment. During that time, residences lack water for showers and toilets, so occupants have to relocate temporarily. They might stay in hotels, at a cost of the GSA per diem for lodging (one room for a household of up to three) plus the GSA per diem rate for meals and incidental expenses (one per each person). It may be that people stay with friends or family or in a shelter at little or no cost, but economists see the value lost as worth something. Residents would rather be at home. The measure of that preference is taken here as the GSA per diem rates.

Businesses cannot operate without functioning bathrooms. If a water treatment plant is inoperative, all businesses are similarly affected. Customers or employees cannot go next door. Nor are there likely to be portable toilets available for the entire community at a moment's notice. The analysis estimates direct business interruption loss as the state-average per-capita daily GDP. Indirect business interruption loss is taken as 0.5 times the sum of additional living expenses and direct business interruption loss, as elsewhere in this study.

In the case of Columbus Junction, Iowa, GSA per diems for accommodations and for meals and incidental expenses are $91 and $51, respectively. The per-capita daily GDP is $139.

***Casualties.*** As discussed elsewhere in this study, the primary cause of death in flooding is due to people drowning when they try to drive through flooded areas. Casualty losses are therefore assumed to be zero in this case, and there seems no reason to suspect that PTSD would occur from temporary loss of potable water service.

***Historic and environmental losses.*** None seem to apply.

***Benefit-cost ratio.*** Considering the foregoing project-specific information presented here, the general procedures presented elsewhere in the study, a 100-year project life, and a cost-of-borrowing discount rate of 2.2%, the project team calculated that the project produced $5.9 million in benefit at a cost of $4.6 million, for an overall BCR of $1.30 saved per $1.00 invested, i.e., 1.3 to 1. Most of the benefits are from reduced business interruption to the community, as shown in Figure 15. Using higher discount rates of 3% and 7%, the BCRs are lower, 1.0 and 0.5, respectively. The BCR is relatively low compared to other mitigation for water treatment plants because the measure relocates the water treatment plant, which is relatively costly, compared with other flood-protection measures considered here, such as building berms and elevating electrical equipment.

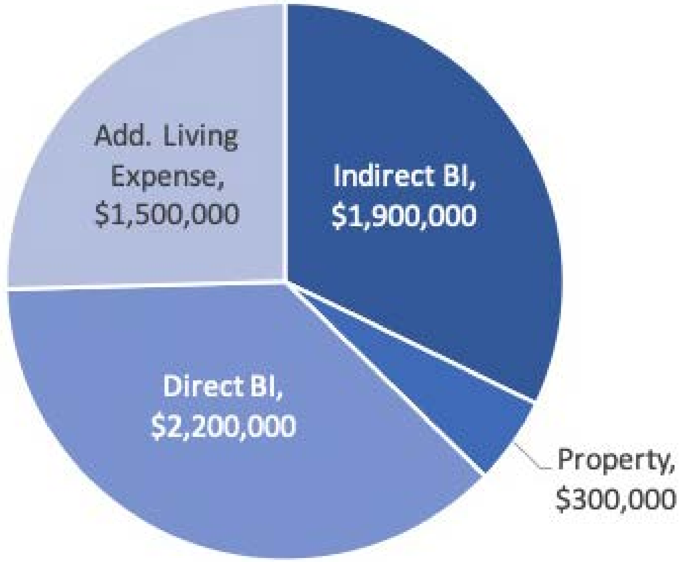


**Figure 15.** Estimated benefits from new water treatment plant in Columbus Junction, Iowa.

## 3.3 Relocate Wastewater Treatment Plant out of Floodplain in Iowa City, Iowa

***Summary of the grant.*** EDA, under its Economic Adjustment Assistance program, provided a grant of $46.5 million in 2010 USD (approximately $54 million in 2018) to Iowa City, Iowa. The purpose of the grant was to redirect wastewater from the city's north wastewater treatment plant, in the FEMA SFHA (the 100-year floodplain), to its south wastewater treatment plant, and expand the south plant to handle the greater demand. Expansion of the south plant cost approximately $40.6 million in 2010 USD ($47 million in 2018). Figure 16 shows the locations of the two facilities.

The grant aimed, during floods, to maintain wastewater service to the city's population of 74,400 people. The ground at the north plant had an elevation of approximately 646 ft ASL. The 100-year and 500-year floodplains near the site of the north plant have upper edges of about 650 ft ASL and 652 ft ASL, respectively. The south plant also had some risk of flooding (see Figure 17), but the expansion mitigated individual buildings and equipment by raising equipment within buildings, raising transformer pads, building berms, and other measures, to a level one ft above the elevation of 500-year flooding. The FEMA FIRMette suggests a 642-ft ASL elevation of the edge of the 100-year floodplain at the south treatment plant. Estimates (Stanley Consultants 2011) placed the upper edge of the 500-year floodplain at approximately 645 ft ASL, and the lowest equipment needing elevation at about 644 ft ASL. Hazus values a medium-sized wastewater treatment plant at $200 million (2003 USD) or $276 million in 2018 USD.

***Flood hazard.*** Using the elevations and exceedance frequencies associated with a 0.2% and 1% annual chance of flooding, the project team estimated a relationship between elevation and exceedance frequency (a flood hazard curve) by assuming that the natural logarithm of exceedance frequency varies linearly with elevation.

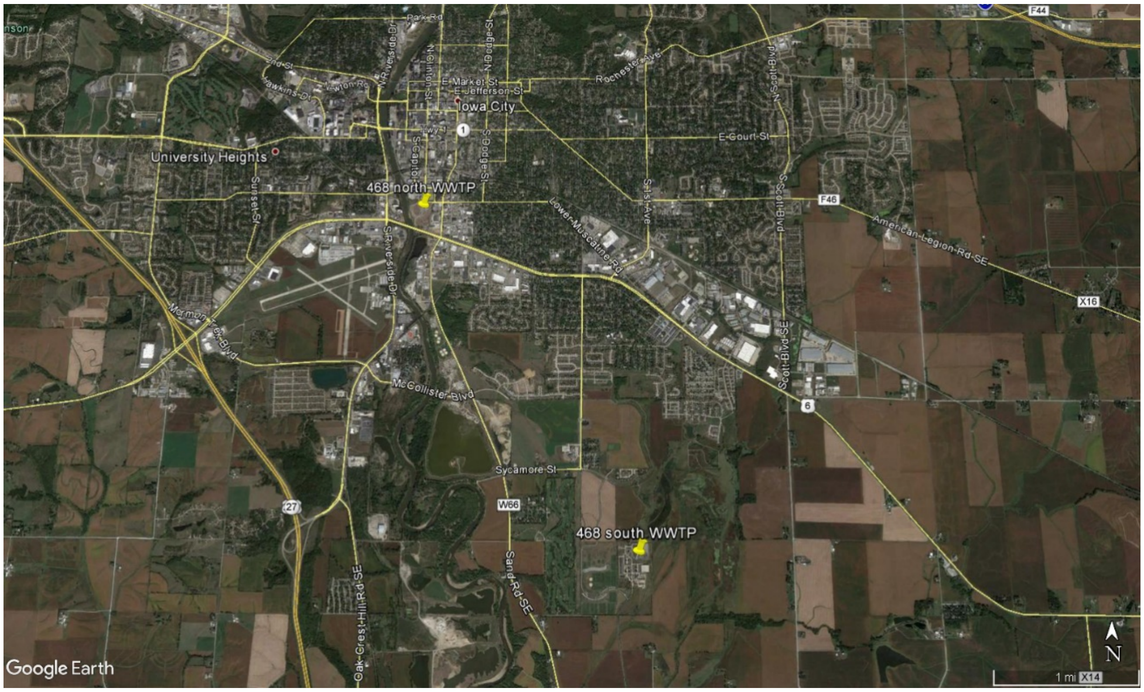

**Figure 16.** Wastewater treatment plant sites in Iowa City, Iowa: the north plant (denoted 468 north WWTP) and the south plant (denoted 468 south WWTP).

***Direct damage to wastewater treatment plant equipment.*** The Hazus Flood Model provides a vulnerability function for wastewater treatment plants. The methodology provides different labels of systems that distinguish them by size (small, medium, and large), but the vulnerability functions for different sizes are identical. The methodology indicates that the system ceases to function when any flooding occurs.

***Loss of use duration and costs.*** It is assumed here that restoring the function of a wastewater treatment plant requires one day per foot of flooding for floodwater to recede (as assumed elsewhere in this study) plus one week to disassemble, clean, and dry motors, pumps, and other rotating equipment, and less time to clean and dry electrical equipment. During that time, if the wastewater treatment plant were damaged, it is assumed here that homes and businesses would be allowed to continue using the sewer system in Iowa City at a voluntarily reduced rate and that untreated wastewater would flow overland, through unnamed creeks, downstream to the Iowa River, then 25 miles past Hills, Columbus Junction, and Wapello to the Mississippi River. It is assumed that by the time it reaches Columbus Junction, the untreated wastewater would be diluted to the point that the Columbus Junction Water Treatment Plant could handle the additional contaminants and that no additional living expenses or business interruption costs would be incurred there.

***Casualties.*** As discussed elsewhere in this study, the primary cause of death in flooding is due people drowning when they try to drive through flooded areas. Casualty losses are therefore assumed to be zero in this case, and there seems to be no reason to suspect that PTSD would occur from temporary loss of wastewater service.


**Figure 17.** The estimated extent of flooding at the south waste water treatment plant in Iowa City, Iowa, before mitigating sensitive buildings and components, using a 0.2% annual exceedance probability (500-year flood). (Stanley Consultants 2011)

***Historic losses.*** None seem to apply.

***Environmental losses.*** Regardless of loss-of-use costs, if either wastewater treatment plant were to flood, untreated wastewater represents a hazardous spill that would pollute the Iowa River and make it unusable for recreation for a season. It is problematic to assign a monetary value to the resulting environmental impact. As noted elsewhere in this study, Whitehead et al. (2000)

estimated the revealed-preference value of $95 per visit to a recreation area (in 2018 USD). The project team assumed that pollution from flooding of the wastewater treatment plant would impair the recreational value of the Iowa River between Iowa City and the Mississippi River for a season. The analysis attributes that amount to each person who lives between Iowa City and the Mississippi River: in Iowa City (population 74,400), Riverside (1,000), Hills (800), Columbus Junction (1,800), and Wapello (2,000), essentially assuming one foregone visit per person near the river. The project team therefore estimated the environmental impact from flooding of either wastewater treatment plant to be worth $7.6 million to avoid.

***Benefit-cost ratio.*** Considering the foregoing project-specific information presented here, the general procedures presented elsewhere in the study, a 100-year project life, and a cost-of-borrowing discount rate of 2.2%, the project team calculated that the project produced $195 million in benefit at a cost of $54 million, for an overall BCR of $3.60 saved per $1.00 invested, i.e., 4 to 1. The BCR is relatively low compared with other water- and wastewater-related grants considered here because of the assumption that Iowa City homes and businesses would not have to cease operations solely because of flooding of either wastewater treatment plant. That assumption may be overly conservative; conceivably, untreated wastewater near businesses at the south end of Iowa City (just downstream of the wastewater treatment plant) might so impair air quality and public safety that some businesses would cease operations until cleanup were completed. In any case, most of the benefits are from property loss to the wastewater treatment plants, as shown in Figure 18. Using higher discount rates of 3% and 7%, the BCRs are lower: 2 and 1, respectively.


**Figure 18**. Estimated benefits from decommissioning the Iowa City, Iowa, north wastewater treatment plant and elevating or otherwise protecting critical equipment at the south plant.

## 3.4 Protect Water and Wastewater Treatment Plants in Greenville, North Carolina from Flood

***Summary of the grant.*** EDA, under its Economic Adjustment Assistance program, provided a grant of $4.8 million in 2001 USD (approximately $6.8 million in 2018) to Greenville, North Carolina to construct a flood-protection berm and pumping station for Greenville’s water treatment plant. The grant also paid to raise a flood protection wall and a retaining wall at the

Northside Wastewater Treatment Plant. Figure 19A shows the locations of the two facilities. The grant aimed to maintain, during floods, the water and wastewater service to the city's population of 91,500 people. The ground at the water treatment plant has an elevation of 21 ft ASL; the crest of the berm rises to 33 ft ASL (Figure 19). The 100-year and 500-year floodplains have upper edges of approximately 24 ft and 27 ft ASL, respectively. Ground level at the wastewater treatment plant is 18 ft ASL; its berm has a crest elevation of approximately 21 ft ASL. The edges of the 100-year and 500-year floodplains are about 17 ft and 19 ft ASL. Hazus values a medium-sized water-treatment plant at $100 million in 2003 USD, or $138 million in 2018 USD. It values a wastewater treatment plant at $200 million in 2003 USD or $276 million in 2018 USD.


**Figure 19**. A. Water treatment plant (denoted 53 WTP) and wastewater treatment plant (denoted 53 WWTP) sites in Greenville, North Carolina. B. Image of the water treatment plant, with berm highlighted in red. C. Image of the wastewater treatment plant.

***Flood hazard.*** Using the elevations and exceedance frequencies associated with a 0.2% and 1% annual chance of flooding, the project team estimated a relationship between elevation and exceedance frequency (a flood hazard curve) by assuming that the natural logarithm of exceedance frequency varies linearly with elevation.

***Direct damage to water treatment plant and wastewater treatment plant equipment.*** The Hazus Flood Model provides a vulnerability function for water treatment plants that operate by pressure and another for wastewater treatment plants. The methodology provides different labels of systems that distinguish them by size (small, medium, and large), but the vulnerability functions for different sizes are identical. The methodology also indicates that the system ceases to function when any flooding occurs.

***Loss of use duration and costs.*** It is assumed here that restoring the function of a water treatment plant or of a wastewater treatment plant requires one day per foot of flooding for floodwater to recede (as assumed elsewhere in this study) plus one week to disassemble, clean, and dry motors, pumps, and other rotating equipment, and less time to clean and dry electrical equipment. During that time, if the water treatment plant is damaged, showers and toilets cannot be used in residences and occupants must relocate temporarily. They might stay in hotels, at a cost taken to be the GSA per diem for lodging (one room for a household of up to three people) plus the GSA per diem rate for meals and incidental expenses (one per person). It may be that people stay with friends or family or in a shelter at little or no cost, but economists still see the lost value as worth something. Residents would rather be at home, and the measure of that preference, in this case, is taken as the GSA per diem rates.

The project team also assumed that businesses cannot operate without functioning bathrooms. If a water treatment plant is inoperative, all businesses are similarly affected. Customers or employees cannot simply go next door. Nor are there likely to be portable toilets available for the entire community at a moment's notice. The analysis therefore assumes that without water, direct business interruption costs the state-average per-capita daily GDP. Indirect business interruption is taken as 0.5 times the total additional living expenses and direct business interruption loss, as elsewhere in this study.

The local GSA per diem rates for accommodations and for meals and incidental expenses are $115 and $59, respectively. The state per-capita daily GDP is $121.

***Casualties.*** As discussed elsewhere in this study, in flooding, the primary cause of death is due to people drowning when they try to drive through flooded areas. Casualty losses are therefore assumed to be zero in this case, and there seems to be no reason to suspect that PTSD would occur from temporary loss of potable water service.

***Historic losses.*** None seem to apply.

***Environmental losses.*** If the wastewater treatment plant floods, untreated wastewater would flow overland to the nearby Tar River, polluting the river as it passes nearby Washington, North Carolina, and 25 miles downstream into Pamlico Sound, part of the Cape Hatteras National Seashore. The pollution would impair the recreational value of Pamlico Sound for approximately one season. Whitehead et al. (2000) used revealed-preference data to value a recreational visit to Pamlico Sound at $64 per user in 2000 USD, or $95 per visit in 2018 USD. The National Park Service reports that 2.4 million people visit the Cape Hatteras National Seashore each year (National Park Service 2018). Thus, the environmental costs of polluting the national park can be estimated at $228 million. In addition, Pamlico Sound produces $20 million per year in commercial fishing (Sea Grant 2017). The project team therefore estimated the acceptable cost to avoid environmental losses associated with flooding of the wastewater treatment plant to be $248 million.

***Benefit-cost ratio.*** Considering the foregoing project-specific information presented here, the general procedures presented elsewhere in the study, a 100-year project life, and a cost-of-borrowing discount rate of 2.2%, the project team calculated that the project produced $212 million in benefit at a cost of $6.8 million, for an overall BCR of $31.00 saved per $1.00 invested, i.e., 31 to 1. The BCR is so high because it costs relatively little to build the flood-protection systems that protect a relatively large value. Most of the benefits are from reduced business interruption to the community, but environmental benefits are also significant, as shown in Figure 20. Using higher discount rates of 3% and 7%, the BCRs are lower: 28 and 13, respectively.

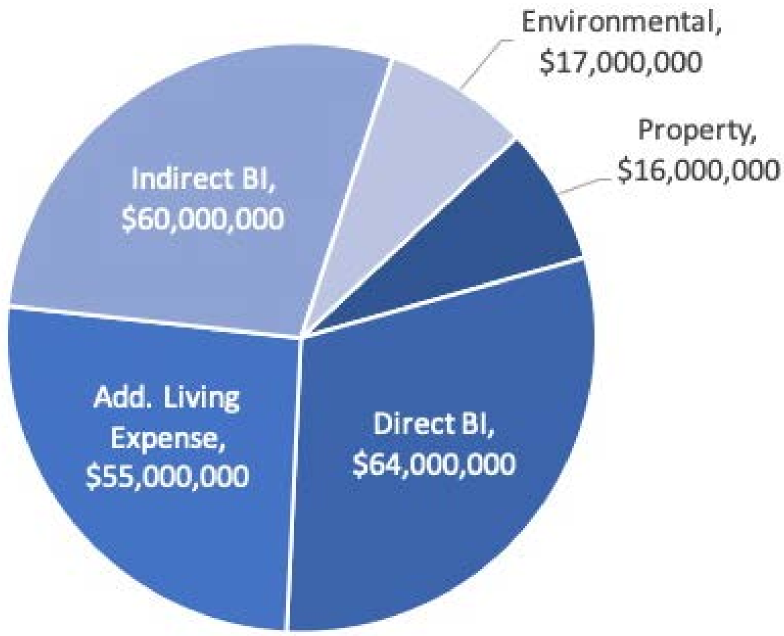


**Figure 20.** Estimated benefits from adding flood protection to the water and wastewater treatment plants in Greenville, North Carolina.

# 4 Flood Mitigation for Electric and Telecommunication Substation

***Summary of the grant.*** EDA, under its Economic Adjustment Assistance program, provided a grant in the amount of $1.8 million (2010 USD) to the city of Reedsburg, Wisconsin. Among its other products, the grant expended $235,000 to build a facility called a telecommunications/ electric switching station, essentially a dual-purpose telephone central office and control building for the adjacent substation yard. The building replaced an older building about 40 feet away but 4 feet lower in elevation. See Figure 21.


**Figure 21.** Electrical and telephone switching stations in Reedsburg, Wisconsin. The old one is to the right with the green cabinet next to it; the new one is to the left, behind the pickup truck.

***Flood hazard.*** A FEMA National Flood Hazard Layer FIRMette shows the old building at the elevation of the 100-year floodplain, 876 feet, and the new one at the elevation of the 500-year floodplain, 880 feet. The project team constructed a flood hazard curve that related depth of flooding to mean exceedance frequency with the common assumption that the natural logarithm of mean exceedance frequency varies linearly with flood elevation. Thus, for example, flooding reaches 878 feet (2 feet above the base of the old building and below the base of the new) with a mean exceedance frequency of 0.004.

***Direct damage to control building equipment.*** The Hazus Flood Model provides a vulnerability function for repair cost to low- and medium-voltage substation equipment. It also implies loss of function when the depth of flooding reaches 4 feet, which appears to apply to yard equipment, not the control building. It seems more reasonable to assume that the control building would become nonfunctional when initially flooded, because operators would deenergize equipment at that stage.

***Loss of use duration and costs.*** Hazus offers no estimate of flood duration or loss-of-use costs. The following analysis assumes that flooding lasts one day per foot of depth, plus one day to clear and reenergize equipment or to replace damaged computers and reinstall control software. It is assumed that loss of function affects all 9,200 inhabitants of Reedsburg. Without power or telecommunications, homes are still occupied, but residents must dine out at a cost (or equivalent value) equal to GSA's per diem rate of $51 per day per person. Insurers commonly call these costs additional living expenses. Without power and telecommunications, businesses do not operate at all (no telecommuting, for example), causing a direct business interruption loss of the Wisconsin per-capita daily GDP, $130. Elsewhere, the project team shows that indirect business interruption amounts to an additional $0.50 per $1.00 of direct business interruption losses and additional living expenses.

***Casualties.*** Elsewhere in this study the project team estimates that a blackout causes deaths at a rate of 0.56 per 100,000 population per day, and nonfatal medical injuries 50 times as high. It is not clear that loss of electricity alone causes PTSD, so no PTSD benefits apply to this project.

***Historic and environmental losses.*** None seem to apply.

***Benefit-cost ratio.*** Considering the foregoing project-specific information presented here, the general procedures presented elsewhere in the study, a 75-year project life, and a cost-of-borrowing discount rate of 2.2%, the project produces $2.2 million in benefit at a cost of $235,000, for an overall BCR of $9.40 saved per $1.00 invested, i.e., 9 to 1. Most of the benefits are from reduced business interruption to the community, as shown in Figure 22. Using higher discount rates of 3% and 7%, the BCRs are lower, 8 and 4, respectively, but still substantially above 1.0.

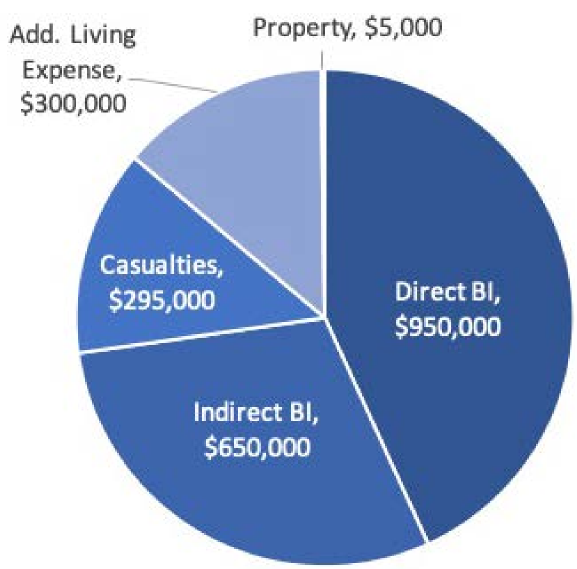


**Figure 22.** Estimated benefits from new telephone and electrical switching building in Reedsburg, Wisconsin.

# 5 Wind Mitigation for Electric and Telecommunications

EDA funded two grants that mitigated wind risk to electric and telecommunication facilities.

## 5.1 Summary of the Grants

***Project 1:*** Replacing aboveground power lines from Derby to West Charleston and Bloomfield to Canaan (both alignments in Vermont). The project description reported by EDA: i) Derby-to West Charleston – replacement of 5.25 miles of 46 kV transmission lines, and ii) Bloomfield to Canaan – replacement of 26 miles of 34.5 kV transmission lines with 520 poles. “The new electrical distribution system will provide more reliable electric service to the area and minimize disruptions to local business operations.”

The project team conducted online research for additional information about the project. Vermont Electric Coop reported that the replacement of aging, single-phase electric lines with three-phase lines would also help to improve the reliability of service to small businesses and farms.

***Project 2:*** Electric power line improvements to The Point, Seabrook, Texas. The project description reported by EDA: infrastructure improvements to The Point, including burying electrical power lines and other utilities in order to aid in disaster resiliency. This aid was provided by EDA in response to damage incurred during Hurricane Ike (2008). In addition to the EDA grant, the city of Seabrook also received a Community Development Block Grant (CDBG) grant awarded by the U.S. Department of Housing and Urban Development (HUD) but administered to the city through the state of Texas.

## 5.2 Methodology

The approach for this task consisted of the following steps: 1) utilize the online ASCE 7 Hazard Tool (ASCE 2018) to determine expected wind speeds for various mean recurrence intervals (MRI) and, in the case of the Vermont alignments, ice thickness; 2) research and select an existing wind damage model for aboveground power poles; 3) identify the exposure and inventory details of the different electric power distribution systems, i.e., confirm rural versus urban details, power pole installations (mainly distances between poles), confirm type of power pole (wooden versus metal), confirm rough power pole height details; 4) research loss estimation or loss avoidance methodologies for wind hazards; and 5) develop a spreadsheet to perform loss estimates (with and without mitigation) and subsequent BCRs.

***ASCE 7 Hazard Tool.*** For this project, the team utilized the ASCE 7 Hazard Tool to obtain wind speeds versus mean return interval for all projects. (The ASCE 7 look-up platform currently uses ASCE/SEI 7-16.) The platform requires the following input in order to return wind speed and ice thickness data: location (latitude and longitude) and risk category. For these grants, the team used the lowest risk, Category I: buildings and other structures that represent a low hazard to human life in the event of failure.

In both sets of projects (Vermont and Texas), the geographic extent of the areas of interest were small enough where the resolution of the ASCE 7 Hazards Tool was not very sensitive to the placement of the position cursor, e.g., the same set of wind speeds and MRIs were returned for both power system alignments in Vermont.

The wind speeds pertain to 3-second gust wind speeds at 33 ft above ground for Exposure Category C. Wind speeds versus MRI for both sets of projects (Vermont and Texas alignments) are contained in Table 3. Figure 23 shows a plot of annual frequency versus wind speed (mph) for the Vermont power distribution alignments.

| Mean recurrence interval (MRI) | Annual frequency ($yr^{-1}$) | Wind speed (mph) | |
|---|---|---|---|
| | | Vermont | Texas |
| 10 years | 0.1 | 73 | 78 |
| 25 years | 0.04 | 80 | 96 |
| 50 years | 0.02 | 84 | 110 |
| 100 years | 0.01 | 89 | 121 |
| 300 years | 0.003 | 99 | 134 |

**Table 3.** Wind speeds versus mean recurrence intervals for Vermont and Texas alignments.

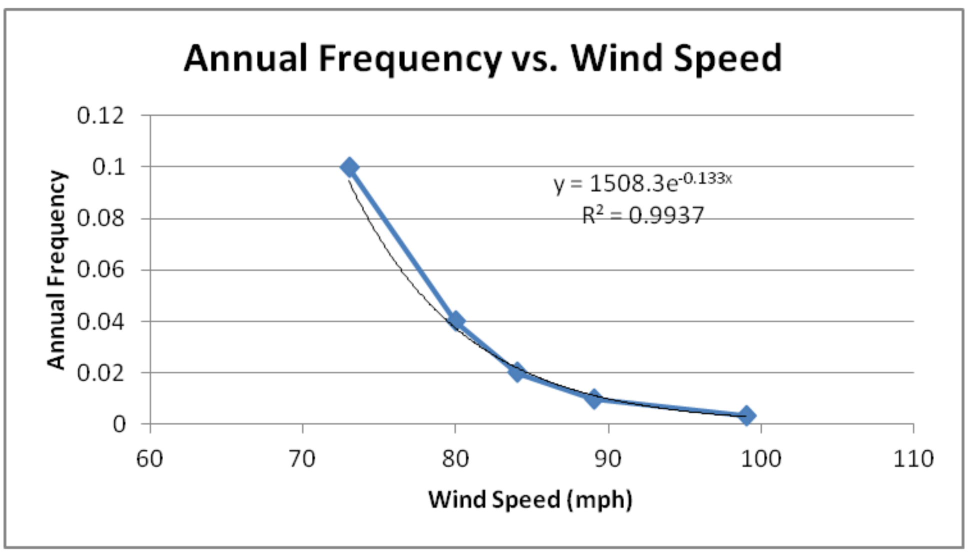


Note: x: wind speed, mph; y: exceedance frequency, events per year; $R^2$: coefficient of determination

**Figure 23.** Annual Frequency versus Wind Speed (mph) for Derby to West Charleston and Bloomfield to Canaan (all in Vermont).

For the Vermont alignments, the project team also extracted ice thickness information from the ASCE 7 Hazard Tool. Based on platform readings, the radial ice thickness value (in) is one (1) inch, which corresponds to a 50 mph, 3-second gust speed. The project team assumed that the MRI associated with this ice thickness value is 50 years.

***Wind damage function for aboveground electric power poles.*** The project team reviewed three publications in order to select an appropriate damage function for aboveground power poles.

- *Fragility Curves for Assessing the Resilience of Electricity Networks Constructed from an Extensive Fault Database* (Dunn et.al. 2018).

  Fragility curves are developed for overhead electrical lines using an empirical approach to model likely failures due to wind storm hazards. To generate these curves, the authors compiled a dataset of 12,000 electrical failures in the United Kingdom and correlated it with the European Reanalysis (ERA) wind storm model. The results are presented in terms of number of assets failed per km as a function of wind speed.

- *Age-Dependent Fragility Models of Utility Wood Poles in Power Distribution Networks against Extreme Wind Hazards* (Shafieezadeh et al. 2014).

  A sampling approach involving a demand and capacity model was used to generate a statistical sample of 20,000 faults that were randomly paired with wind velocity. Fragility models were generated for new wood poles, and poles that are 25, 50, 75, and 100 years old. The results are presented in the form of probabilities of failure as a function of wind velocity and ANSI pole class.

- *Effects of Adjacent Spans and Correlated Failure Events on System-Level Hurricane Reliability of Power Distribution Lines* (Darestani et al., 2017).

  This paper investigates the effects of environmental conditions that may impact the decay rate of wooden power poles and ultimately the impact on system reliability. The results are presented in terms of probability of failure versus 3-second gust wind speeds for a mean pole age of 30 years.

Based on the ease of use and the dependency on pole age, the project team decided to use the Shafieezadeh et al. (2014) fragility curve for modeling wind damage to aboveground power poles. See Figure 24.

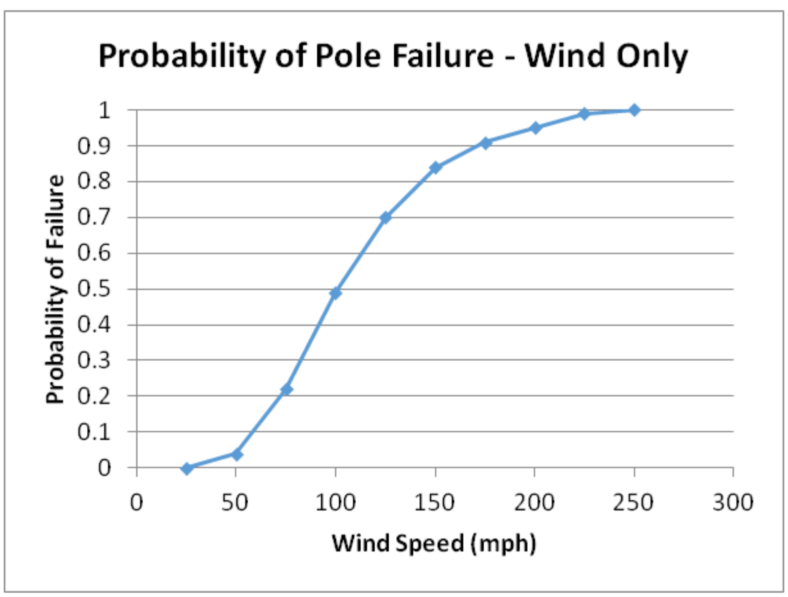


**Figure 24**. Power pole fragility model for wind effects (Shafieezadeh et al., 2014).

In order to estimate damage due to excessive ice loads, the project team used a model developed for the FEMA study, *Electrical Transmission and Distribution Mitigation: Loss Avoidance Study* (FEMA 2008). That study analyzed mitigation effectiveness of various measures as applied to power transmission and distribution lines in Nebraska and Kansas. For this effort, the project team adapted the methodology for loss avoidance presented in that study by substituting local wind hazard information and scaling some of the damage models presented in the FEMA study (more discussion below). The damage/pole failure model used in the FEMA study for ice hazards is a function of three parameters: the *National Electrical Safety Code* (NESC) (Grade N for older systems and Grade C or B for all new improvements); tree clearance (from zero: tree clearance exceeds 10 feet in all locations to three: tree clearance may be less than 10 feet at some locations), from 11 to 20 spans per miles of circuit; and radial ice index (from zero to three inches). In the FEMA report, for a condition that is associated with one inch radial ice thickness, NESC Grade N , and tree clearance index of 3, the probability of pole failure is 0.055. Based on the location of the Vermont alignments, this probability is associated with a MRI of 50 years. To scale ice thickness to different MRIs, the project team used the wind speed-MRI distribution provided by the ASCE 7 Hazard Tool.

***Loss avoidance calculation.*** To estimate projected losses based on wind and ice load hazards, the project team adopted the methodology presented in FEMA 2008. The methodology provides a stepwise calculation procedure that begins with an initial statement of exposure (i.e., rural versus urban, number of power poles, population) and hazard levels (ASCE 7). For many of the equations, FEMA 2008 references an earlier FEMA document (FEMA 2003), especially for quantifying ice load risks. For convenience, the calculation steps are reproduced below.

**Step 1:** Number of poles damaged:

$$N = \text{poles damaged} = P_f \times (\text{length of power lines in miles}) \times (\text{no. poles per mile})$$

**Step 2:** Number of wires damaged:

$$W = N \times 3 \text{ (for rural) or } N \times 6 \text{ (for urban)}$$

**Step 3**: Number of cross-arms damaged (pole does not require repair):

$$C = N \times 0.1$$

**Step 4:** Number of guy wires damaged:

$$G = N \times 0.01$$

**Step 5:** Number of pole-mounted transformers to be repaired:

$$T = N \times 0.2$$

**Step 6:** Hours by lineman in the field:

$$H = N \times 8 + W \times 2 + C \times 4 + G \times 4 + T \times 2$$

**Step 7:** Number of lineman available:

$$L = \text{population served} \times 0.005$$

**Step 8:** Estimate no. of days to complete restoration of service:

$$D100 = H / (12 \times L)$$

**Step 9:** Estimate losses based on FEMA (2003) unit costs: $7,502 to repair a damaged pole and $220 per person per day of lost service (costs have been scaled to 2018 costs)

## 5.3 Exposure or Inventory Information

**Vermont Alignments:**

| | Population at risk (source: 2010 Census) | Line Length (source: EDA report) | Poles per mile (source: FEMA 2003, 2008) |
|---|---|---|---|
| Derby to West Charleston | Total: 5,254<br>Derby: 4,613<br>West Charleston: 641 | 5.25 miles | 18, default for rural areas |
| Bloomfield to Canaan | Total: 3,680<br>Canaan: 972<br>West Stewartstown: 386<br>Colebrook: 1,394<br>Lemington: 104<br>Columbia: 603<br>Bloomfield: 221 | 26 miles | 20 |

**Table 4.** Exposure and inventory information for Project 1.

**Texas Alignments:**

| | Population at risk (source: 2010 Census) | Line Length (source: EDA report) | Poles per mile (source: FEMA 2003, 2008) |
|---|---|---|---|
| Seabrook, Texas | Total: 11,952 | 1,950 feet | 66 |

Notes: Power pole is a Class 5 (more narrow pole) and around 75 years old, based on age of Seabrook (roughly 60 years). Assume Risk Level 1 for power poles – lowest implemented. Distance between poles is 80 feet, based on measuring separation in several Google Street Views and Google Maps.

**Table 5.** Exposure and inventory information for Project 2.

## 5.4 Results for Vermont Alignments

To determine the total benefit of these pole replacements, the project team calculated, on an annualized basis, the avoided losses from wind and ice damage for both projects. This section presents the intermediate and final results from this analysis.

***Project 1: Vermont alignments***

Based on the EDA data, the project team assumed aboveground power line replacements from i) Derby to West Charleston—replacement of 5.25 miles of 46 kV transmission lines, and ii) Bloomfield to Canaan—replacement of 26 miles of 34.5 kV transmission lines with 520 poles.

i) Derby to West Charleston

Table 6 contains the mean pole failure probability ($P_f$) from wind and ice damage as a function of wind speed. The table contains both the conditional probability of failure and the probability of failure weighted by wind speed probability ($P_{ws}$), that is

$$P_f = P_{f\,|WS} \times P_{WS},$$

where WS is wind speed (mph).

| Wind speed (mph) | $P_{f\,\vert WS}$ | $P_{WS}$ | $P_f$ |
|---|---|---|---|
| 10 | 0.024 | - | - |
| 30 | 0.073 | - | - |
| 50 | 0.122 | 0.484 | 0.059 |
| 70 | 0.170 | 0.480 | 0.082 |
| 90 | 0.219 | 0.034 | 0.007 |

**Table 6**. Pole failure probabilities (Derby to West Charleston alignment).

After calculating the pole failure probability, the project team followed the procedure presented above to produce an annual loss estimate. The calculation process begins by first estimating the total number of damaged components (N). Table 7 lists the values at each step of the calculation for the Derby to West Charleston power distribution alignment.

| | Damage parameters | | | | | | |
|---|---|---|---|---|---|---|---|
| Wind speed (mph) | $P_f$ | N | W | C | G | T | H |
| 10 | - | - | - | - | - | - | - |
| 30 | - | - | - | - | - | - | - |
| 50 | 0.059 | 5.563 | 16.688 | 0.556 | 0.056 | 1.113 | 82.55 |
| 70 | 0.082 | 7.728 | 23.184 | 0.773 | 0.077 | 1.546 | 114.68 |
| 90 | 0.007 | 0.695 | 2.085 | 0.070 | 0.007 | 0.139 | 10.31 |

**Table 7.** Damage (Derby to West Charleston alignment).

The project team estimated the number of linemen available to work on repairs in Step 7 as outlined in Section 2.4.2. Based on the total population at risk for the service area (5,2,54), the total number of linemen available for repairs is 5,254 × 0.005 = 26.

Table 8 shows the number of days until 100% service is restored ($D_{100}$). The FEMA (2008) methodology assumes that in these emergency repair situations, linemen will work shifts of 12 hours per day, 7 days per week until all service is restored.

| Wind speed (mph) | $D_{100}$ (days) |
|---|---|
| 10 | - |
| 30 | - |
| 50 | 0.26 |
| 70 | 0.36 |
| 90 | 0.03 |

**Table 8.** Days to full service restoration (Derby to West Charleston alignment).

The expected loss based on pole damage/failure is the sum of the total repair cost plus the cost that is incurred because of power disruption. As indicated in Table 3, $7,502 is used to reflect the cost to repair a damaged pole and $220 per person per day is assumed to cover loss of service. Both numbers have been scaled up to 2018 to reflect inflation increases. Table 9 lists each loss type by wind speed. The sum of all losses over all wind speeds is the expected annualized loss (EAL) for the project.

| Wind speed (mph) | Physical damage ($) | Loss of function ($) | Loss ($) |
|---|---|---|---|
| 10 | - | - | - |
| 30 | - | - | - |
| 50 | 41,731 | 372,849 | 414,580 |
| 70 | 57,976 | 517,989 | 575,964 |
| 90 | 5,214 | 46,584 | 51,798 |
| Expected annualized loss | 104,921 | 937,422 | 1,042,343 |

**Table 9.** EAL from wind and ice damage to poles (Derby to West Charleston alignment).

ii) Bloomfield to Canaan

Table 10 presents the mean pole failure probability (wind and ice hazards) for power lines between Bloomfield and Canaan.

| Wind speed (mph) | $P_{f\,\vert WS}$ | $P_{WS}$ | $P_f$ |
|---|---|---|---|
| 10 | 0.0110 | - | - |
| 30 | 0.0330 | - | - |
| 50 | 0.0550 | 0.5462 | 0.0300 |
| 70 | 0.0770 | 0.4194 | 0.0323 |
| 90 | 0.0990 | 0.0318 | 0.0031 |

**Table 10.** Pole failure probabilities (Bloomfield to Canaan alignment).

Table 11 shows the damage calculation values for the Bloomfield to Canaan alignment. Because of the longer length of this alignment compared to the Derby to West Charleston line, the damage calculation values are higher by a factor of at least two.

| | Damage parameters | | | | | | |
|---|---|---|---|---|---|---|---|
| Wind speed (mph) | $P_f$ | N | W | C | G | T | H |
| 10 | - | - | - | - | - | - | - |
| 30 | - | - | - | - | - | - | - |
| 50 | 0.030 | 15.622 | 46.866 | 1.562 | 0.156 | 3.124 | 231.83 |
| 70 | 0.032 | 16.793 | 50.378 | 1.679 | 0.168 | 3.359 | 249.20 |
| 90 | 0.003 | 1.636 | 4.908 | 0.164 | 0.016 | 0.327 | 24.28 |

**Table 11**. Damage (Bloomfield to Canaan alignment).

The total number of linemen available for repairs, based on a population of 3,680, is estimated at

Number of linemen: $3{,}680 \times 0.005 = 18.4$

Table 12 presents the total number of days until 100% of service is restored. Table 13 provides the total EAL.

| Wind speed (mph) | $D_{100}$ (days) |
|---|---|
| 10 | - |
| 30 | - |
| 50 | 1.05 |
| 70 | 1.13 |
| 90 | 0.11 |

**Table 12.** Number of days to full service restoration (Bloomfield to Canaan alignment).

| Wind speed (mph) | Physical damage ($) | Loss of function ($) | Loss ($) |
|---|---|---|---|
| 10 | - | - | - |
| 30 | - | - | - |
| 50 | 117,196 | 1,047,094 | 1,164,290 |
| 70 | 125,978 | 1,125,561 | 1,251,539 |
| 90 | 12,273 | 109,656 | 121,930 |
| Expected annualized loss | 255,447 | 2,282,312 | 2,537,759 |

**Table 13**. EALs due to wind and ice damage to poles (Bloomfield to Canaan alignment).

Table 14 lists the total EAL for Project 1 (Derby to West Charleston and Bloomfield to Canaan).

| Community | Physical damage ($) | Loss of function ($) | Total ($) |
|---|---|---|---|
| Canaan to Bloomfield | 255,447 | 2,282,312 | 2,537,759 |
| Derby to West Charleston | 104,921 | 937,422 | 1,042,343 |
| Expected annualized loss | 360,367 | 3,219,735 | 3,580,102 |

**Table 14.** Total EAL for Project 1 by loss type.

***Benefit-cost ratios.*** Table 15 presents the BCR for Project 1 (undergrounding Vermont alignments) for four different time horizons (25, 50, 75, and 100 years). The assumption here is that relocating power lines below ground will eliminate any wind or ice load hazards, and thus, the calculated annual losses will be zero. This analysis did not consider any new hazards that may affect the lines while buried, e.g., land movement, flooding, construction, etc. The project team used the discount rate of 2.2% in this analysis to discount future benefits (the rate used for other projects in the overall study). Therefore, the benefits presented in Table 14 are the losses avoided over the specified time period or horizon. Table 15 presents the BCR by time horizon, based on the benefits calculated and the original project cost (extracted from the EDA grant information), which is $17,228,894.

| Time horizon | Benefit | BCR |
|---|---|---|
| 25 years | $71,862,364 | 4.17 |
| 50 years | $111,493,407 | 6.47 |
| 75 years | $134,495,275 | 7.81 |
| 100 years | $147,439,304 | 8.56 |

**Table 15.** BCRs for undergrounding Vermont alignments, by time horizon.

## 5.5 Results for Seabrook, Texas Alignment

The Texas project involved infrastructure improvements at The Point in Seabrook, Texas, including the burial of electrical power lines and other utilities in order to aid in disaster resiliency. Table 16 presents the pole failure probabilities (mainly from wind effects).

| Wind speed (mph) | $P_{f\|WS}$ | $P_{WS}$ | $P_f$ |
|---|---|---|---|
| 25 | 0 | - | - |
| 50 | 0.04 | 0.712 | 0.028 |
| 75 | 0.22 | 0.222 | 0.049 |
| 100 | 0.49 | 0.051 | 0.025 |
| 125 | 0.7 | 0.012 | 0.008 |
| 150 | 0.84 | 0.003 | 0.002 |
| 175 | 0.91 | 0.001 | 0.001 |
| 200 | 0.95 | 1.4E-04 | 1.3E-04 |
| 225 | 0.99 | 3.2E-05 | 3.2E-05 |
| 250 | 1 | 7.3E-06 | 7.3E-06 |

**Table 16**. Pole failure probabilities (Seabrook, Texas alignment).

Table 17 contains the damage calculated using the steps outlined in Section 2.4.2 of the *2017 Interim Report*. Since the wind hazard is more significant in this area, the range of possible wind speeds and their probabilities of occurrence (and the impact on the damage parameters) is much broader than in the Vermont case.

| | Damage parameters | | | | | | |
|---|---|---|---|---|---|---|---|
| Wind speed (mph) | $P_f$ | N | W | C | G | T | H |
| 25 | - | - | - | - | - | - | - |
| 50 | 0.028 | 0.694 | 2.082 | 0.069 | 0.007 | 0.139 | 10.30 |
| 75 | 0.049 | 1.192 | 3.576 | 0.119 | 0.012 | 0.238 | 17.69 |
| 100 | 0.025 | 0.607 | 1.822 | 0.061 | 0.006 | 0.121 | 9.01 |
| 125 | 0.008 | 0.199 | 0.596 | 0.020 | 0.002 | 0.040 | 2.95 |
| 150 | 0.002 | 0.054 | 0.163 | 0.005 | 0.001 | 0.011 | 0.81 |
| 175 | 0.001 | 0.014 | 0.041 | 0.001 | 1.4E-04 | 0.003 | 0.20 |
| 200 | 1.3E-04 | 0.003 | 0.010 | 3.2E-04 | 3.2E-05 | 0.001 | 0.05 |
| 225 | 3.2E-05 | 0.001 | 0.002 | 7.7E-05 | 7.7E-06 | 1.5E-04 | 0.01 |

**Table 17**. Damage (Seabrook, Texas alignment).

Based on a total population at risk of 11,952, the number of linemen available to participate in the repair effort is estimated as 11,952 × 0.005 = 59.76.

Table 18 shows the number of days required to completely restore service ($D_{100}$) for different wind speeds. As in the Vermont case, the project team assumed that linemen will work 12 hours per day, 7 days per week until all service is restored.

| Wind speed (mph) | $D_{100}$ (days) |
|---|---|
| 25 | - |
| 50 | 0.014 |
| 75 | 0.025 |
| 100 | 0.013 |
| 125 | 0.004 |
| 150 | 0.001 |
| 175 | 2.8E-04 |
| 200 | 6.7E-05 |
| 225 | 1.6E-05 |

**Table 18**. Days to full restoration (Seabrook, Texas alignment).

Using the same unit cost values as in the Vermont case, Table 19 lists the expected losses by type and by wind speed.

| Wind speed (mph) | Physical damage ($) | Loss of function ($) | Total loss ($) |
|---|---|---|---|
| 25 | - | - | - |
| 50 | 5,206 | 46,512 | 51,718 |
| 75 | 8,943 | 79,899 | 88,842 |
| 100 | 4,557 | 40,713 | 45,270 |
| 125 | 1,489 | 13,306 | 14,795 |
| 150 | 409 | 3,653 | 4,062 |
| 175 | 101 | 905 | 1,007 |
| 200 | 24 | 216 | 240 |
| 225 | 6 | 52 | 57 |
| Expected annualized loss | 20,735 | 185,256 | 205,991 |

**Table 19**. EALs from wind damage to poles (Seabrook, Texas alignment).

***Benefit-cost ratios.*** Table 20 presents the total benefits and BCR for each time horizon. A 2.2% discount rate has been assumed; the total project cost (as recorded by the EDA grant package) is $3,668,691.

| Time horizon | Benefit | BCR |
|---|---|---|
| 25 years | 4,134,794 | 4.13 |
| 50 years | 6,415,072 | 6.41 |
| 75 years | 7,738,546 | 7.73 |
| 100 years | 8,483,315 | 8.47 |

**Table 20.** BCRs for undergrounding by time horizon (Seabrook, Texas alignment).

## 5.6 Conclusions and Limitations

The calculations of future benefits over varying time horizons suggest that the mitigation measures undertaken in the EDA projects (i.e., burying electric power distribution lines) are highly cost effective even for short time horizons (25 years). That is, the return on investment (in the form of avoided losses) is highly likely given the measures that have been taken and the projected risks of hazard occurrence.

In this study, the project team did not explore new risks that may have emerged as a result of burying these distribution lines. For example, there may be new risks from local flooding, land movement caused by settlement or landslides, or construction accidents. However, it is assumed that any of these new risks would be significantly smaller than those that have been mitigated (wind and ice) and, therefore, would be negligible.

# 6 Benefit-Cost Analysis of a Resilient Water Supply Grid

## 6.1 Introduction

As part of its research, the project team examined the benefits and costs of implementing a resilient grid in an urban water supply network; that is, whether it is cost effective to improve network resilience by reducing the vulnerability or otherwise improving all or some trunk lines, thereby forming a *resilient grid* (Davis 2017). Specifically, the project team assumed the stress event affecting the network would be an earthquake. Figure 25 shows a schematic network. The figure shows that a transmission line brings raw water from the source (in the figure, a reservoir) to a treatment plant. Treated water is conveyed to terminal reservoirs and then the distribution network. Within the distribution network, trunk lines convey water to distribution lines. Some or all of the trunk lines can form the resilient grid. In most U.S. cities, the distribution piping often has diameters of 6 or 8 inches. Trunk lines typically have diameters between 12 and 24 inches. Because of topography and other geographic features, as well as historical development, water distribution networks in actual cities each have their own peculiarities. Therefore, to draw general conclusions for cities in high seismic hazard locations, rather than examining a particular real system, the project team examined an idealized water supply network that seems generally representative of a medium-sized U.S. city.

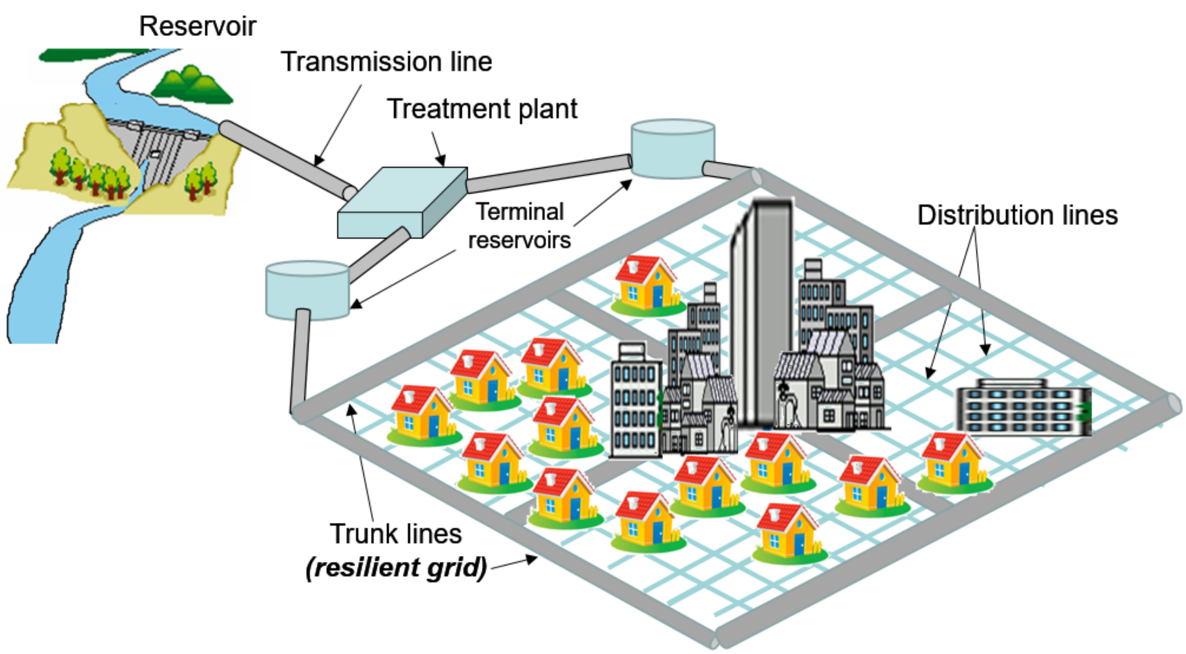


**Figure 25**. Schematic of water supply network.

The project team used a three-phased approach for this study:

1. In Phase 1, the team examined various configurations of distribution and trunk lines to arrive at a water supply network or grid representative of a medium-sized U.S. city (the study region). The region is supplied from a water source outside the region via two

transmission lines supplying two terminal reservoirs, a grid of larger trunk lines, and a network of smaller distribution pipes. The region is square-symmetric to eliminate bottlenecks or other complicating factors. The size and spacing of distribution pipes and trunk lines were selected so as to provide typical average day demands, including ordinary fire flows. The ordinary fire flows are two 5,000 gpm demands. The project team termed this network the *as-is network*.

2. In Phase 2, the project team stressed the as-is network with random breaks and leaks resulting from earthquake excitation, together with extraordinary fire demands associated with the phenomenon of fire following earthquake. (Other natural hazards can also increase demand on a water supply system. Tsunamis, for example, can also ignite fires and increase demands for firefighting water supply.) Under earthquake excitation, the as-is system can experience damage-associated costs of repairs, as well as a shortfall of supply; that is, insufficient water pressure to continue serving all its customers and to provide firefighting water supply. The shortfall results because the system was not designed with such disasters in mind. This shortfall then has consequences in terms of loss of service, leading to larger fires and more time to recover.
3. In Phase 3, the project team improved the as-is system to form a resilient grid. The improvement consists of replacing trunk lines (only) with lower-vulnerability pipe, that is, pipe that experiences less damage when subjected to earthquake excitation. For example, one might replace cast iron or asbestos cement trunk lines with earthquake-resistant ductile iron pipe (ERDIP). The project team then determined the shortfall and resulting consequences of this resilient grid system, stressed with the same scenario, and compared them with those of the as-is system.

The difference in loss of service, fire size, time to recovery, and costs between the as-is and resilient grids is a measure of the benefit of the resilient grid. Benefits include reduced losses in several categories:

- Water-system repair costs
- Fire-related property losses
- Direct business interruption losses associated with loss of water service and fire damage
- Indirect business interruption losses to the rest of the economy that does business with customers who lose water service or suffer fire damage
- Deaths, injuries, and instances of PTSD resulting from fire following earthquake

The project team converted the benefits to equivalent dollar amounts. In the case of deaths, nonfatal injuries, and PTSD, dollar amounts are assigned as in the *2017 Interim Report*.

Note that the benefits shown are not exhaustive. They are the ones that can be readily quantified and monetized. Mitigation produces other intangible benefits that are not considered here, such as prevention of loss of heirlooms, pets, etc.

The project team estimated the benefit per year by integrating benefits with frequency of hazard. The team estimated the present value of benefits over a time horizon by applying a discount rate equal to the real cost of borrowing. The present value of benefits divided by cost is the BCR for the resilient grid.

## 6.2 Analytical Method

### 6.2.1 Selecting a Characteristic Study Region

To develop a study region representative of a medium-sized U.S. city, the project team compiled data for all U.S. cities with 2016 (est.) populations greater than 100,000, as shown in Figure 26, which encompass a total population of 93 million. Because of the decreasing ratio of repair resources with increasingly larger populations, the issue of resilient grids is more important the larger the city. Therefore, the initial focus of this study is on larger cities. For this purpose, the project team examined the 50 largest cities, as shown in Figure 27, which encompass a total population of 50 million. The mean population of these 50 largest cities is 998,000 and the median population is 646,000, so a study area with population on the order of 750,000 persons was deemed representative of large U.S. cities.

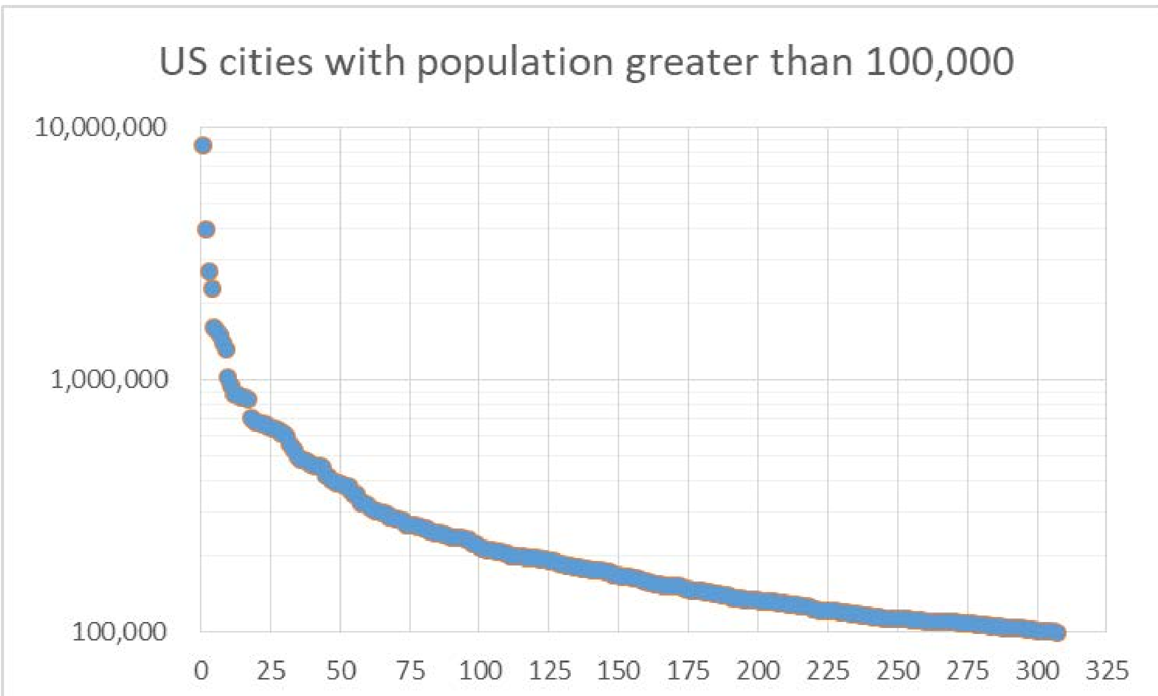


Data source: U.S. Census Bureau (2018).

**Figure 26.** Frequency plot of U.S. cities with population greater than 100,000.

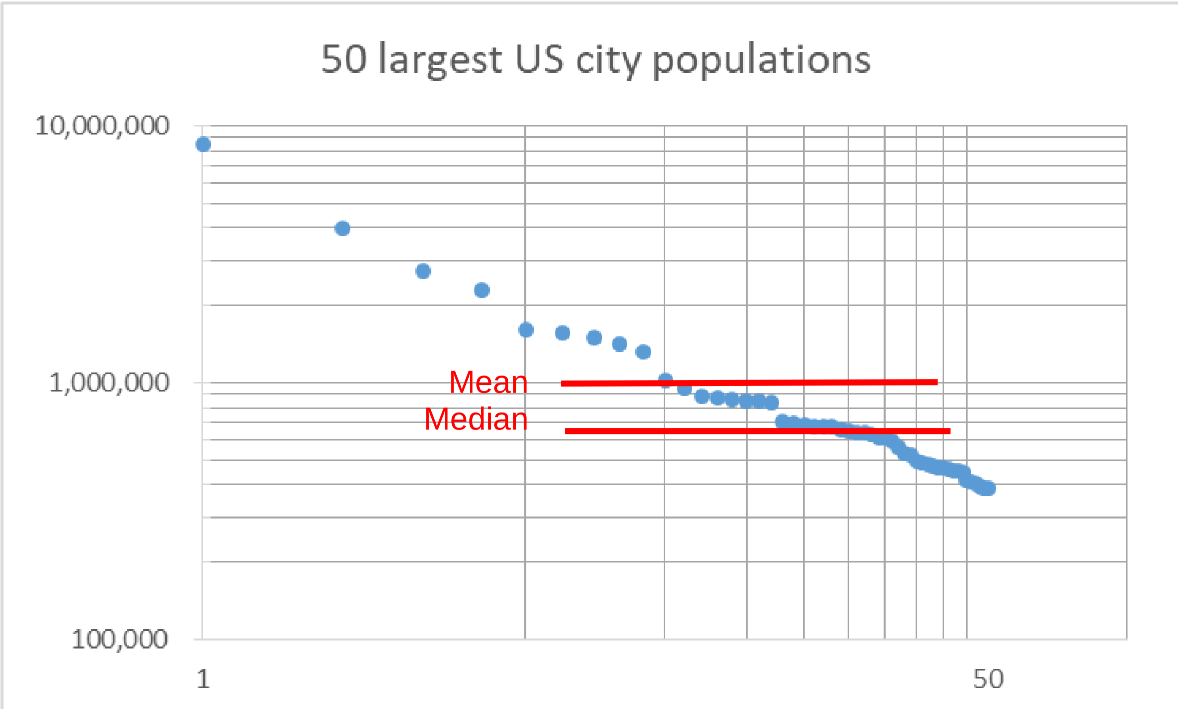


Data source: U.S. Census Bureau (2018).

**Figure 27**. Distribution of 50 largest U.S. city populations, mean (998,000) and median (646,000).

### 6.2.2 Initial Configuration

The project team selected a square grid *b* × *b* blocks, each block being *L* (feet) square, as shown in Figure 28, as representative of a city of about a 750,000 population. The study grid is intended to be representative of the distribution system of a medium-sized city. The grid consists of *b* + 1 lines of north-south and east-west distribution pipes at regular *L* spacing (depicted as gray lines). Specific values were *b* = 60 and *L* = 600 feet. The grid consists of 61 lines of north-south and 61 lines of east-west distribution pipes regularly spaced at *L* (depicted as gray lines), so that the grid is 36,000 ft (6.82 miles) on a side with an area of 46.5 square miles. Trunk lines of the resilient grid are placed every *n* distribution pipes (depicted by bold blue lines in the figure as every 5th distribution pipe, or a grid of 3,000 ft). The source is to the south of the grid, which supplies two terminal reservoirs placed symmetrically in the east and west parts of the city via transmission lines (in red – the transmission lines are not part of the model). The distribution grid is not connected to the trunk grid except at intersections of the trunk grid. Table 21 lists all parameters.

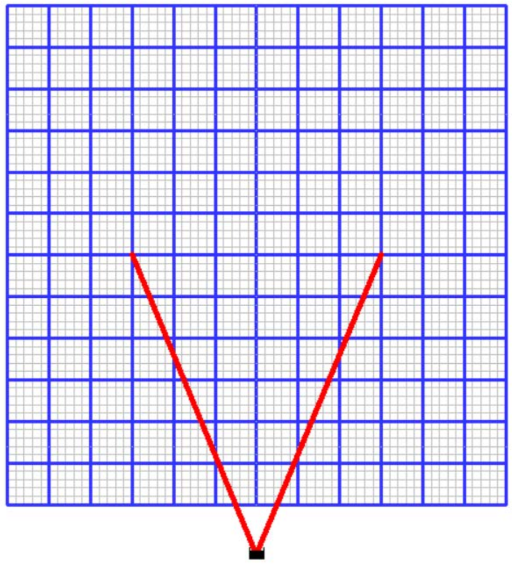

**Figure 28.** Study grid.

| Symbol | Parameter | Value |
|---|---|---|
| $A_{cont}$ | Additional replacement value for contents | 50% |
| $B$ | No. of blocks | 60 |
| $B\ pa$ | Benefits per annum | To be solved for |
| $BCR$ | Benefit-cost ratio | To be solved for |
| $B_{LF}$ | Buildings per large fire | 312.5 (derived) |
| $C$ | Per capita water consumption (gallons per day) | 90 |
| $C$ | Project cost per inch-diam. per ft. of installed pipe | $50 |
| $C_{bldg}$ | Replacement cost for buildings | $200 per sq. ft. |
| $C_{cust}$ | Cost to customers | To be solved for |
| $C_{HI}$ | Value lost or cost of human injury | To be solved for |
| $C_{los}$ | Cost of loss of service per day per service connection | $720 |
| $C_{morb}$ | Value lost due to an injury | $0.55 million |
| $C_{mort}$ | Value lost due to a fatality | $9.4 million |
| $C_{prop}$ | Replacement cost for buildings and contents | A variable |
| $C_{PTSDpc}$ | Value lost or cost of PTSD, per person | $33,750 |
| $C_{PTSDpLF}$ | Value lost or cost of PTSD, per large fire | To be solved for |
| $Cr$ | Cost of labor for repairs (dollars per hour per worker | $100 per hour |
| $C_{rep}$ | Cost of repairs | $= C_{utility} + C_{cust}$ |
| $C_{rep/hr}$ | Cost of repair per hour | $= F_{repMatls} \times C_{repLabor}$ |
| $C_{repLabor}$ | Labor cost per hour for repairs, 4 pers. crew | $400 |

| Symbol | Parameter | Value |
|---|---|---|
| $C_{utility}$ | Cost to utility | To be solved for |
| *D* | Distribution pipe diameter (inches) | Varied; *d* = 6" finally employed |
| $D_c$ | No. of days required to complete all repairs | To be solved for |
| *EOD* | Equivalent orifice diameter | $EOD = d \times (0.5d^{-0.155})$ |
| *FD* | Normal fire demand on the system (gpm) | 10,000 |
| *FFi* | Fire flow initial (gpm) | 3,000 |
| $f_{morb}$ | Nonfatal injuries per million dollars of property loss | 1.73 |
| $f_{mort}$ | Fatalities per million dollars of property loss | 0.36 |
| $F_{repMatls}$ | Factor on labor for materials and equipment | 30% |
| *H* | No. of households (HH) per block | 62.5 |
| $H_{day}$ | No. of hours per day worked by crews | 12 |
| *Igns* | Number of ignitions | A variable |
| $K_1$ | A factor to account for pipe material | Varies by material |
| *L* | Length of a block (ft.) | 600 |
| *MMI* | Modified Mercalli Intensity | VI~IX (denoted 6~9) |
| *N* | Interval of trunk lines vis-à-vis distribution lines | Varied; *n* = 10 finally employed |
| $N_{dr}$ | No. of distribution repairs | To be solved for |
| *NFE* | Number of fire engines = *f(P)* | 45 |
| $N_{tr}$ | No. of trunk line repairs | To be solved for |
| $N_{tr}$ | Total number of repairs to trunk lines | To be solved for |
| *P* | No. of persons per HH | 3.5 |
| *P* | Residential population in thousands | 787,500 |
| *PGA* | Peak ground acceleration (g) | A variable |
| *PGD* | Permanent ground deformation | A variable |
| $P_{LF}$ | Population per large fire | 1,084 (derived) |
| *PTSD* | Post-traumatic stress disorder | An acronym |
| *PV(B)* | Present value of all future benefits | To be solved for |
| $R_d$ | Crew-hours for distribution line repair | 7.6 |
| *RR* | Repair rate | A variable |
| $R_t$ | Crew-hours for trunk line repair | 16.1 |
| $T_{crew}$ | Total no. of repair crews employed by a system | $B^2h$/10,000 |
| *TFA* | Total floor area (sq. ft.) | 504 million |
| $TFA_{LF}$ | Total floor area per large fire, sq. ft. | 700,000 sq. ft. (derived) |
| *TFApc* | Average total floor area per capita (sq. ft. pc) | 640 |
| $T_{ma}$ | Mutual aid crew increase per day | 20% |

| Symbol | Parameter | Value |
|---|---|---|
| $T_{max}$ | Upper limit of $(1+ T_{ma})^{Dc}$ | 2 |
| WP | Wave propagation | An acronym |
| $Z$ | Reservoir head above grid (ft.) | 300 |

**Table 21.** Parameters and acronyms used in the study and their values.

Trunk lines are placed every *n* distribution pipes (depicted by bold blue lines in the figure as $n$ = 5 or every 5th distribution pipe, or a trunk grid of 3,000 ft). The source is to the south of the grid and supplies two terminal reservoirs placed symmetrically in the east and west parts of the city via transmission lines (shown in red – the transmission lines' vulnerability is not considered in the model). The distribution grid is connected to the trunk grid only at intersections of the trunk grid. Both grids are assumed to be at 0 feet elevation connected to the terminal reservoirs at *Z* (feet) elevation with negligible head loss from each reservoir to the connection to the trunk line intersection. That is, an unlimited amount of water is delivered at two locations to the trunk and distribution grids, at a head of $Z$ = 300 feet, equivalent to 130 psi pressure, prior to any frictional losses.

Each block has *h* households (HH) with one service connection per household and $p$ = 3.5 persons per HH[4], so that there are $b^2h$ = 225,000 service connections for a total population of $b^2hp$ = 787,500, a value which is between the median and mean of the 50 largest U.S. cities. Based on data shown in Figure 29 for 2005-2010 for selected U.S. cities (Kenny and Juracek 2012), a value of $c$ = 90 gallons per day (gpd) per capita for domestic water use was employed in this study.

The as-is network consists of two grids: (a) the distribution grid of fixed spacing *bL* and a diameter to be determined in Phase 1, and (b) the trunk line grid whose diameter and spacing is also determined in Phase 1. The pipe material in the as-is grid is assumed to be 50% cast iron and 50% ductile iron. The distribution and trunk line grids are hydraulically connected at all of their respective intersections, and the two grids are connected at each trunk line intersection.

[4] The 2017 U.S. national average population per household is 2.77 (https://www.census.gov/quickfacts/fact/table/US/PST045217). The value of 3.5 reflects urban daytime population—see McKenzie et al. (2010).

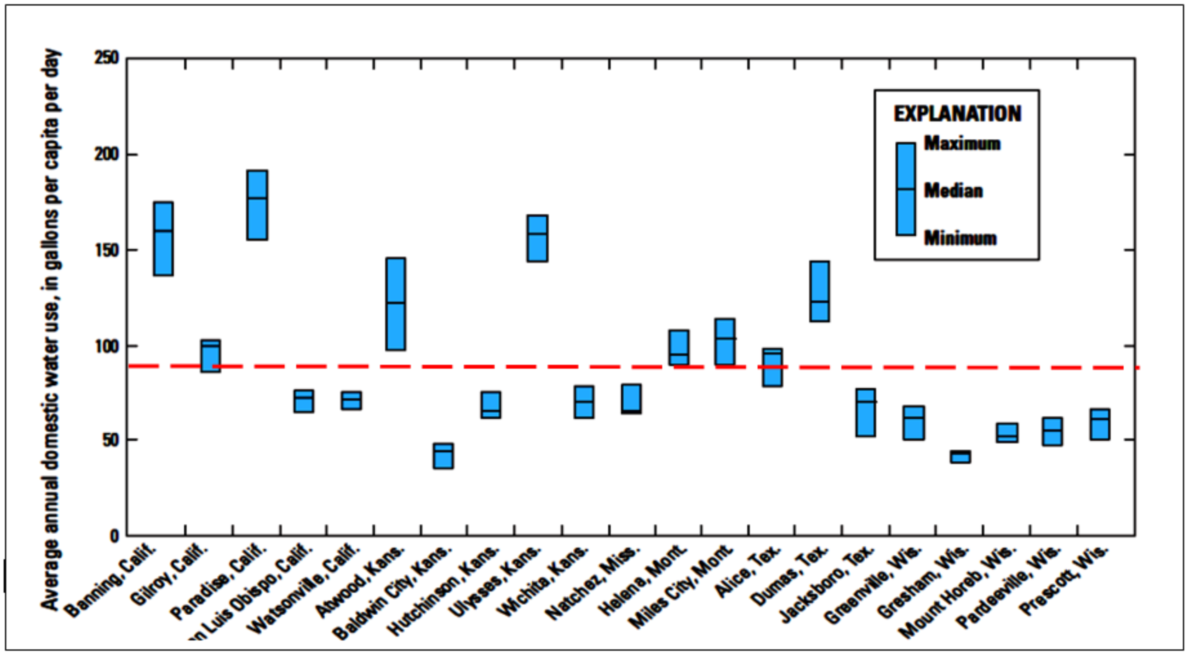


Note: Dashed red lines = 90 gpd per capita, employed in this study. (Kenny and Juracek 2012).

**Figure 29.** Data on 2005-2010 domestic water use for selected U.S. cities.

### 6.2.3 Hydraulic Analysis and Sizing

The network (i.e., the two interconnected sub-grids) was hydraulically modeled using EPANET (Rossman 2000) in a pressure-driven analysis (PDA) mode, with one demand per one node for each block; that is, the target demand per block is $h \times p \times c$ = 19,687 gpd = 13.67 gpm per node/block, with a target nodal pressure of 70 psi and a minimum acceptable pressure of 20 psi[5]. Thus, the total target service connection demands on the system are $h \times p \times c \times b^2$ = 13.67 × 3600 = 49,212 gpm = 70.865 million gallons per day (mgd). Added to this is a normal fire demand *FD* consisting of two fires each requiring 5,000 gpm or a total of 10,000 gpm. Thus, the total demand on the as-is system is 59,212 gpm.

There are an infinite number of ways to configure the two grids to meet these targets. System design is usually accomplished as a cost-minimization problem subject to the constraints of acceptable flow and pressure, as well as practical considerations, i.e., that distribution pipes are typically 6-inch or 8-inch in diameter and trunk lines are 12 inches to 16 inches in diameter. Cost *C* was treated here as project cost per inch-diameter per foot of installed pipe[6], including all valves, hydrants, and other appurtenances. Project cost means all engineering, overhead, contingency, and other costs are included. Costs for installation of new ductile iron water supply pipe mains vary dramatically, because of factors such as the size of the project; whether the pipe

[5] The values of 20 and 70 psi were determined based on discussions with several system operators. The lower value is the minimum acceptable pressure for firefighting water supply, and the higher acceptable value is the maximum pressure in mains supplying residences. A somewhat lower value (40~60 psi) may be more typical, but the higher value of 70 psi was employed knowing that the system would be subjected to numerous leaks.
[6] "per inch-foot" is a common rule of thumb for estimating installed pipe cost. If the cost is $10 per inch-foot, then an 8" pipe costs $80 per foot installed, and a 20" pipe $200 per foot installed.

is being installed in a new development or is replacing existing pipe already in service; regional variations in labor costs; the constraints imposed by season and weather; costs associated with rerouting traffic; joint type; overhead burden; and many other factors. Discussions with system operators in California and a review of recent cost data from Arkansas, Ohio, and North Carolina found a range of costs of \$10 to \$100 per inch-foot, with so-called soft costs, such as engineering and project management, ranging from 30% to extremes of 100%. Given this wide variation, this study employed an installed pipe cost where $C$ = \$50 per inch-foot If a reader feels that a different cost is more appropriate for a specific application (say \$20 per inch-foot) the costs can simply be multiplied by the ratio (i.e., 0.4).

#### 6.2.4 As-Is Design and Validation

Given the above parameters, a least-cost network configuration can be determined. The project team started with Case 1, which consisted of all distribution pipes being 6 inches in diameter and no trunk lines, as shown in Figure 30. Using $C$ = \$50 per inch-foot, this proposed system has a replacement value of $2dbLC(b + 1)$ = \$1.32 billion. This is the total of the costs of installing the distribution grid and the trunk line grid, in this case the latter being zero. However, hydraulic analysis shows this configuration is unable to furnish adequate pressure almost anywhere, so the project team rejected it.

Cases 2 through 9 are shown in Figure 31 through Figure 37 and are summarized in Table 22, from which it can be seen that Case 5, consisting of a distribution grid of 6-inch diameter pipe with a trunk line grid of 16-inch pipe every $10^{th}$ distribution pipe, is the least-cost solution (at \$1.72 billion) that satisfies the target goals with a median nodal pressure of 55 psi (with 2 × 5,000 gpm fire flows) and 73 psi (no fire flows), as Case 5A shows in Figure 38. Case 5 has a total of 4.9 million feet of pipe (927 miles), consisting of 4.39 million feet (831 miles, 89.7% of all lengths) of 6-inch distribution pipe and 504,000 feet (96 miles, 10.3%) of 16-inch trunk line pipe. This as-is system has a replacement value of \$1.32 billion for the distribution system and \$403 million for the trunk line system, or a total of \$1.72 billion.

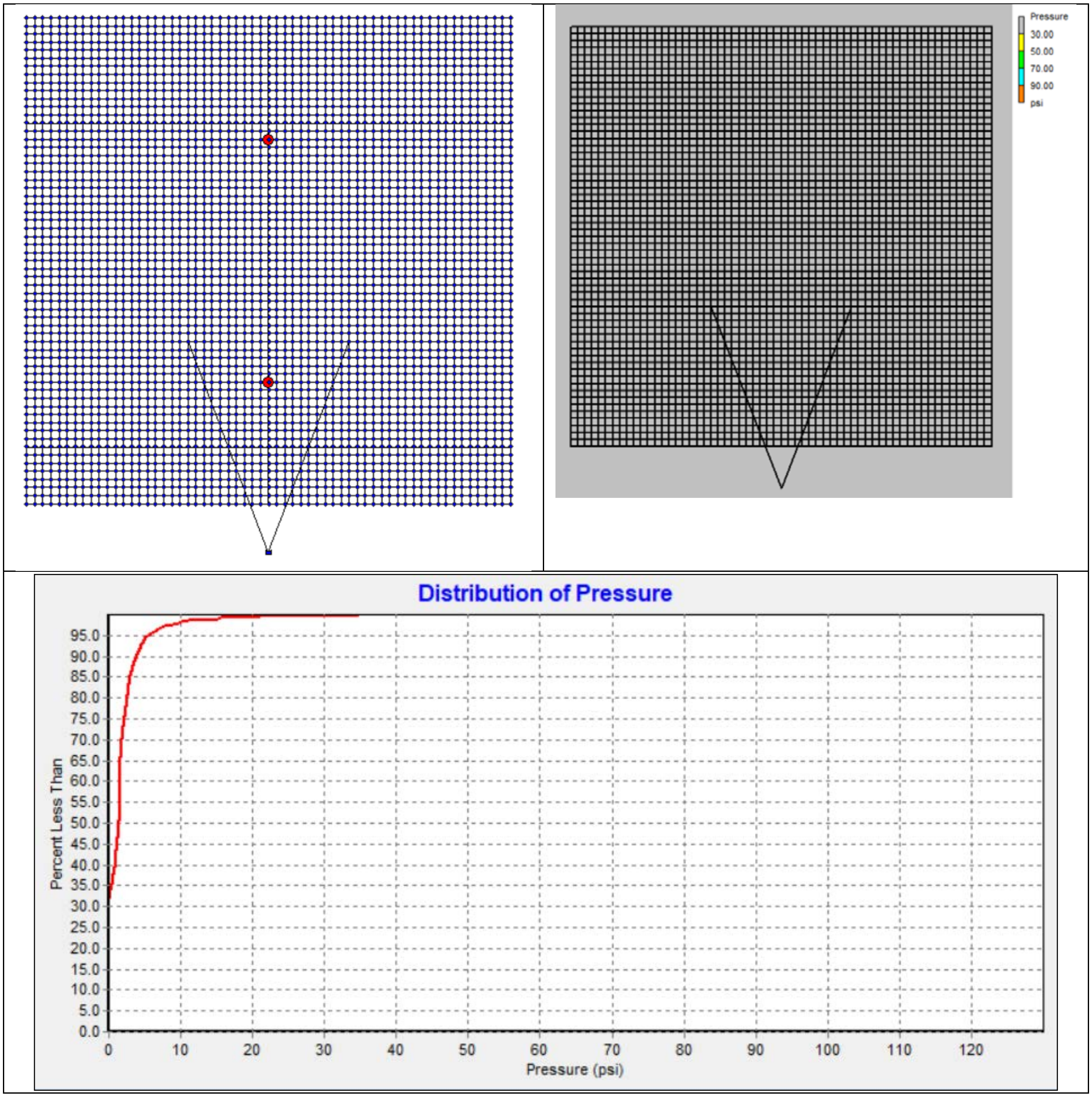


Note: (top left) 6-inch distribution pipe, no trunk lines, two red nodes are the 5000 gpm fire demands; (top right) resulting pressure distribution, gray - less than 30 psi everywhere. Total cost = $1.32 billion. (bottom) frequency distribution of nodal pressures, from which it can be seen that almost 100% of nodes have less than 30 psi pressure, with a median nodal pressure ($\breve{P}_n$) of about 2 psi, which is unacceptable.

**Figure 30.** Water network Case 1: first round of initial design.

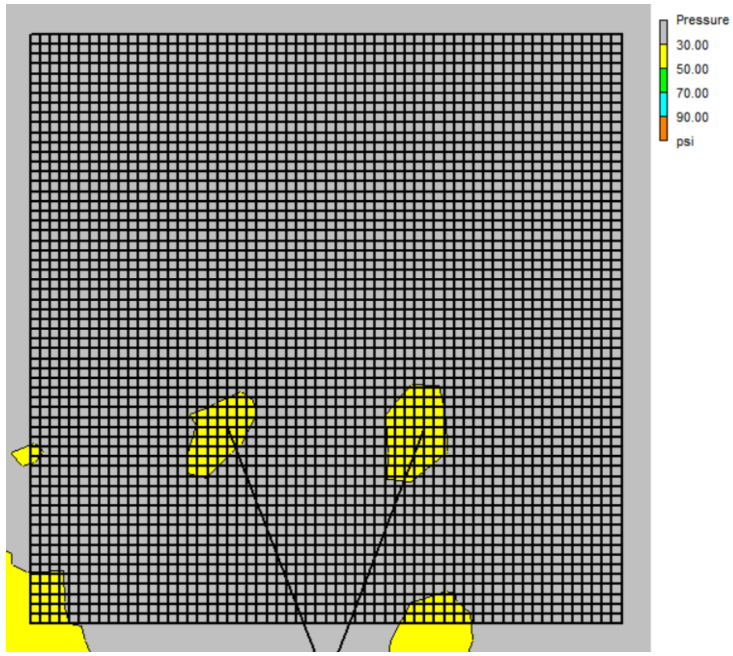


Note: 6-inch distribution, 16-inch trunk lines every 20th distribution pipe; resulting pressure distribution, less than 30 psi almost everywhere. Total cost = $1.65 billion, but unacceptable due to inadequate pressures.

**Figure 31.** Water network Case 2: second round of initial design.

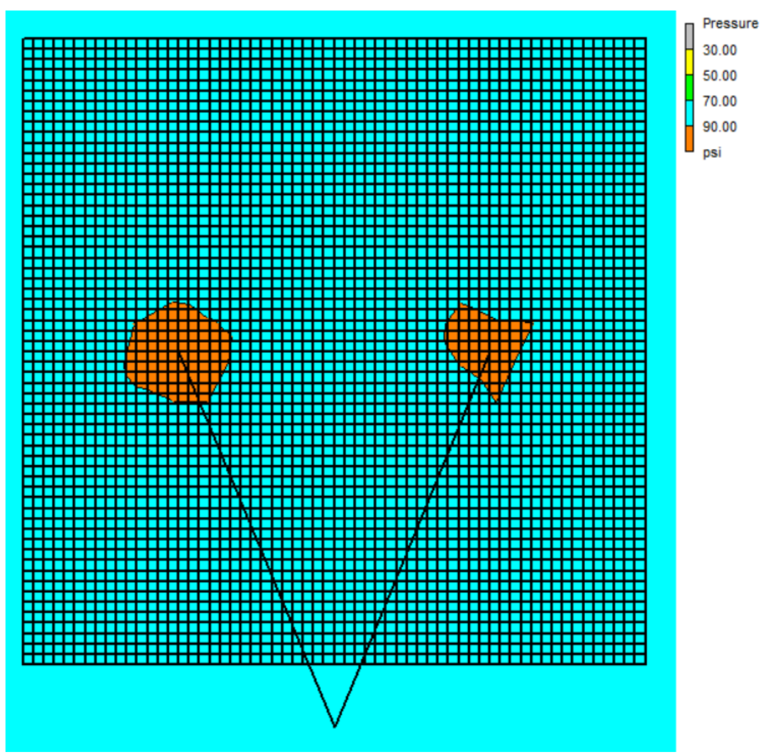


Note: 6-inch distribution pipe, 16-inch trunk lines every 5th distribution pipe; pressure distribution adequate everywhere. Total cost = $2.07 billion. $\breve{P}_n$ = 83 psi, which is acceptable.

**Figure 32.** Water network Case 3.

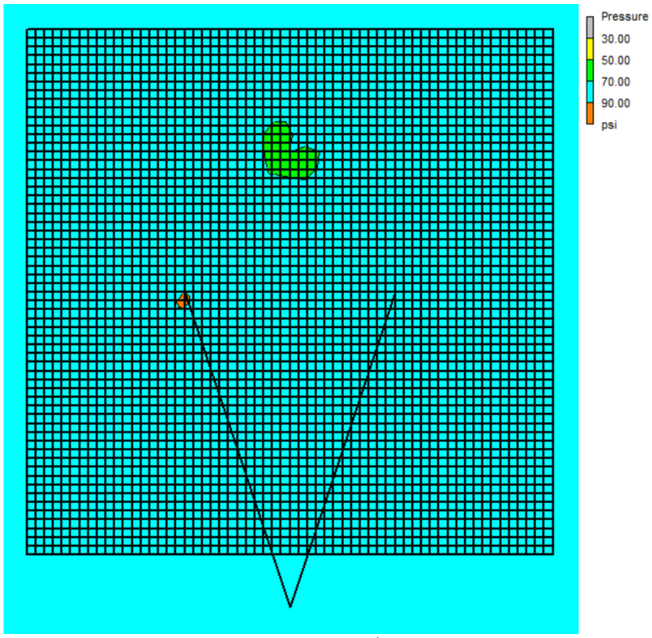


Note: 6-inch distribution pipe, 16-inch trunk lines every 6th distribution pipe; pressure distribution adequate everywhere. Total cost = $1.95 billion.

**Figure 33.** Water network Case 4.

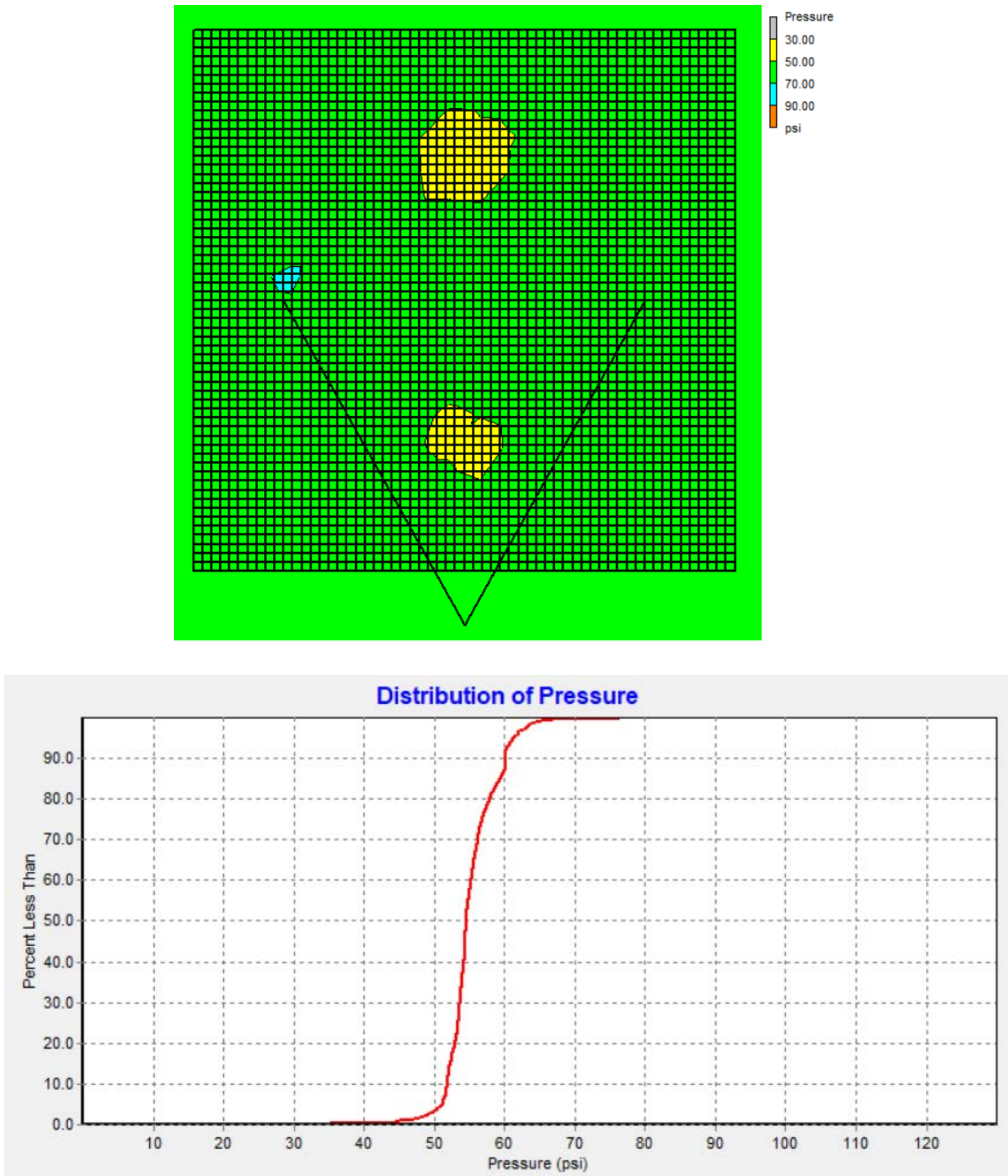


Note: 6-inch distribution pipe, 16-inch trunk lines every 10th distribution pipe; pressure distribution adequate everywhere. Total cost = $1.72 billion, median nodal pressure 55 psi, acceptable.

**Figure 34.** Water network Case 5.

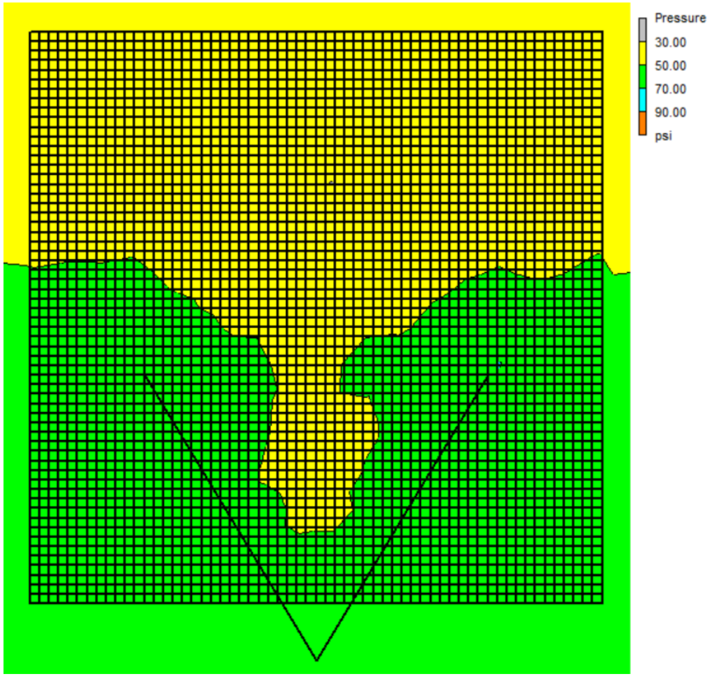


Note: 6-inch distribution pipe, 16-inch trunk lines every 12th distribution pipe; pressure distribution adequate everywhere. Total cost = $1.66 billion.

**Figure 35.** Water network Case 6.

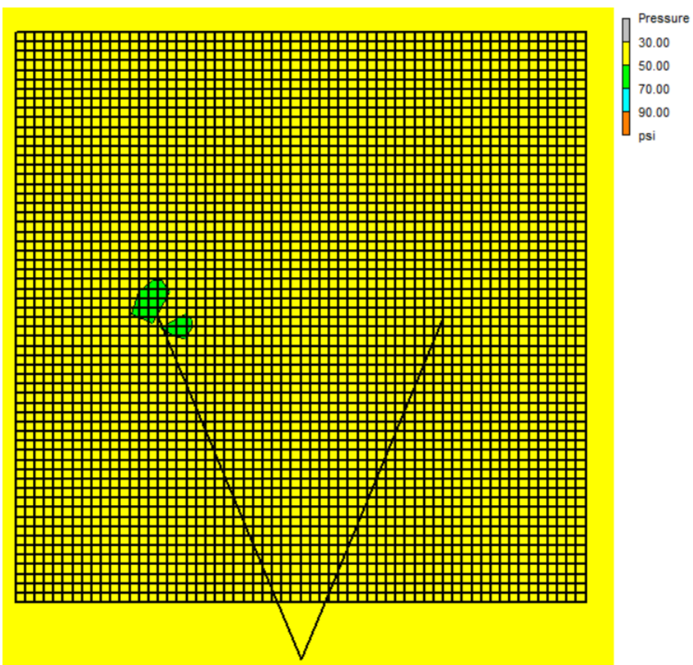


Note: 6-inch distribution pipe, 16-inch trunk lines every 15h distribution pipe; pressure distribution barely adequate everywhere. Total cost = $1.61 billion.

**Figure 36**. Water network Case 7.

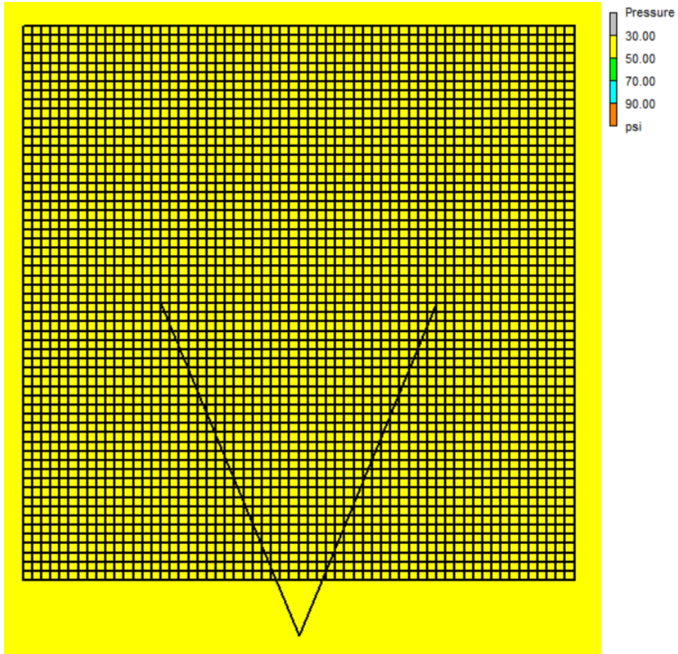


Note: 8-inch distribution pipe, 12-inch trunk lines every 15th distribution pipe; pressure distribution barely adequate everywhere. Total cost = $1.76 billion.

**Figure 37.** Water network Case 8.

| Case | Distrib. Diam. (inches) | Trunk lines | | Cost (billions $) | Median nodal pressure ($\breve{P}_n$) | Acceptable? |
|---|---|---|---|---|---|---|
| | | Diam. (inches) | Spacing | | | |
| 1 | 6 | none | none | $1.32 | 2 | No |
| 2 | 6 | 16 | 20th | $1.55 | 6 | No |
| 3 | 6 | 16 | 5th | $2.07 | 83 | marginal |
| 4 | 6 | 16 | 6th | $1.95 | 75 | OK |
| 5 | 6 | 16 | 10th | $1.72 | 55 | OK |
| 5A | 6 | 16 | 10th | $1.72 | 73 | OK (no fire flow) |
| 6 | 6 | 16 | 12th | $1.66 | 50 | OK |
| 7 | 6 | 16 | 15th | $1.61 | 42 | marginal |
| 8 | 8 | none | none | $1.76 | 10 | No |
| 9 | 8 | 12 | 15th | $1.98 | 35 | marginal |

**Table 22.** Phase 1 as-is design results.

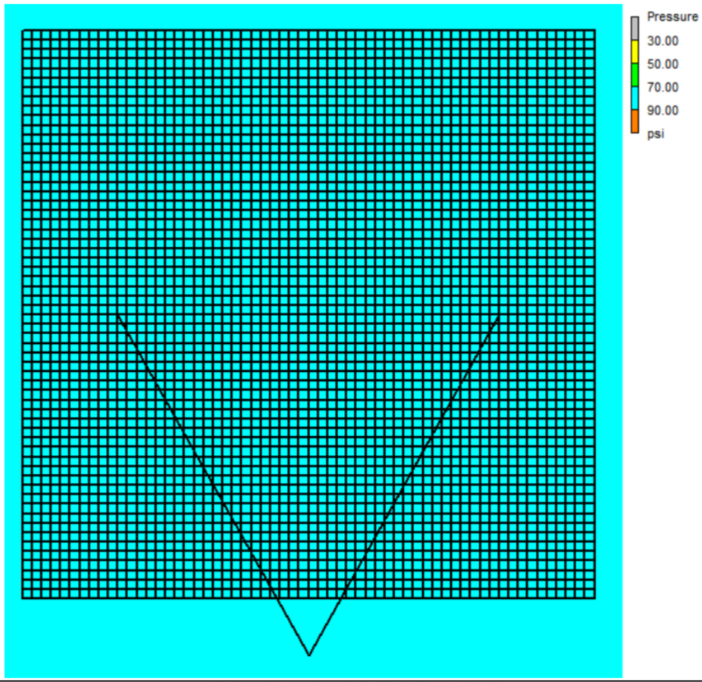


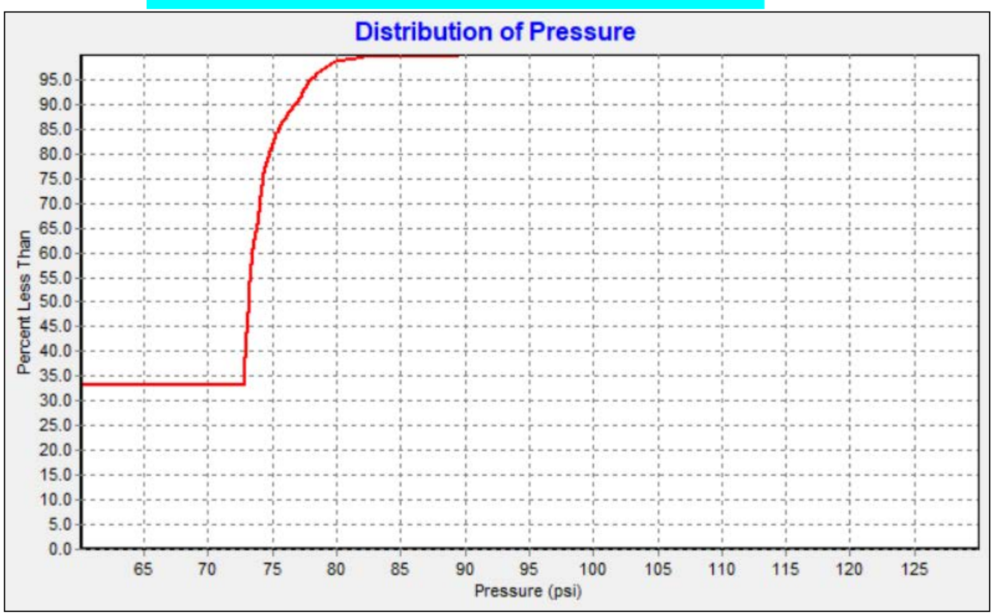


Note: 6-inch distribution pipe, 16-inch trunk lines every 10th distribution pipe; median nodal pressure 73 psi, Acceptable. Total cost = $1.72 billion.

**Figure 38**. Water network Case 5A, no fire flow.

As a form of validation, the project team compared the configuration of this initial design with the distribution system of the city of San Francisco, as shown in Table 23, demonstrating the as-is model is reasonably representative of a large U.S. city. Table 24 and Figure 39 show the comparison of the frequencies of distribution pipe diameters for several systems, and Table 25 and Figure 40 show the frequencies for pipe materials, showing that, given the somewhat simplified nature of the model, reasonable agreement with real systems.

| Parameter | | As-is design | San Francisco |
|---|---|---|---|
| 2016 population (est.) | | 787,500 | 870,887 |
| Area (sq. mi.) | | 47 | 47 |
| Retail water use per capita (mgd, 2014-15) | | 70 | 77 |
| total length pipe (millions ft) | | 4.9 | 6.5 |
| length breakdown by size (%) | 6" | 90% | 29% |
| | 8" | - | 37% |
| | 10" | - | - |
| | 12" | - | 12% |
| | 14" | - | - |
| | 16" | 10% | 7% |
| | 18" | - | 0.2% |
| | 20" | - | 1.9% |
| | > 20" | - | 7.9% |

**Table 23.** Comparison of as-is design and San Francisco water distribution parameters.

| Diameter | As-is | San Francisco | EBMUD | LADWP |
|---|---|---|---|---|
| 6 | 90% | 29% | 49% | 50% |
| 8 | 90% | 66% | 76% | 75% |
| 10 | 90% | 66% | 77% | 76% |
| 12 | 90% | 78% | 88% | 87% |
| 14 | 90% | 78% | 88% | 87% |
| 16 | 100% | 85% | 92% | 90% |
| 18 | 100% | 85% | 92% | 90% |
| 20 | 100% | 87% | 94% | 91% |
| 24 | 100% | 95% | 96% | 93% |

**Table 24.** Distribution of pipe diameters for as-is and selected water districts.

| Material | SF | EBMUD | LADWP |
|---|---|---|---|
| Asbestos cement (AC) | | 30% | 8% |
| Cast iron (CI) | 62% | 34% | 61% |
| Ductile iron (DI) | 29% | | 14% |
| Polyvinyl chloride (PVC) | | 10% | 0% |
| Steel (STL) | 6% | 26% | 15% |

**Table 25**. Distribution of pipe materials for selected water districts.

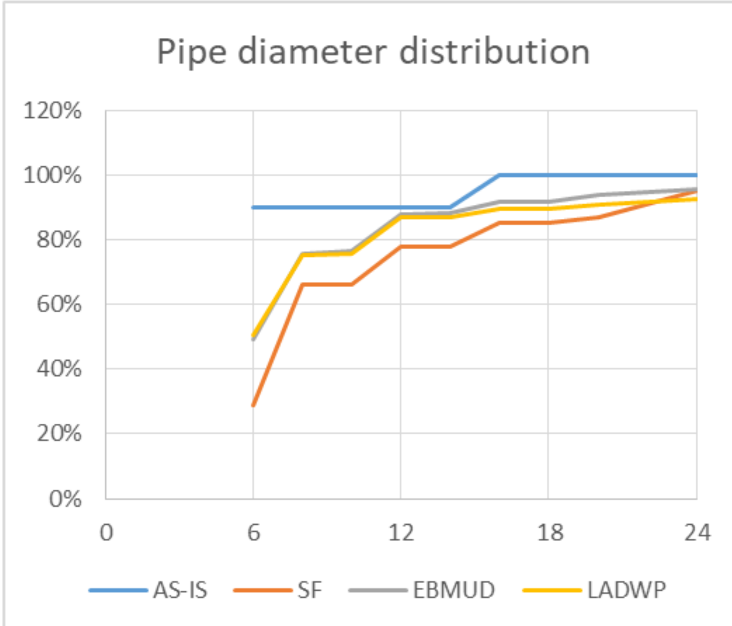


**Figure 39.** Distribution of pipe diameters for as-is and selected water districts.

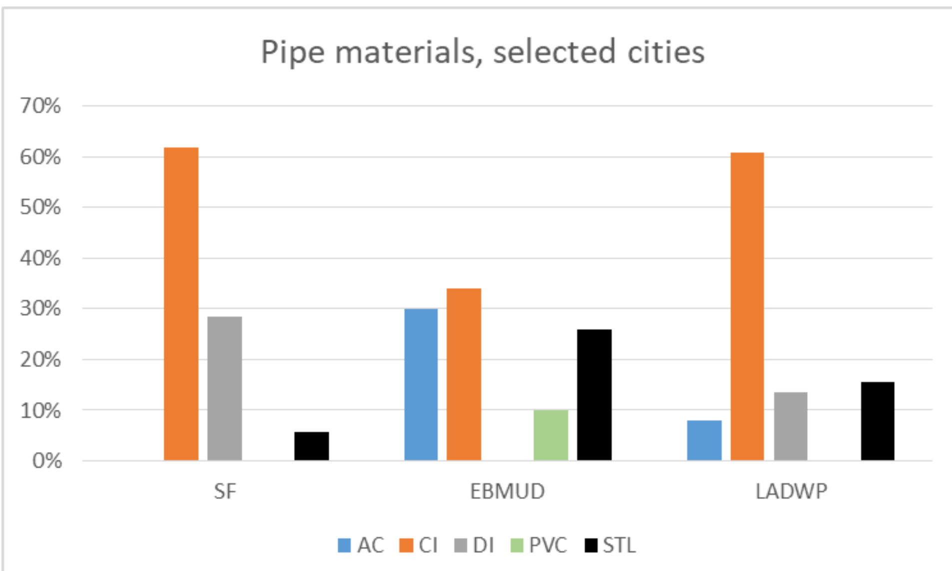


**Figure 40.** Distribution of pipe materials for selected water districts.

### 6.2.5 Rationale for a Resilient Grid

In the previous section, a system representative of a medium-sized U.S. city was sized to meet daily demands, including fire flows, in a manner similar to how most water supply networks are sized. Designing in this manner, however, may fail to meet the demands of extraordinary events such as earthquakes. Such extraordinary demands can be met by several means. Designers can wholly increase the pipe diameter size of the distribution network, using new but ordinary pipe with its seismic vulnerabilities. However, this can be rather expensive. Alternatively, a designer can construct a wholly independent special system, such as San Francisco's Auxiliary Water Supply System or Vancouver, British Columbia's Dedicated Fire Protection System (Scawthorn et al. 2017; Scawthorn, Ballantyne, and Blackburn 2000), although such systems may also be expensive.

Another option is to create a resilient grid that will survive the extraordinary event and facilitate temporary measures to meet the extraordinary demands. “A resilient network places seismically robust pipes at key locations and alignments to help increase the probability of continuous water delivery and reduce the time to restore areas suffering a loss of water services after an earthquake” (Davis 2017). This study examines the resilient grid concept. However, rather than piecemeal replacement of only selected pipes at key locations, the project team left the distribution grid untouched and replaced the entire trunk line grid with ERDIP, which would be hydraulically isolated from the distribution line grid by seismically actuated valves following a major earthquake. In calculating benefit-cost, the project team included the cost of replacing the entire trunk line grid, even though portions of the trunk line grid in some cases might not require replacement (thus, the benefit-cost calculated in this study is probably an underestimate).

### 6.2.6 Pipeline Damage and Restoration

Earthquake damage to the pipe network is typically due to one of two mechanisms: “the *wave propagation* hazard and the *permanent ground deformation (PGD)* hazard. The wave propagation hazard is transient and corresponds to ground shaking. It results in transient strains in buried pipelines, strains that disappear when the shaking has stopped. The wave propagation hazard occurs in every event and generally leads to low to moderate damage rates for buried pipe (repairs per kilometer of pipe) over wide areas.” (O'Rourke and Liu 2012).

The effects of *PGD* are much more damaging to pipes than wave-propagation effects, but *PGD* typically occurs only over a portion of a network, whereas wave-propagation effects typically affect the entire network. For example, in San Francisco in the 1989 Loma Prieta Earthquake, there were 123 repairs concentrated in the relatively small Marina district (O'Rourke et al. 1990), all due to *PGD* effects, and only 35 repairs spread over the rest of the city (some of which were also due to *PGD* effects), so that the ratio of repair rates from permanent ground deformation to those of wave propagation was approximately 135/23 or about 6 to 1.

To model leaks and breaks in pipe due to wave-propagation effects, the project team used the American Lifelines Alliance repair rate estimate for buried pipe (ALA 2001):

$$RR = K_1\, 0.00187 \times PGV$$

(Equation 1)

where $K_1$ is a factor to account for pipe material, $RR$ = repairs per 1,000 feet of main pipe and $PGV$ is peak ground velocity in units of inches/second. The project team used $K_1 = 0.75$ to account for the as-is model being a mix of CI, DI, and other pipe types. The 0.75 factor was arrived at after a review of such factors in ALA (2001). Thus, the total number of repairs to distribution pipe, denoted here by $N_{dr}$, and the total number of repairs to trunk lines, denoted by $N_{tr}$, can be estimated given the total length of distribution and trunk lines affected by various levels of $PGV$, respectively.

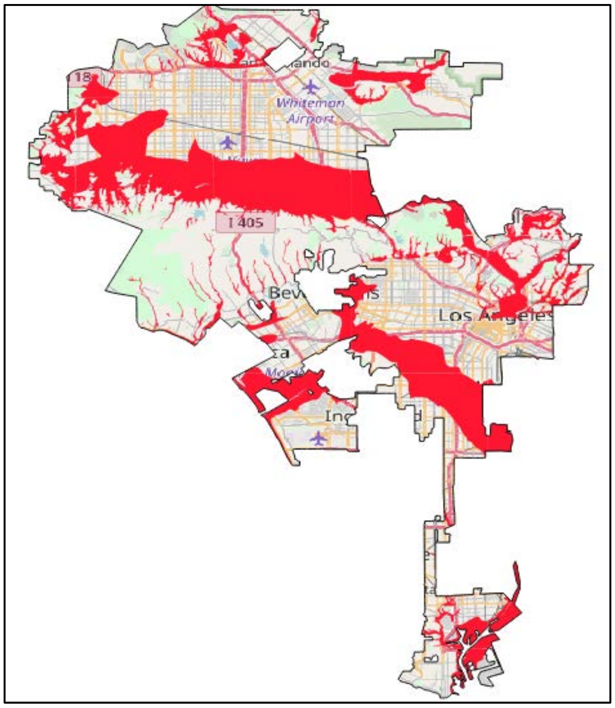


Source: http://geohub.lacity.org/datasets/4842ad85584c430481246852280257c2_9.

**Figure 41.** City of Los Angeles, with potential liquefaction zones shown in red.

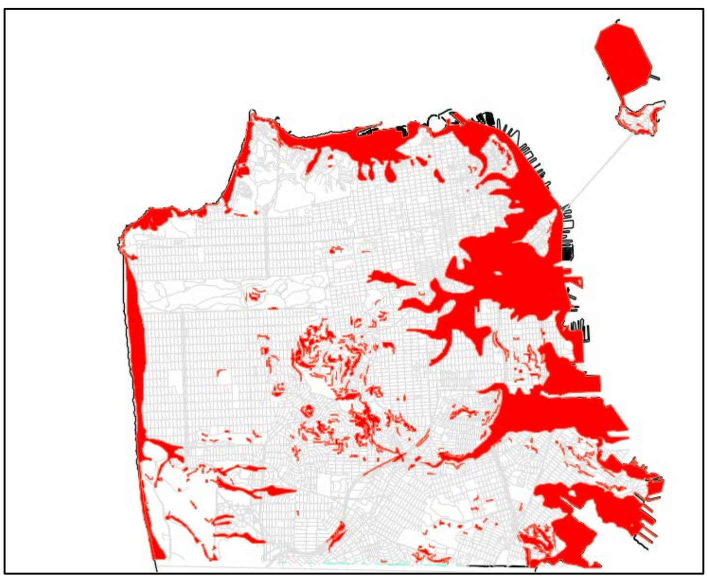

Source: https://data.sfgov.org/City-Infrastructure/San-Francisco-Seismic-Hazard-Zones/7ahv-68ap/data.

**Figure 42**. City of San Francisco, with hazard zones (almost entirely liquefaction, some landslide in the middle of the city) shown in red.

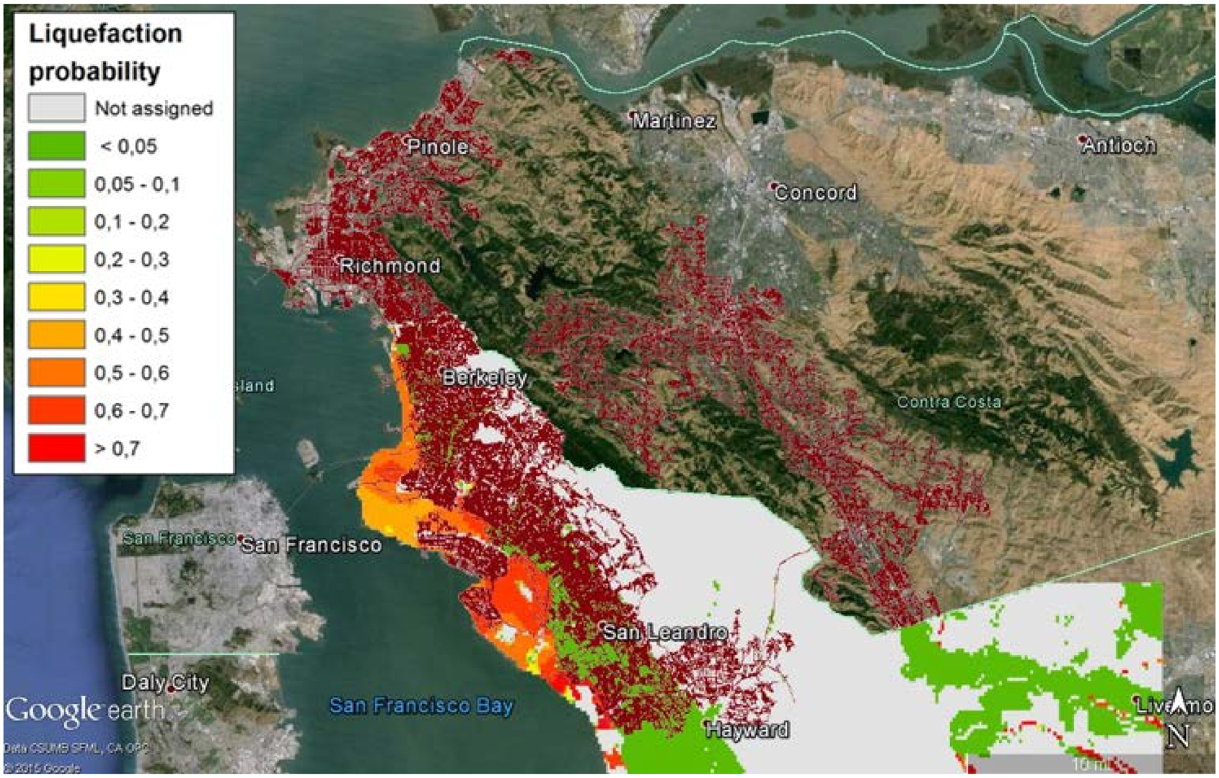


**Figure 43.** EBMUD liquefaction zones (Porter 2018).

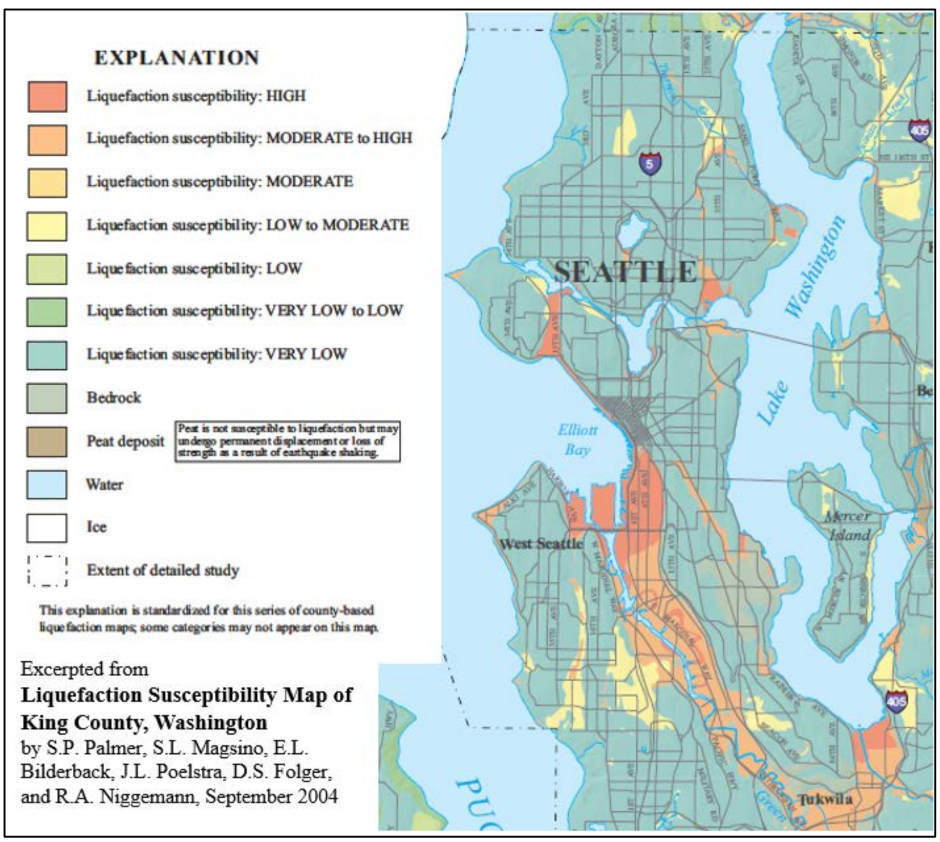


**Figure 44.** City of Seattle liquefaction zones.

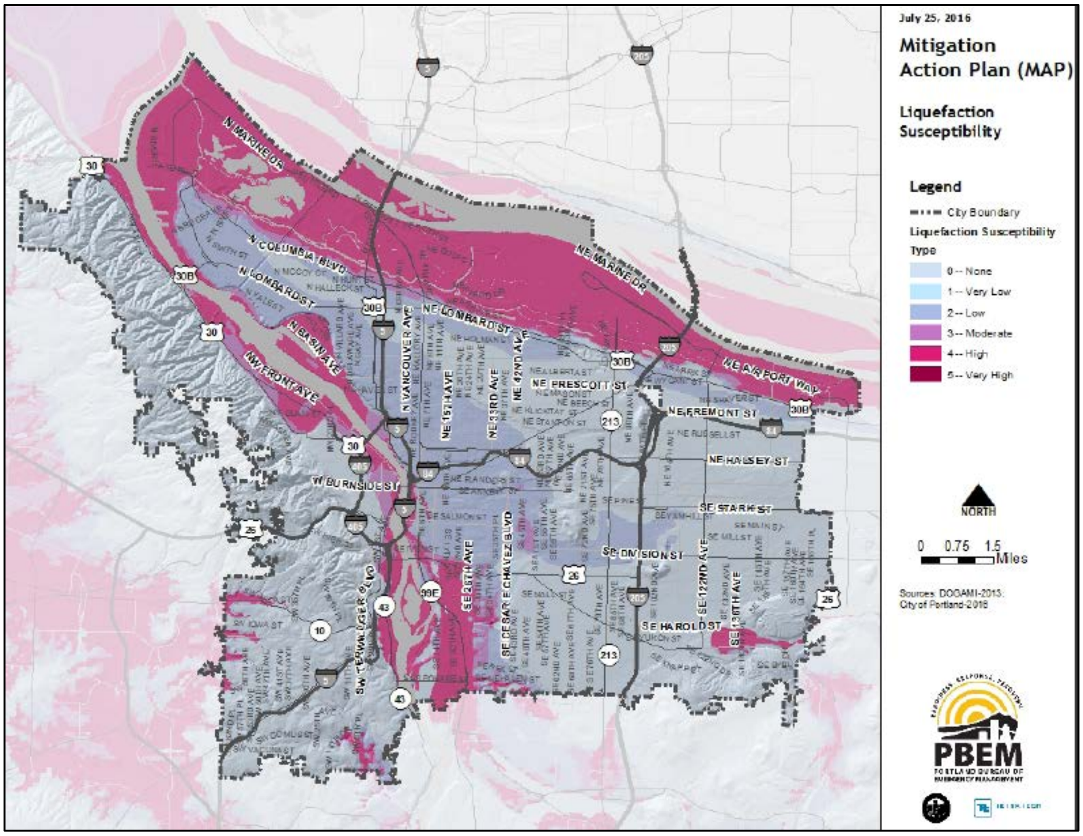


Source: https://www.portlandoregon.gov/pbem/.

**Figure 45.** City of Portland liquefaction zones.

Following commonly accepted assumptions, (Cornell University 2008; DHS 2003) 80% of repairs are due to wave passage (*PGV* effects) repair leaks and the remaining 20% are due to repair breaks. Leaks come in four possible types: annular, round, longitudinal, and local loss of wall (also called windowpane). Using relations and frequencies (Cornell University 2008) for equivalent orifice area (EOA) for each leak type, the project team developed an overall average EOA, which it employed for random repairs. The specific equivalent orifice diameter (EOD) is well approximated by EOD = $d \times (0.5d^{-0.155})$. Thus, if the pipe diameter $d$ is 6 inches, then the average EOD is 2.29 inches, including a 20% weighting of a full pipe break.

Modeling leaks and breaks in pipe due to *PGD* effects is more problematic for this study because the location(s) of *PGD* needs to be specified. *PGD* effects (mostly liquefaction, lateral spreading, landslide, and fault slip) typically only affect a portion of a network. For example, Figure 41 to Figure 45 show potential liquefaction zones for several major West Coast cities. Moreover, the location of the *PGD*-impacted area, whether it is central to the system, or near the major supply nodes, or on the far margins of the network, will greatly affect the impact on the network. Rather than specify a location or take a probabilistic approach, the project team considered ground-failure effects by averaging *PGD* repair rates over the entire region, and combining them with wave-propagation repair rates. That is, the project team assumed approximately 1/6$^{\text{th}}$ (16.7%) of the study region is subject to *PGD* effects, with a 6 to 1 ratio of repair rates from *PGD* to those of wave propagation, resulting in the overall number of repairs due to *PGD* effects being equal in number to those due to wave-propagation effects, so that by simply doubling Equation 1, *PGD* effects are reasonably accounted for. It should be noted that repairs associated with *PGD* are more likely to be breaks than leaks, possibly by as much as a factor of four (ALA 2001). So, this study may underestimate breaks resulting from *PGD*, their hydraulic consequences, and, ultimately, benefits of the resilient grid.

A fully probabilistic Monte Carlo analysis would be of interest, but the additional effort does not seem necessary to achieve the objectives of the this project.

Regarding recovery, the method of Porter (2018) is followed in a somewhat simplified manner. Repairs to distribution pipe require $R_d$ = 7.6 crew-hours to accomplish, while repairs to trunk lines require $R_t$ = 16.1 crew-hours. Crews work $H_{day}$ hours per day, assumed to be 12 hours per day, until all repairs are completed, and several crews can work on one repair to shorten the time required for completing the repair. Repairs are assumed to be initiated immediately following the earthquake, and to progress at the above rates until completed. The duration of repairs depends on the number of repair crews available. The total number of repair crews, denoted by $T_{crew}$, is estimated as the total number of service connections normally in service, divided by 10,000 (Porter 2018):

$$T_{crew} = \text{(total number of service connections)}/10{,}000$$

(Equation 2)

That is, if a water agency has 225,000 service connections (e.g., the project study area), it has 23 crews. These are in-house crews.

For extraordinary events, crews are added by mutual aid. They are assumed to arrive gradually, with an additional $T_{ma}$ = 20% of the number of crews already on site arriving each day after the first day. Mutual-aid crews arrive until the number of mutual-aid crews equals the number of in-house crews, which happens on the Day 6 after the earthquake. Mutual-aid crews are assumed to stay until the repairs from the mainshock are completed. (This analysis excludes repairs associated with aftershocks.) For the above example, on Day 1, the agency can draw on 23 crews, on Day 2 there are 28 crews, and so on, as shown in Table 26 with the corresponding number of repairs.

| Day | 1 | 2 | 3 | 4 | 5 | 6 | 7 | 8 | 9 | 10 |
|---|---|---|---|---|---|---|---|---|---|---|
| Number of crews | 23 | 28 | 34 | 41 | 46 | 46 | 46 | 46 | 46 | 46 |
| Distrib. repairs per day | 36 | 44 | 53 | 64 | 72 | 72 | 72 | 72 | 72 | 72 |
| Cum. distrib. repairs | 36 | 80 | 133 | 197 | 269 | 341 | 413 | 485 | 557 | 629 |
| Trunk repairs per day | 17 | 21 | 25 | 31 | 34 | 34 | 34 | 34 | 34 | 34 |
| Cumulative trunk repairs | 17 | 38 | 63 | 94 | 128 | 162 | 196 | 230 | 264 | 298 |

**Table 26.** Maximum possible repairs per day.

Given the above, solve for $D_c$, the total number of days required to complete all repairs, using Equation 3:

$$2(R_d N_{dr} + R_t N_{tr}) = \sum_{D=0}^{D_c} \left\{ T_{crew} \left[ (1 + T_{ma})^D \leq T_{max} \right] H_{day} \right\}$$

(Equation 3)

The left-hand side of the equation gives crew-hours required to perform $2 \times (R_d + R_t)$ repairs, the factor of 2 accounting for pipe repairs associated with ground failure, not included in Equation 1. The right-hand side of the equation gives the number of crew-hours expended by Day $D_c$. The inequality in the right-hand side of Equation 3 is shorthand notation to cap at $T_{max}$ the number of crews on Day $D$ as a multiple of $T_{crew}$. The multiple is taken here as $T_{max} = 2$.

### 6.2.7 Modeling Fire Ignition, Growth, and Firefighting Response

For fires following earthquake, the project team assumed an average total floor area per capita, for all types of building occupancies of $TFApc$ = 640 square feet, taken from ATC-52-1 (Applied Technology Council 2010) for a total floor area ($TFA$) of 504 million square feet for the entire as-is model. The project team estimated the number of ignitions using Equation 4, in which shaking is measured using peak ground acceleration, $PGA$, measured in units of gravity, $g$. See SPA Risk (2009).

$$Igns = (0.5819 \times PGA^2 - 0.0294 \times PGA) \times TFA$$

(Equation 4)

In the equation, $Igns$ refers to the number of ignitions and is rounded to the nearest whole number, and $TFA$ is measured in units of millions of square feet. For example, $PGA = 0.3g$ produces a mean of 22 ignitions for the study area. In the present calculations, ignitions are random and may vary around this mean.

Estimating the water needed for fire suppression is a complex matter (TCLEE 2005). This study assumes a modest delay in reporting and response such that the equivalent of three structures are involved when firefighters arrive at the fire. Using guidelines in DHS (2003), to fight a fire involving three structures requires a fire flow (a flow of firefighting water) of 3,000 gpm. Large fires require significantly larger fire flows. For 10 ignitions, the total required fire flow equates to 30,000 gpm. For reference, a normal fire engine’s maximum capacity is 1,500 to 2,000 gpm.

Thus, if the system were subjected uniformly to shaking of Modified Mercalli intensity ($MMI$) = 7, the total demands on the system include the ordinary service connection demands of 49,212 gpm; no ordinary fire demands; break and leak demands (assuming full pressure for the full 4.9 million feet of pipe) of about $4.9 \times 17{,}700 = 86{,}765$ gpm; and extraordinary fire demands of 39,000 gpm, for a total of 174,977 gpm. This is the desired total flow. The question is whether the damaged system can furnish it.

The number of fire engines is assumed to total only those belonging to the jurisdiction, on the assumption that (at least initially) nearby jurisdictions are all affected by the earthquake and cannot assist for the first 12 hours. (This assumption is dependent on mutual aid and other factors, and should probably be examined further.) The number of engines for a jurisdiction is estimated as

$$NFE = 3.82 + 0.052 \times P \qquad n = 202,\ r^2 = 0.45$$

(Equation 5)

The equation is based on unpublished work by Scawthorn. In the equation, $NFE$ = number of fire engines (rounded to nearest whole number) and $P$ is residential population in thousands. The value $n$ = 202 in the equation refers to the number of jurisdictions examined, and $r^2$ refers to the coefficient of determination from the regression analysis that produced the equation. For the study area, with a population of 787,500, Equation 5 rounds to 45 engines. By comparison, the city of San Francisco, with a 2016 population of 871,000, has 44 engines. Using Equation 5 would produce an estimate of 49 fire engines for San Francisco, suggesting reasonable agreement. (San Francisco has experienced very rapid population growth recently. Its 2010 population was 805,000, which would equate to 46 engines, and its 2000 population was 777,000, which would imply 44 engines).

Firefighting is a complex matter (TCLEE 2005). The project team used simplified but reasonable assumptions typical of West Coast cities (e.g., wood-based residential construction), as follows:

- Ignitions initially require two engines to respond. Thus, for the study area, if there are more than 22 ignitions, the number of ignitions exceeding 22 are initially unfought because of insufficient engines. Those fires grow. They are referred to here as large fires because they will rapidly grow to involve a large number of buildings.
- Ignitions that are within 1,000 feet of a node with at least 20 psi pressure are responded to first, by two engines, and are confined to three buildings (or a very few neighboring buildings) such that the property loss is small relative to conflagrations that develop from large fires. These smaller fires are neglected for present purposes.
- Ignitions that are farther than 1,000 feet from a node with pressure of at least 20 psi require an additional engine for each increment of 1,000 feet for hose-relay purposes. If there are insufficient engines to relay water, the ignition grows to become a large fire, because responding fire engines will not have water to suppress the fire.
- Large fires within a few tens of minutes grow to involve several buildings that, under ordinary circumstances, would require a second or greater alarm[7] (i.e., at least two engines). If the number of fire engines available for a large fire is five or more, the property loss is still relatively small, and is neglected for present purposes. If fewer than five engines are available, then a large fire grows to a size that cannot be contained, and will cross several firebreaks (e.g., streets). The actual extent is highly dependent on wind speed, street width, building setback, building cladding, roofing, and other factors. Based on a review of typical conditions in the San Francisco Bay and Los Angeles regions (Scawthorn 2018; Scawthorn 2011), it is assumed here that the average large fire burns five city blocks. This may seem an extraordinarily large area, but it must be kept in mind that by definition large fires are unfought, either because of insufficient engines or insufficient water. As such, there is nothing to stop their spread, save the cumulative probability of not crossing a firebreak. Given reasonable ranges of this probability, it can be shown that five city blocks is an average total burned area. For the study area, this equates on average to buildings per large fire, $B_{LF} = 5 \times 62.5 = 312.5$, which have a total population per large fire, $P_{LF}$ of $3.5 \times 312.5 = 1{,}094$ occupants. Given there are 640 square feet of floor area per occupant, equivalent to 2,240 square feet per building, $TFA_{LF}$, or total floor area per large fire is 700,000 square feet.

[7] The meaning of and number of fire engines responding to a "greater alarm" varies by department due to such factors of department size, building density, and construction. In general, a first alarm has a response of two or three engines (as well as other apparatus, not relevant here) with another two or three engines for each additional alarm.

### 6.2.8 Estimating Water and Fire Losses

Losses associated with damage to water supply include:

- Pipeline repair cost, denoted here by $C_{utility}$
- Direct business interruption loss to water customers who lose service, denoted by $C_{DBI,w}$
- Buildings that burn in fires that grow only because of lack of adequate firefighting water supply, resulting in:
    - Cost of property damage, denoted by $C_{PL}$
    - Deaths, financially quantified here in terms of the U.S. Department of Transportation (DOT) acceptable cost to avoid statistical deaths and denoted by $C_{mort}$
    - Nonfatal injuries financially quantified here in terms of the DOT acceptable cost to avoid a statistical serious injury (abbreviated injury scale, AIS, level 3; Association for the Advancement of Automotive Medicine 2001) and denoted by $C_{morb}$
    - Cost of PTSD among occupants, denoted here by $C_{PTSD}$
    - Direct business interruption loss to customers, denoted by $C_{DBI,f}$
- Indirect business interruption to the rest of the economy that does business with the customers whose homes or buildings burn down because of fires that grow only because of inadequate firefighting water, denoted by $C_{IBI,f}$

The total property loss associated with repairs (denoted here by $C_{rep}$) includes the actual cost to the water utility of the repair (i.e., labor and materials), plus $C_{cust}$ the cost to customers of the loss of service:

$$C_{rep} = C_{utility} + C_{cust}$$

(Equation 6)

Cost to the water utility for all repairs is:

$$C_{utility} = \sum_{D=0}^{D_c} \left( C_{\frac{rep}{hr}} T_{crew}\, H_{day} D \right)$$

(Equation 7)

where $C_{rep/hr}$ is cost of repairs per hour equal to $C_{repLabor}$ dollars per hour per worker, assumed here to be $100 per hour per worker, and a four person crew times a factor $F_{repMatls}$ to account for cost of materials and equipment, assumed here to be 30% so that the hourly cost of repairs is

$$C_{rep/hr} = F_{repMatls} \times C_{repLabor}$$

(Equation 8)

while $D_c$, $H_{day}$ and $T_{crew}$ are defined in the section on repairs above.

Cost to customers $C_{cust}$ is assumed solely to be due to the cost of loss of service $C_{los}$, which is estimated at $720 per day per service connection, based on the total regional economic loss attributed to loss of water in the 2008 Shakeout study (Jones et al. 2008), divided by the number of customers affected. Thus, for example, if one incident of pipe damage removes 100 service lines from service, and the repair cannot be made until three days following the incident, the cost of loss of service to customers is 3 × 100 × $720 = $216,000.

The total cost due to fires, $C_F$, is the sum of the financial cost due to human casualties, property losses, and direct business interruption:

$$C_F = C_{PL} + C_{HI} + C_{BI}$$
(Equation 9)

where $C_{PL}$ is the cost of property losses, $C_{HI}$ is the value lost or cost of human injury, and $C_{BI}$ is the cost of direct business interruption, in millions of dollars.

Regarding property losses, a replacement value $C_{bldg}$ for buildings typical of West Coast cities of $200 per square foot (RSMeans 2016) is employed with an addition for contents of $A_{cont}$ of 50%, for a total $C_{prop}$ of $300 per square foot. Given that the total floor area destroyed per large fire, $TFA_{LF}$ is 700,000 square feet, the property loss per large fire is a $C_{PL}$ of $210 million per Equation 10.

$$C_{PL} = TFA_{LF} \times C_{prop}$$
(Equation 10)

Estimating the value lost due to human injury $C_{HI}$ follows the methods in MMC (2018) and is the sum of values lost, or costs, due to mortality and morbidity $C_{MM}$ and cost due to PTSD $C_{PTSD}$:

$$C_{HI} = C_{MM} + C_{PTSD}$$
(Equation 11)

Estimating the frequencies of mortality and morbidity due to post-earthquake fires is difficult. Many earthquakes have very few deaths due to fires, but a few earthquakes are dominated by fire (Spence, So, and Scawthorn 2011; TCLEE 2005). On the one hand, earthquakes can be regarded as an alarm that will alert the population so that they will not be trapped by fire, while on the other hand, collapsed buildings may trap people who cannot extricate themselves from the path of fires.

The project team employed a simple approach here, consisting of a review of U.S. fire statistics for the period of 2003 to 2015 (USFA 2018). In that period, on average, there were 0.27 fatalities and 1.39 injuries per million dollars of property loss, which are the ratios used here for $f_{mort}$ and $f_{morb}$ per million dollars of property loss. See Table 27. The value of a statistical life, or cost $C_{mort}$ due to a fatality is $9.4 million, and value of a statistical injury, or cost $C_{morb}$, due to an injury is $0.55 million (MMC 2018)

$$C_{MM} = C_{PL}\,(C_{mort} f_{mort} + C_{morb} f_{morb})$$
(Equation 12)

which equates to (0.27 × $9.4 + 1.39 × 0.55) = $3.3 million per million dollars of property loss. That is, the cost of mortality and morbidity is 3.3 times larger than the property loss.

Regarding PTSD, the project team assumed all customers in buildings destroyed by large fires suffer PTSD, due to which there is a value lost or cost $C_{PTSDpc}$ of $33,750 per person (MMC 2018).

Given that the affected population per large fire, $P_{LF}$, is 1,094 persons, the cost of PTSD per large fire is:

$$C_{PTSDpLF} = C_{PTSDpc} \times P_{LF}$$
(Equation 13)

or $36.9 million per large fire. Given $C_{PL}$ the property loss per large fire is $210 million, the total cost of human injury per large fire is then 3.3 × 210 million + $36.9 – that is, $C_{HI}$ = $667 million.

Regarding business interruption, the project team used the approach in the *2017 Interim Report* of $69 per day per household for additional living expenses, for a period of 720 days. For a large fire, then 5 blocks × 62.5 HH/blk × $69 per day × 720 days = $C_{BI}$ = $15.5 million business interruption costs per large fire.

| Year | All building fires | Deaths | Injuries | $ Loss ($Mil) | Deaths / $Mil Loss | Injuries / $Mil Loss |
|---|---|---|---|---|---|---|
| 2003 | 484,400 | 3,185 | 14,825 | 10,258.9 | 0.31 | 1.45 |
| 2004 | 491,700 | 3,120 | 14,850 | 9,759 | 0.32 | 1.52 |
| 2005 | 477,900 | 2,935 | 14,775 | 10,478.1 | 0.28 | 1.41 |
| 2006 | 491,600 | 2,565 | 13,900 | 10,569.6 | 0.24 | 1.32 |
| 2007 | 493,300 | 2,855 | 14,800 | 11,459.6 | 0.25 | 1.29 |
| 2008 | 475,300 | 2,750 | 14,350 | 1,263.1 | 0.22 | 1.14 |
| 2009 | 445,400 | 2,570 | 14,100 | 11,069.1 | 0.23 | 1.27 |
| 2010 | 447,000 | 2,635 | 14,650 | 9,834.4 | 0.27 | 1.49 |
| 2011 | 449,900 | 2,530 | 15,000 | 957.5 | 0.26 | 1.57 |
| 2012 | 466,800 | 2,450 | 14,500 | 9,883.5 | 0.25 | 1.47 |
| 2013 | 474,000 | 2,820 | 13,875 | 9,500 | 0.30 | 1.46 |
| 2014 | 479,000 | 2,825 | 13,275 | 9,487.6 | 0.30 | 1.40 |
| 2015 | 485,500 | 2,635 | 12,800 | 9,790.4 | 0.27 | 1.31 |
| mean | 473,985 | 2,760 | 14,285 | 10,330.5 | 0.27 | 1.39 |
| Standard deviation | 16,308 | 217 | 644 | 887.2 | 0.03 | 0.12 |

**Table 27.** U.S. fire statistics 2003-2015 (USFA 2018).

In summary then, the cost of a large fire, which on average destroys five city blocks, is $C_F$ = ($C_{PL}$ = $210 million) + ($C_{HI}$ = $667) + ($C_{BI}$ = $15 million) = $892 million.

The project team applied these values and methodology to the study area for increasing earthquake shaking intensities, using hydraulic analysis to determine how the water supply network will cope with these demands. Based on the response of the network, the project team determined the number of large fires, and final burnt area, as well as the number and duration of households without water service.

### 6.2.9 Benefit-Cost Analysis

The project team calculated the benefit of a resilient grid as the present value of the reduction in losses, accounting for the frequency of shaking that causes those losses. The *2017 Interim Report* presented the mathematics, which are also calculated in a later section of this report.

## 6.3 Vulnerability Under As-is Conditions

As used here, vulnerability means loss conditioned on a level of environmental excitation. This section estimates losses and then applies the extraordinary demands on the as-is system resulting from increasingly strong shaking, quantified in terms of a uniform level of seismic intensity applied across the entire region. The project team used *PGV* for estimation of pipe damage, and PGA for estimation of ignitions, as discussed above. Calculations are performed using these two measures of ground motion, but for presentation purposes only, results are presented in terms of MMI 6, 7, 8, 9, and 10[8], converted to MMI using Wald et al. (1999). Given a level of ground shaking, the demands on the system are the ordinary demands excluding ordinary fire flows, plus leaking and broken pipes, plus fire flows from fires arising from the extraordinary event.

For MMI 6, using the above methodology, stochastic analysis finds 29 distribution pipe and no trunk line repairs are required, with 4 ignitions. See Figure 46. Total flow increases to 69,220 gpm (versus normal flow of 59,212 gpm including normal fire flows), virtually all nodal pressures exceed 10 psi pressure, so no services lose water, about 70% of nodes have pressures exceeding 20 psi (minimum for fire flow) so that the initial fire flow demands of 3,000 gpm for the 4 extraordinary fires are largely (not fully) met, averaging about 1600 gpm.

The project team calculated that the 29 repairs would all be completed within one day, for a cost to the utility of about $110,000. Financial loss due to the loss of service is negligible.

[8] MMI are denoted in Arabic (rather than Roman) numerals.

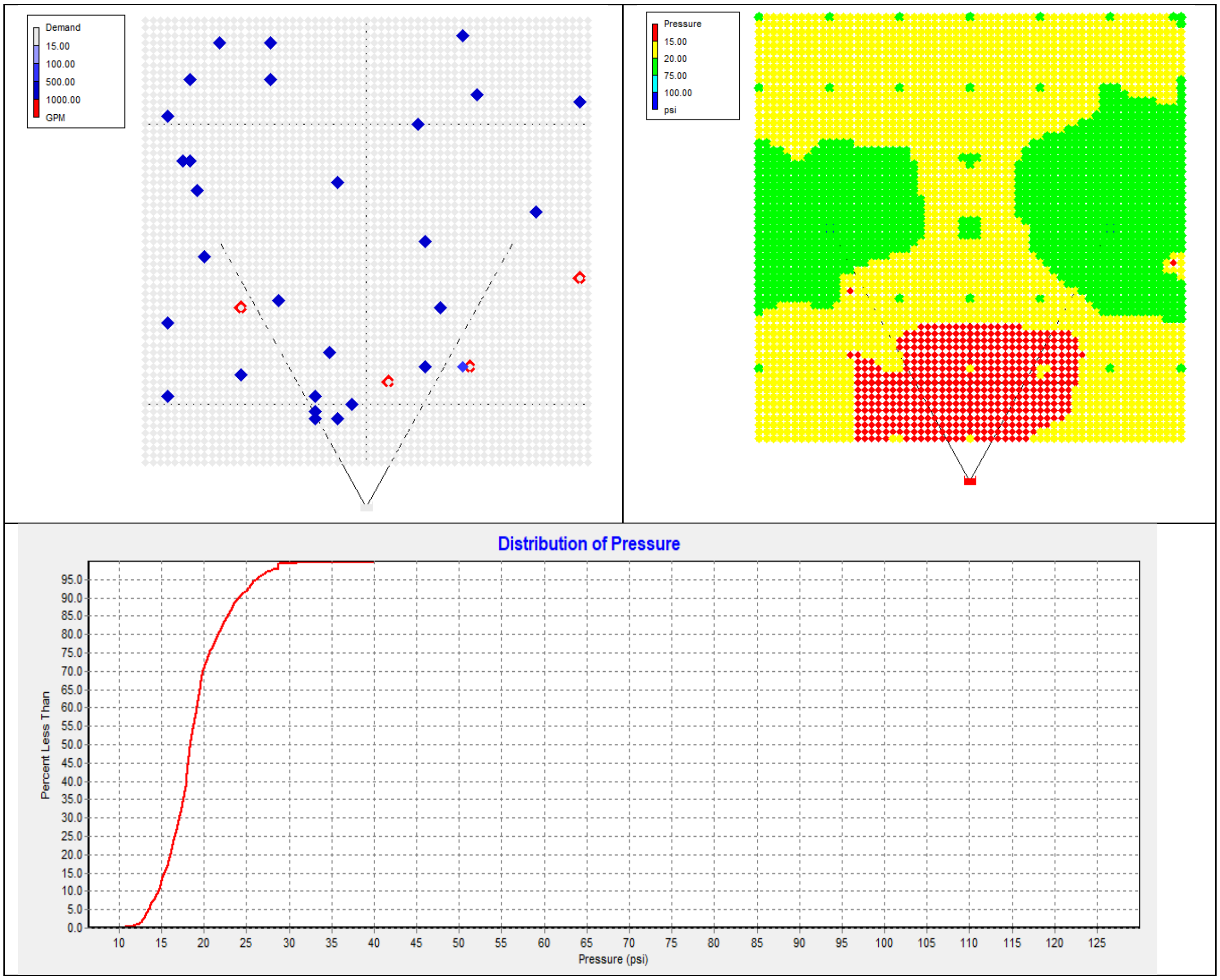


Note: Top left: 6-inch distribution lines every block and 16-inch trunk lines every 10th distribution line. Demand: normal demand (13.67 gpm) is light gray. The 29 leaks and breaks, and fires, are shown as blue or red diamonds; (top right) nodal pressure – virtually all nodes have pressures > 10 psi but 70% are less than 20 psi; (bottom) frequency distribution of pressure. Total system demand = 69,220 gpm.

**Figure 46.** MMI 6 with as-is design.

Regarding fires, while fire demands are not fully met initially, the small number of fires compared to the resources (45 engines) would suggest a low likelihood fires develop into large fires, so fire losses are negligible.

For MMI 7, stochastic analysis finds 63 distribution pipe and 7 trunk line repairs are required, and 6 ignitions occur, with total flow of 73,386 gpm. See Figure 47. Immediate impacts are:

- Nodal pressures are less than 10 psi for 85% of the population, so that Day 1 economic loss due to loss of water service is 85% × 225,000 services × $720 loss/service/day, or $138 million.
- All nodal pressures are less than 20 psi. However, there are more than 5 engines per fire so no fires grow to be large fires.

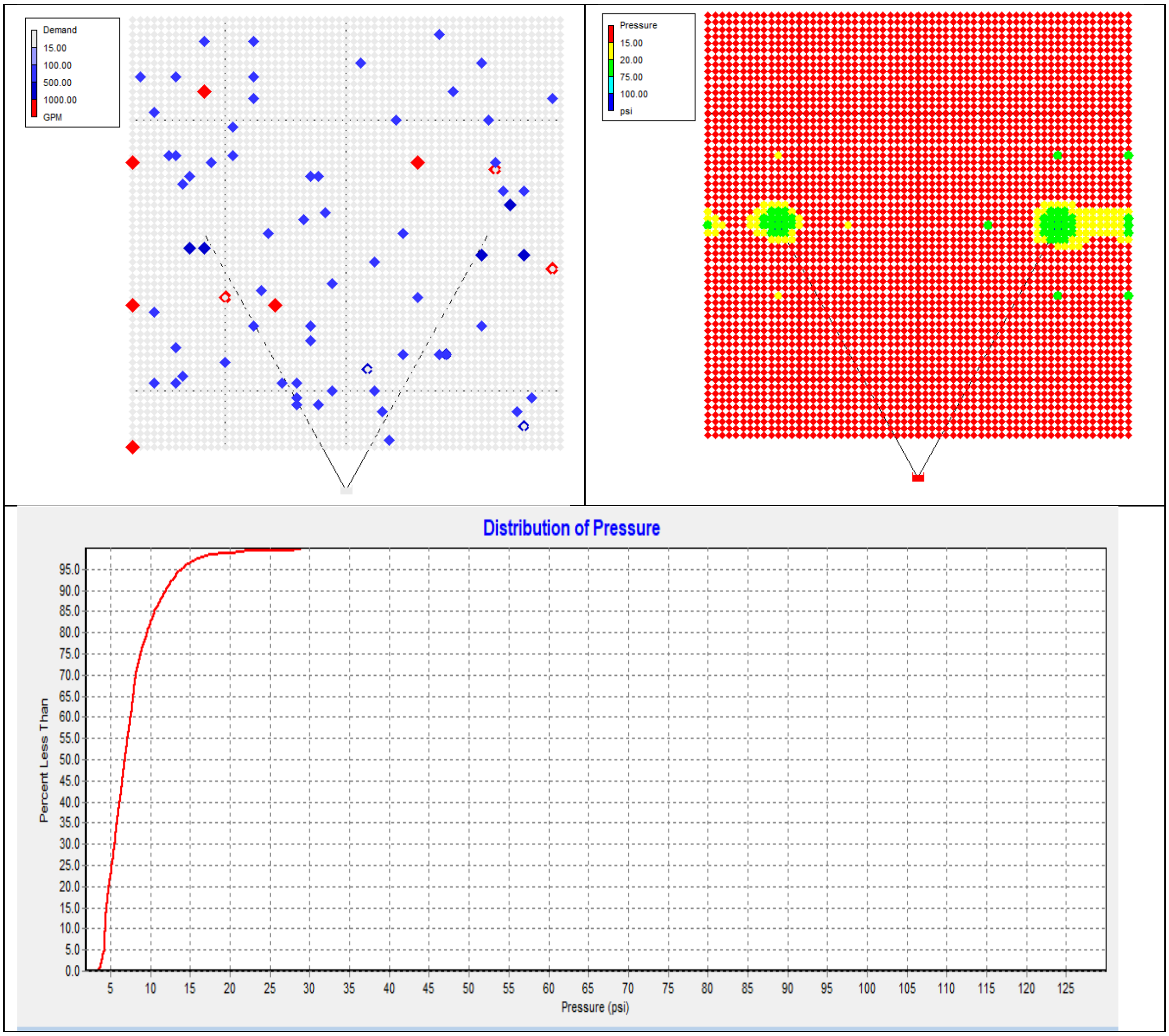


**Note:** Demand: normal demand (13.67 gpm) is light gray, 70 total leaks and breaks and the 6 fires shown as diamonds; (upper right and bottom) about 85% nodes have pressures > 10 psi but all are < 20 psi. Total system flow = 73,386 gpm.

**Figure 47.** MMI 7, as-is design.

At 24 hours after the event (i.e., end of Day 1), all fires are extinguished or burnt out, all trunk line and all distribution line repairs have been completed and all services have been restored. Total losses then are $138 million for loss of service and $0.32 million for utility cost of repairs.

For MMI 8, stochastic analysis finds 111 distribution pipe and 9 trunk line repairs are required, with 21 ignitions, see Figure 48. Total flow increases to 74,817 gpm. Immediate impacts are:

- All nodal pressures are less than 10 psi, so that Day 1 economic loss due to loss of water service is $162 million.
- All 21 fires have insufficient water and grow to be large fires, so that total fire loss is $18.7 billion. It should be noted that even with perfect water supply, a maximum of 22 fires could be responded to, so that this loss can be attributed entirely to loss of water.

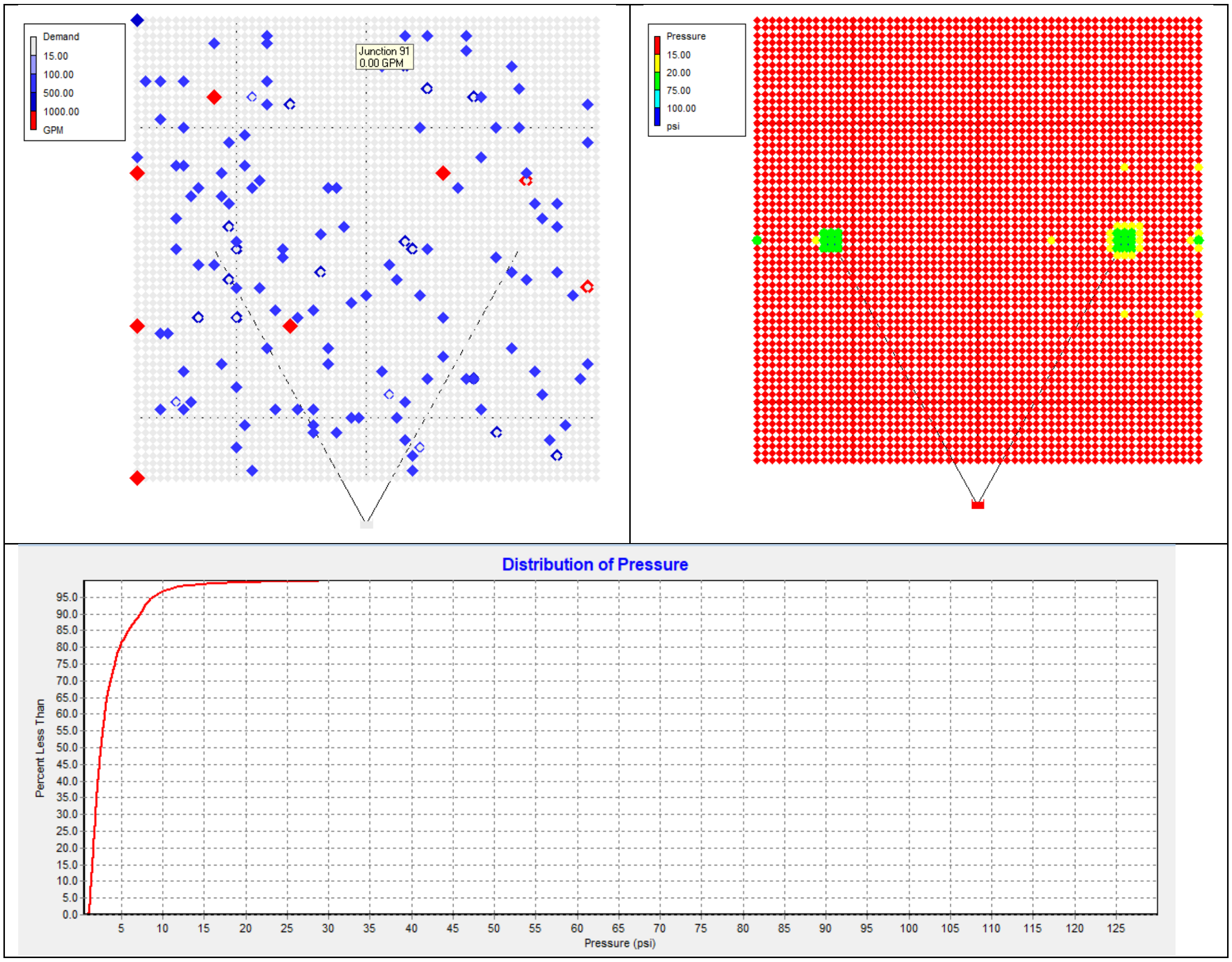


Note: Virtually all nodal pressures are below 10 psi. Total system flow is 74,817 gpm.

**Figure 48**. MMI 8 as-is design sustains 111 distribution and 9 trunk line repairs, and 21 ignitions occur.

At 24 hours after the event (i.e., end of Day 1), all fires are extinguished or burnt out, all 9 trunk line repairs and 17 distribution line have been completed. See Figure 49. These repairs reduce flow to 72,164 gpm so that 70% of service pressures are less than 10 psi, resulting in $113 million in economic loss.

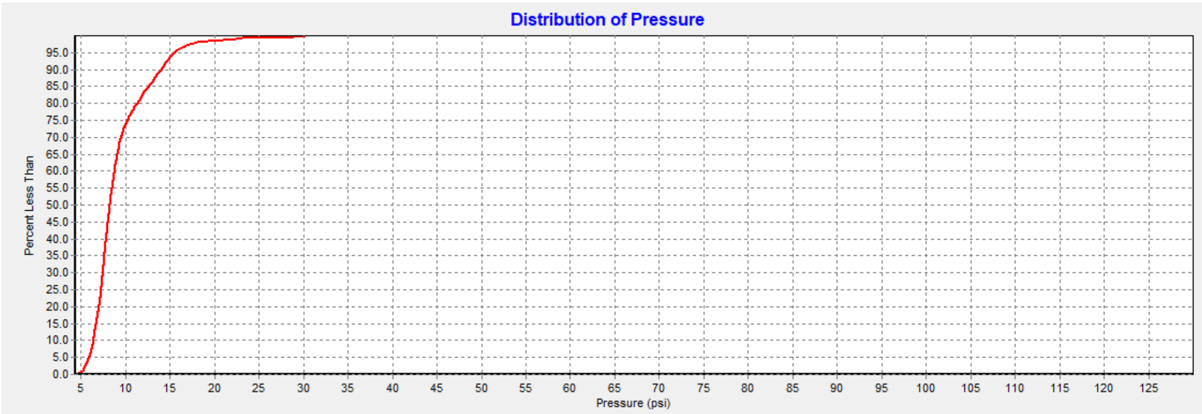


Note: Total flow is 72,096 gpm. It can be seen 70% of nodal pressures are < 10 psi.

**Figure 49.** MMI 8 nodal pressure distributions at the end of Day 1, when all fires are out, all trunk line repairs and 17 distribution line repairs are completed, and 94 remain.

At the end of Day 2, all trunk line and 61 distribution repairs are completed, which reduces flow to 69,851 gpm and 100% of services with pressure greater than 10 psi. Total utility cost of repairs is $0.53 million.

Total economic loss due to loss of water services is therefore $18.7 billion due to fire and $276 million in economic loss, for a total of $19 billion.

For MMI 9, stochastic analysis finds 205 distribution pipe and 14 trunk line repairs are required, with 59 ignitions. See Figure 50. Total flow is 94,296 gpm. Immediate impacts are:

- Virtually all nodal pressures are less than 10 psi so that Day 1 economic loss due to loss of water service is $162 million.
- All 59 fires have insufficient water and grow to be large fires, so that total fire loss is $8.32 billion. However, even with perfect water supply, only 22 of these fires could have been responded to, so that only 22 fires equivalent to $19.6 billion in losses should be attributed to loss of water supply, and the remainder of the loss ($33 billion) to insufficient fire resources.

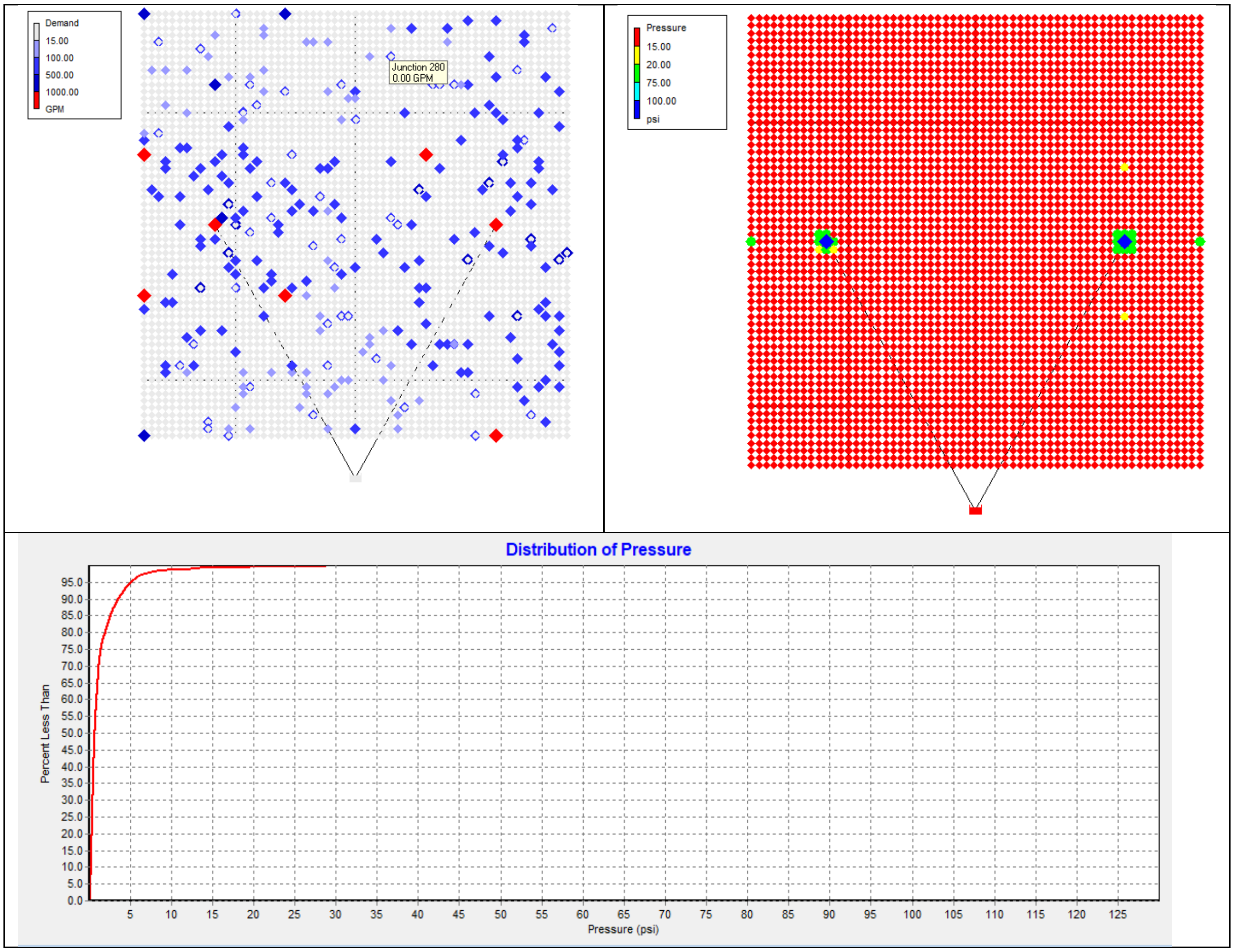


Note: All nodal pressures on day “0” are below 20 psi. Total system flow is 94,296 gpm.

**Figure 50.** MMI 9, as-is design sustains 205 distribution and 14 trunk line repairs, and 59 ignitions occur.

At 24 hours after the event (i.e., end of Day 1), all fires are extinguished or burnt out, and all trunk line repairs and 7 distribution lines have been completed. These repairs leave 95% of services still without water, resulting in $154 million in economic loss. Day 2 sees 44 more distribution repairs, which still leaves 93% of services without water. Day 3 sees 54 more distribution repairs, but 80% of services are still without water. By Day 4, a total of 170 distribution repairs have been completed to date, and 100% of services are restored. By Day 5, all repairs are completed. Figure 51 shows this process. The total economic loss due to loss of service for the four days while service was being restored is $596 million. The total economic loss due to fire given loss of water is $19.6 billion, for a total loss attributable to loss of water of $20.2 billion, and a total loss for all reasons of $53.2 billion, mostly due to fire.

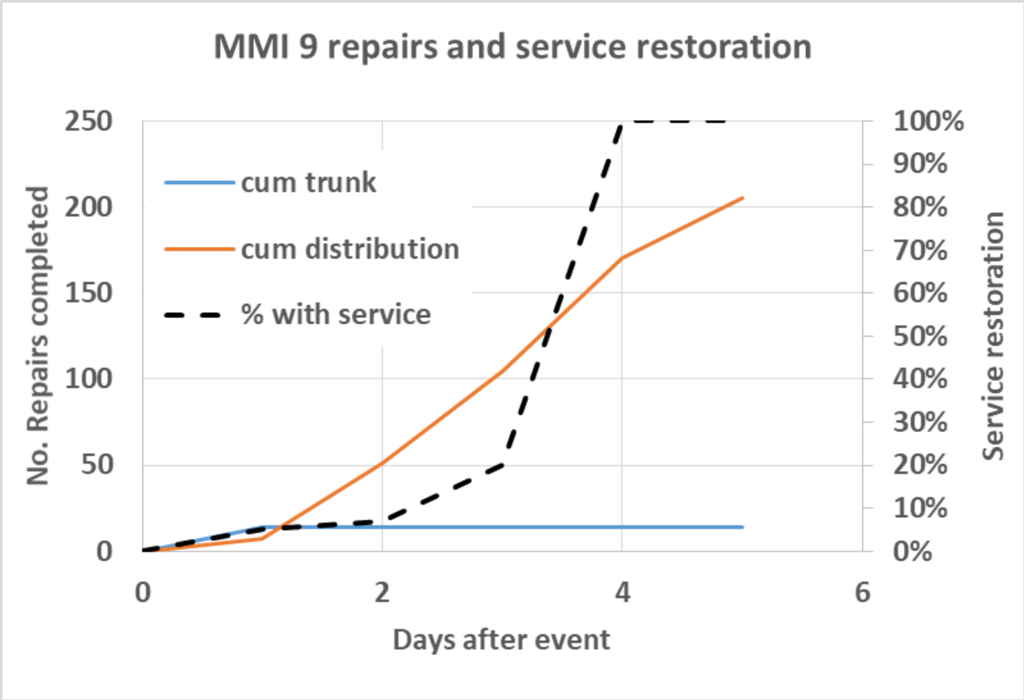

**Figure 51.** MMI 9, cumulative repairs and service restoration vs. days after event.

For MMI 10, stochastic analysis finds 371 distribution pipe and 31 trunk line repairs are required, with 170 ignitions. Total flow is 105,054 gpm. Plots of initial demand pressure distributions differ little from those for MMI 9, and are not shown here. Immediate impacts are:

- Virtually all nodal pressures are less than 10 psi, so that Day 1 economic loss due to loss of water service is $162 million.
- All 170 fires have insufficient water and grow to be large fires, so that total fire loss is $152 billion. However, even with perfect water supply, only 22 of these fires could have been responded to, so that only 22 fires equivalent to $19.6 billion in losses should be attributed to loss of water supply.

Completion of all repairs requires eight days, with all services restored by Day 7, so that the total economic loss due to loss of service for the seven days while service was being restored is $1.13 million, and the total economic loss due to fire given loss of water is $19.6 billion, for a total loss attributable to loss of water of $20.8 billion, and a total loss for all reasons of $153 billion, mostly due to fire. The foregoing results are summarized in Table 28.

| | MMI 6 | | MMI 7 | | MMI 8 | | MMI 9 | | MMI 10 | |
|---|---|---|---|---|---|---|---|---|---|---|
| Trunk (16") repairs | 0 | | 7 | | 9 | | 14 | | 31 | |
| Distribution (6") repairs | 29 | | 63 | | 111 | | 205 | | 371 | |
| Repairs per 1000 ft. of all pipe | 0.0059 | | 0.0143 | | 0.0245 | | 0.0447 | | 0.0821 | |
| Total number of repairs | 29 | | 70 | | 120 | | 219 | | 402 | |
| Cost of repairs | $ 0.11 | | $0.32 | | $ 0.53 | | $ 0.94 | | $ 1.72 | |
| Initial flow (normal = 59,212 gpm) | 68,680 | | 73,386 | | 74,817 | | 94,296 | | 105,054 | |
| Initial flow (normal = 85 mgd) | 98.9 | | 105.7 | | 107.7 | | 135.8 | | 151.3 | |
| **Customers without service (loss of service, LOS, %) and economic loss ($mil)** | | | | | | | | | | |
| | **LOS** | **$mil** | **LOS** | **$mil** | **LOS** | **$mil** | **LOS** | **$mil** | **LOS** | **$mil** |
| LOS, day 0 | 0 | - | 85 | 138 | 100 | 162 | 100 | 162 | 100 | 162 |
| LOS, day 1 | | | | | 70 | 113 | 95 | 154 | 100 | 162 |
| LOS, day 2 | | | | | | | 93 | 151 | 100 | 162 |
| LOS, day 3 | | | | | | | 80 | 130 | 100 | 162 |
| LOS, day 4 | | | | | | | | | 100 | 162 |
| LOS, day 5 | | | | | | | | | 100 | 162 |
| LOS, day 6 | | | | | | | | | 100 | 162 |
| Total customer-days LOS | 0 | | 191,250 | | 382,500 | | 828,000 | | 1,575,000 | |
| Mean LOS days (= tot cust-days/tot customers) | - | | 0.850 | | 1.700 | | 3.680 | | 7.000 | |
| Total economic loss due to loss of water | $ - | | $ 138 | | $ 275 | | $596 | | $1,134 | |
| **Fires and economic loss** | | | | | | | | | | |
| Total ignitions | 4 | | 6 | | 21 | | 59 | | 170 | |
| Total no. large fires | 0 | | 0 | | 21 | | 59 | | 170 | |
| Large fires due to loss of water | 0 | | 0 | | 21 | | 22 | | 22 | |
| Economic fire loss given loss of water ($mil) | $ - | | $- | | $ 18,732 | | $ 19,624 | | $ 19,624 | |
| Total economic loss due to fire ($mil) | $ - | | $- | | $ 18,732 | | $ 52,628 | | $151,640 | |
| **Total economic loss given loss of water ($mil)** | **$0.1** | | **$ 138** | | **$ 19,008** | | **$20,221** | | **$20,760** | |
| **Total economic loss ($mil)** | **$ -** | | **$ 138** | | **$ 19,007** | | **$ 53,224** | | **$152,774** | |

**Table 28.** Results for as-is system for increasing seismic intensity.

## 6.4 Vulnerability with a Resilient Grid

The foregoing analysis allows easy assessment of a resilient grid by the project team. The analyst assumes the trunk line is resilient, rebuilt to have negligible vulnerability (as is currently assumed for ERDIP), and with automatic seismic valves that can quickly isolate the trunk line from the distribution system. The trunk line will now be integral and function immediately following an earthquake. It will (a) immediately be able to provide water for firefighting if the fire is within a relay-able distance, assumed here to be 1,000 feet per engine;[9] (b) be able to convey potable water to within a few blocks of most of the population, which suffices for emergency conditions for a few days; and (c) greatly increase the restoration of service to many customers, since breaks in the distribution system will have a more limited impact. For these reasons, a low-vulnerability trunk line system capable of being isolated from the more-vulnerable distribution system constitutes a resilient grid. The project team thus assessed the reduction in loss resulting from benefits of the resilient grid. Table 29 summarize the results.

For MMI 6, the loss of service and impact of fire was nil. The trunk line sustained no damage, so reduction in cost of repairs, and all benefits, are nil.

For MMI 7, 85% of the population lost service on Day 1, while losses due to the 6 fires was negligible. The benefit of water within a few blocks of 85% of the population is difficult to estimate; the cost of no water was estimated to be $720 per service connection, so the project team assumed this limited emergency provision at selected points along the resilient grid is worth $100 per customer connection, or a total of 85% × 225,000 × $100 = $19 million.

For MMI 8, 55% of the 21 ignitions will be within a relay-able distance of 1,000 feet from the resilient grid, reducing the fire-related losses to $8.4 billion for a benefit of $10.3 billion. Losses due to loss of service to customers is estimated at $620/$720 × $275 = $237 million. Reduction in utility cost of repairs to trunk lines exists but is modest. Total benefits of the resilient grid are thus about $10.5 billion.

For MMI 9, 55% of the 59 ignitions will be within a relay-able distance of 1,000 feet from the resilient grid, so that 22 of the ignitions can be prevented from becoming large fires, for a benefit of $19.6 billion (although there are still $33 billion in fire losses). Losses due to loss of service are $513 million, or a reduction of $83 million. Total benefits of the resilient grid are thus about $19.7 billion.

Comparably, for MMI 10, the benefit of the resilient grid is $19.8 billion.

[9] "Relay" here refers to the series deployment or "daisy-chaining" of fire engines, so as to serially pump water from a source to the fireground. A Class A fire engine is typically able to pump 1,500 gpm 1000 feet through a 5-inch hose, termed large diameter hose (LDH), which is within the capability of most urban fire departments (although the supply of LDH may be limited). Frictional loss in the hose is the limiting factor on distance and pressure.

| | MMI 6 | MMI 7 | MMI 8 | MMI 9 | MMI 10 |
|---|---|---|---|---|---|
| Losses without resilient grid | $- | $138 | $19,007 | $53,224 | $152,774 |
| Losses with resilient grid | $- | $119 | $8,667 | $33,517 | $132,993 |
| Benefit of resilient grid | $- | $19 | $10,341 | $19,707 | $19,782 |
| Cost of resilient grid | $403 | $403 | $403 | $403 | $403 |
| Benefit-cost ratio | 0 | 0.05 | 25.7 | 48.9 | 49.1 |

**Table 29.** Summary of losses and benefits with and without resilient grid given MMI shaking ($ millions).

## 6.5 Results

The as-is system consists of 4.39 million feet of 6-inch distribution pipe and 504,000 feet of 16-inch trunk line pipe, with a replacement value at $50 per inch-feet of $1.32 billion and $403 million, respectively. This system provides potable and firefighting water for a study region with a population of 787,500 and value of $100.8 billion.

Benefits of a resilient grid are defined as reduction in losses attributable to the resilient grid, which are determined as fire losses and economic losses due to loss of service for the as-is system, minus those for the system with a resilient grid. These are summarized in Table 29 for selected levels of seismic intensity, and are seen to increase with increasing seismic intensity. It should be noted that these benefits are conditioned on the occurrence of the event.

Annual frequency of seismic intensity is inversely correlated and varies by location in the United States, as can be seen in Figure 52 for several West Coast cities.

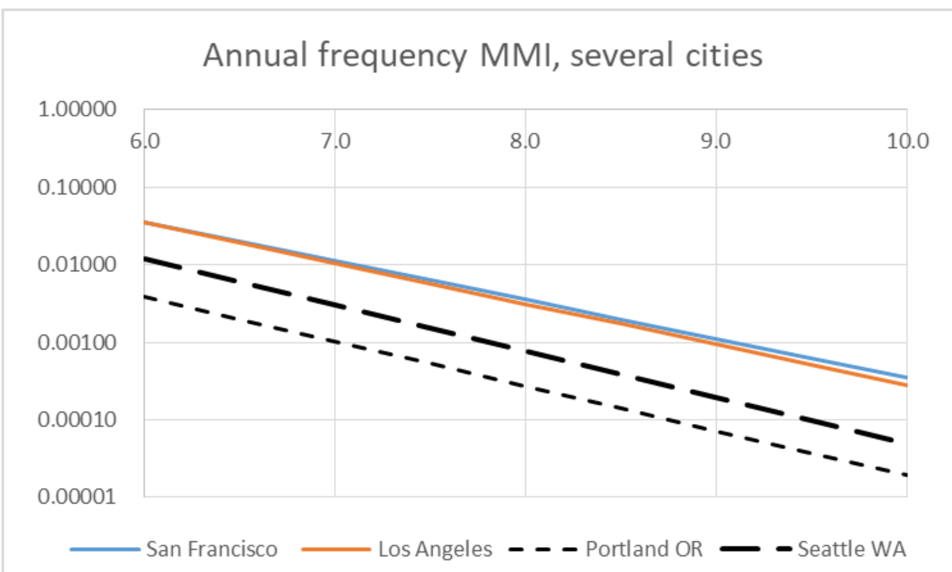


Source: adapted from https://earthquake.usgs.gov/hazards/interactive/.

**Figure 52.** Annual frequency of MMI for Los Angeles, San Francisco, Portland, and Seattle, vs. 300 mps.

Given these intensity curves and the benefit data (interpolated linearly between integer values of *MMI*), the project team numerically integrated to determine the benefit per annum, $B_{pa}$, attributable to a resilient grid:

$$B_{pa} = \sum_{MMI=6}^{9} B(MMI)f(MMI)\Delta MMI$$

(Equation 14)

where *B(MMI)* is the benefit as a function of *MMI, f(MMI*) is the annual frequency of *MMI*, and $\Delta MMI$ is the *MMI* interval employed in the numerical summation. This calculation was performed for four West Coast cities using ground motion annual frequency data obtained from OpenSHA (Field et al. 2005) for San Francisco and Los Angeles, and Peak Ground Acceleration (PGA) for Portland and Seattle obtained from USGS national seismic hazard maps. This data was converted to MMI using Wald et al. (1999). The present value of all future benefits *PV(B)* is then:

$$PV(B) = \int_0^T B_{pa} e^{-It} dt$$

(Equation 15)

where *I* is the cost-of-borrowing discount rate per annum, and *T*, the time horizon of interest, was taken as 100 years. Using these values and integrating benefits and annual frequency of occurrence of *MMI*, the project team found the present value of all future benefits for the hypothetical study region sited so as to have the seismic hazard of several West Coast cities. Dividing the present value of all future benefits by the replacement value of the resilient grid (which assumes the existing trunk lines are rebuilt with ERDIP pipe and seismic isolation valves), the project team determined the benefit cost ratio, *BCR*:

*BCR* = *PV(B)* / replacement cost

(Equation 16)

This has been done for the four West Coast cities using a cost-of-borrowing discount rate of 2.2%, as shown in Table 30. The higher seismic hazard locations of San Francisco and Los Angeles have BCRs of about 6 to 8, Seattle 1.7, and Portland less than 1. Table 31 shows BCRs for discount rates of 2.2%, 3%, and 7%, indicating that resilient grids are clearly cost-beneficial for cities in high to very high seismic regions (i.e., Seattle, San Francisco, and Los Angeles) but may not be cost-beneficial for a moderate region such as Portland.

However, it should be noted that these BCRs are all based on long-term seismic hazard probabilities and not time-dependent probabilities. All four cities are judged to be at high risk of a major earthquake in the near term, which, if taken into account, would increase the BCRs significantly.

| | San Francisco | Los Angeles | Portland OR | Seattle WA |
|---|---|---|---|---|
| Benefit per annum, $B_{pa}$ ($ million) | $82.1 | $62.27 | $5.85 | $17.10 |
| *PV(B)* ($ million) | $3,340 | $2,534 | $238 | $696 |
| Replacement value resilient grid ($ million) | $403 | $403 | $403 | $403 |
| Benefit-cost ratio, *BCR* | 8.3 | 6.3 | 0.6 | 1.7 |

**Table 30.** Summary of benefits and BCR, four West Coast cities (cost-of-borrowing discount rate of 2.2%).

## 6.6 Summary and Conclusions

The project team examined the benefits of an urban water distribution resilient grid concept using an idealized study region that was representative of a typical medium-sized U.S. city. The study region was modeled as a buried water distribution network consisting of a 600 feet rectangular grid of 6-inch diameter distribution pipes, with 16-inch trunk lines spaced every 10$^{th}$ distribution pipe. The project team selected this sizing to provide adequate potable and firefighting demands for the study region, and is representative of an urban water grid. The grid is fed from supplies arriving at two relatively central points on the trunk line grid, typical of terminal reservoirs.

The examined stress event, earthquake, affects the grid in two ways: (a) the earthquake causes numerous leaks and breaks (collectively termed repairs) by shaking and ground failure, and (b) the earthquake also causes fires to ignite due to the shaking, which create extraordinary fire flow demands on the system. Modeling follows accepted guidelines for pipe repairs (ALA 2001) and post-earthquake ignitions, fire growth, and fire flow demands (SPA Risk 2009, TCLEE 2005). PGD effects are modeled as a simple increase in repair rates averaged over the entire system, rather than focused in a few areas of the network.

Given these demands, the network is hydraulically analyzed in a PDA mode using EPANET (Rossman 2000) to determine the network capacity vis-à-vis these demands. As summarized in Table 31, repairs and ignitions vary from 29 repairs and 4 ignitions for MMI 6, to 402 repairs and 170 ignitions at MMI 10, with losses increasing from approximately nil at MMI 6 to $153 billion at MMI 10, dominated by fire losses. Because the fire service is overwhelmed after approximately 22 ignitions, only a portion of the fire losses should be attributed to a water system lack of capacity, so that water-related losses are capped at approximately $20 billion for fire, while losses due to lack of potable supply continue to increase at a more modest rate. Thus, water system-related losses approximate nil at MMI 6 to $20.7 billion at MMI 10. All of these losses are for the as-is system, without a resilient grid; that is, repairs are required to both the distribution and trunk lines.

The resilient grid concept involves replacement of the trunk lines with low-vulnerability pipe, such as is currently available by ERDIP type pipe. The resilient grid then is considered not significantly damaged by earthquake, and isolated from the damaged distribution network by seismically actuated valves. Such valves are quite feasible. For example, they have been employed on the San Francisco Auxiliary Water Supply System since the 1990s. The resilient grid has a 6,000 feet spacing so that, combined with hose lays by the fire service, it brings potable supply to within 3,000 feet of all customers, thus providing firefighting water supply at

55% of the ignitions. In this manner, fire losses are significantly reduced, especially at moderate MMI intensities (i.e., 6~8) and potable water supply is significantly improved. While not quantified, it is quite likely that only a few repairs to the distribution system, combined with the resilient grid, would allow quick re-establishment of water supply to large numbers of customers in selected portions of the grid.

Using conservative estimates of the benefits accruing to the resilient grid, and taking the cost of the resilient grid as full replacement of all existing trunk lines, benefits are determined, and range from approximately nil at MMI 6 to $20 billion at MMI 10. Applying annual frequencies of these intensities for four West Coast U.S. cities, the project team found that the resilient grid has a BCR of about 6 to 8 for seismic environments typical of Los Angeles and San Francisco, a value of 1.7 for Seattle, and 0.6 for Portland, based on a cost-of-borrowing discount rate of 2.2%. If higher discount rates are employed, these BCRs decline, for a discount rate of 3%, to 5 to 6 for Los Angeles and San Francisco, and 1.3 and 0.5 for Seattle and Portland, respectively, and for a discount rate of 7%, to 2 to 3 for Los Angeles and San Francisco, and 0.6 and 0.2 for Seattle and Portland, as summarized in Table 31.

| Discount rate (pa) | San Francisco | Los Angeles | Portland OR | Seattle WA |
|---|---|---|---|---|
| 2.2% | 8.3 | 6.3 | 0.59 | 1.73 |
| 3.0% | 6.4 | 4.9 | 0.46 | 1.34 |
| 7.0% | 2.9 | 2.2 | 0.21 | 0.61 |

**Table 31.** Summary of resilient watergrid BCRs for several discount rates, four West Coast cities.

In summary, the resilient grid concept is cost-beneficial in high to very high seismic regions (i.e., Seattle, San Francisco, and Los Angeles). These BCRs are based on long-term seismic hazard probabilities. Since all four cities are judged to be at high risk of a major earthquake in the near term, if time-dependent hazard probabilities are taken into account the BCRs would increase significantly. Observations include:

- The major benefit of the resilient grid is due to improved supply of firefighting water.
- The benefit of the resilient grid is constrained by the capacity of the fire service. For the study area, this plateaus at about 22 ignitions. If the fire service can increase its capacity, for example, by having a greater capacity to move water via tanker trunks or portable water supply systems, then the resilient grid is much more beneficial.
- The above observation reinforces the point that the resilient grid concept is not solely a water department initiative, but would need to be pursued in close cooperation with the fire service.
- Irrespective of the fire aspect, however, the resilient grid is quite likely to result in significantly reducing the time to restore the water supply to customers.
- Closer spacing of the resilient grid may not significantly increase the BCR. That is, while closer spacing (e.g., trunk lines at every 5th or 6th distribution line, rather than every 10th) increases benefits, it also increases costs. If the trunk line spacing is every 5th distribution line, for example, then the cost of a resilient grid is more than $800 million. The project team did not perform in detail the calculation of BCRs for closer (or more sparse) trunk line spacing, but examination of the results for the 1 to 10 spacing of the study region

indicates that the BCRs would in fact remain about the same if the spacing were made 1 to 5.

- The above findings on BCRs are based on the conservative assumption that the resilient grid requires the replacement of 100% of the trunk lines, which is probably overly conservative. If, alternatively, it is assumed that only a portion of the resilient grid requires replacement (e.g., say 50% of the existing trunk lines are considered of low vulnerability), then the above BCRs are doubled.

In conclusion, based on a limited examination of an idealized study region representative of a medium-sized U.S. city, the concept of a resilient grid is clearly cost-beneficial for high seismicity regions. Future studies might examine the resilient grid for other types of stress events, such as flooding or tropical cyclones.

# 7 Benefit-Cost Analysis of a Resilient Electric Grid

## 7.1 Purpose and Focus

The purpose of this sub-task was to examine the benefits and costs of achieving electric power grid resilience. As noted in the *Quadrennial Energy Review* of the Department of Energy (DOE 2017), "The reliability of the electric system underpins virtually every sector of the modern U.S. economy." Note that quotations in this section are from DOE (2017) unless otherwise noted.

Electric power is not only important in itself, it also underpins virtually all other infrastructure and economic activity, as shown in Figure 53. This importance has been underscored in very large blackouts, which have affected tens of millions of people. Examples include the 2012 blackout in India, which affected 700 million, and the 2003 U.S. Northeast Blackout, which affected 50 million (Duddu 2015). Such blackouts have typically been due to overload or equipment failure, rather than extreme external events such as hurricanes or earthquakes, although extreme events are a significant cause. See Table 32.

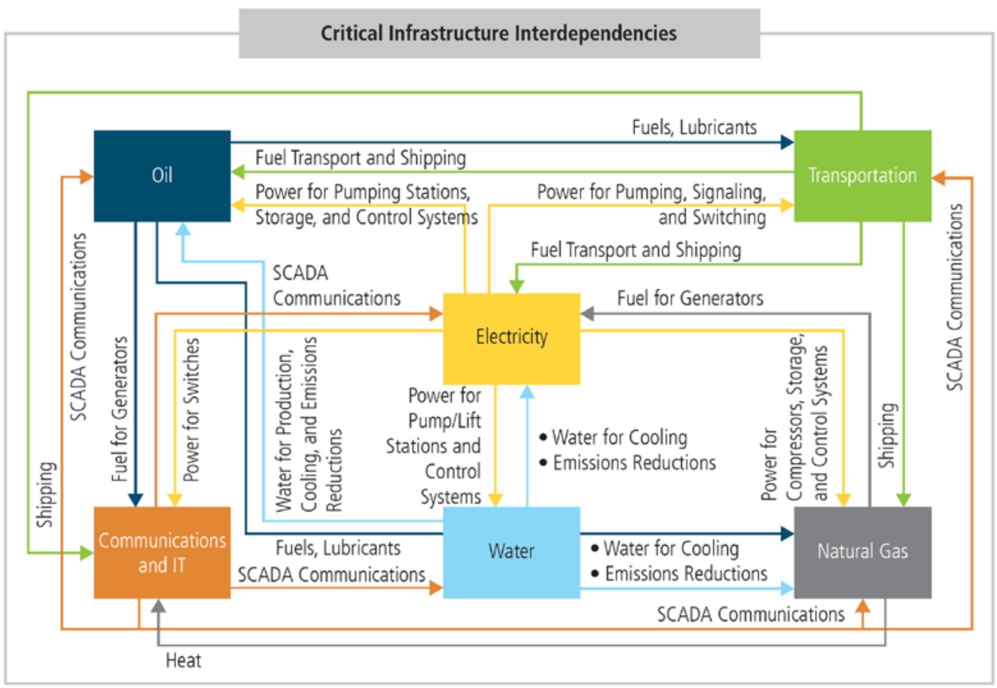


**Figure 53**. Importance of electric power and critical infrastructure dependencies (DOE 2017).

| Cause | Percent of events | Mean size (MW) | Mean size (customers) |
|---|---|---|---|
| Earthquake | 0.8 | 1,408 | 375,900 |
| Tornado | 2.8 | 367 | 115,439 |
| Hurricane/tropical storm | 4.2 | 1,309 | 782,695 |
| Ice storm | 5 | 1,152 | 343,448 |
| Lightning | 11.3 | 270 | 70,944 |
| Wind/rain | 14.8 | 793 | 185,199 |
| Other cold weather | 5.5 | 542 | 150,255 |
| Fire | 5.2 | 431 | 111,244 |
| Intentional attack | 1.6 | 340 | 24,572 |
| Supply shortage | 5.3 | 341 | 138,957 |
| Other external cause | 4.8 | 710 | 246,071 |
| Equipment failure | 29.7 | 379 | 57,140 |
| Operator error | 10.1 | 489 | 105,322 |
| Voltage reduction | 7.7 | 153 | 212,900 |
| Volunteer reduction | 5.9 | 190 | 134,543 |

Note: MW = megawatts

**Table 32.** Blackout initiating events (Source: NERC data 1986-2003, from Hines et al. 2008).

Regarding measuring resilience, "… a number of resilience metrics and measures have been proposed; however, there has not been a coordinated industry or government initiative to develop consensus or implement standardized resilience metrics", so this study employs the decrease in expected service outage as a measure of resilience, together with the associated decreases in economic losses. A significant contributor to resilience is grid reliability: "Reliability of the grid is a growing and essential component of national security… [and]…Standard definitions of reliability have focused on the frequency, duration, and extent of power outages" and have not considered in a systematic manner the potential for widespread long-duration outages due to major natural disasters.

Note that DOE (2017) defines and measures reliability as "the ability of the system or its components to withstand instability, uncontrolled events, cascading failures, or unanticipated loss of system components. Resilience is the ability of a system or its components to adapt to changing conditions and withstand and rapidly recover from disruptions…reliability is formally defined through metrics describing power availability or outage duration, frequency, and extent…One metric applied with the goal of improving system performance with respect to reliability indicators is the System Average Interruption Duration Index (SAIDI). SAIDI measures the total duration of an interruption for the average customer given a defined time period…As most outages occur on the distribution system rather than the bulk power system, these reliability indices are commonly used to measure distribution level reliability. NERC [National Electric Reliability Corporation] uses a number of bulk power system reliability indices…utilities have historically reported SAIDI ... statistics in inconsistent ways… only 33 percent of utilities report these statistics, covering 91 percent of the electricity sales in the Nation, which indicates that there is room for improving reliability reporting practices." Note that other metrics of electric system performance exist, and they too are often reported inconsistently.

The electric power grid is complex, with multiple types of electric generation and storage, and transmission and distribution to the end user, as schematically depicted in Figure 54. These elements are subjected to a number of threats, as shown in Figure 55, from which it can be seen that one of the more critical elements of the system are substations. This is emphasized in Figure 56, which shows that substations are probably the most crucial element of the electric power system, due both to their vulnerability as well as the topology of the grid (multiple sources and transmission paths, but multiple paths converging at substations).

It should be noted that the electric power system is evolving and a new grid is emerging with more controllability ("With the advent of more two-way flows of information and electricity—communication across the entire system from generation to end use, controllable loads, more variable generation, and new technologies such as storage and advanced meters—reliability needs are changing…") as well as more end-user, close-in generation (e.g., photovoltaic). However, the system model used here (source-transmission-substation-distribution-end-user) is what currently exists, and will exist for a significant period going forward.

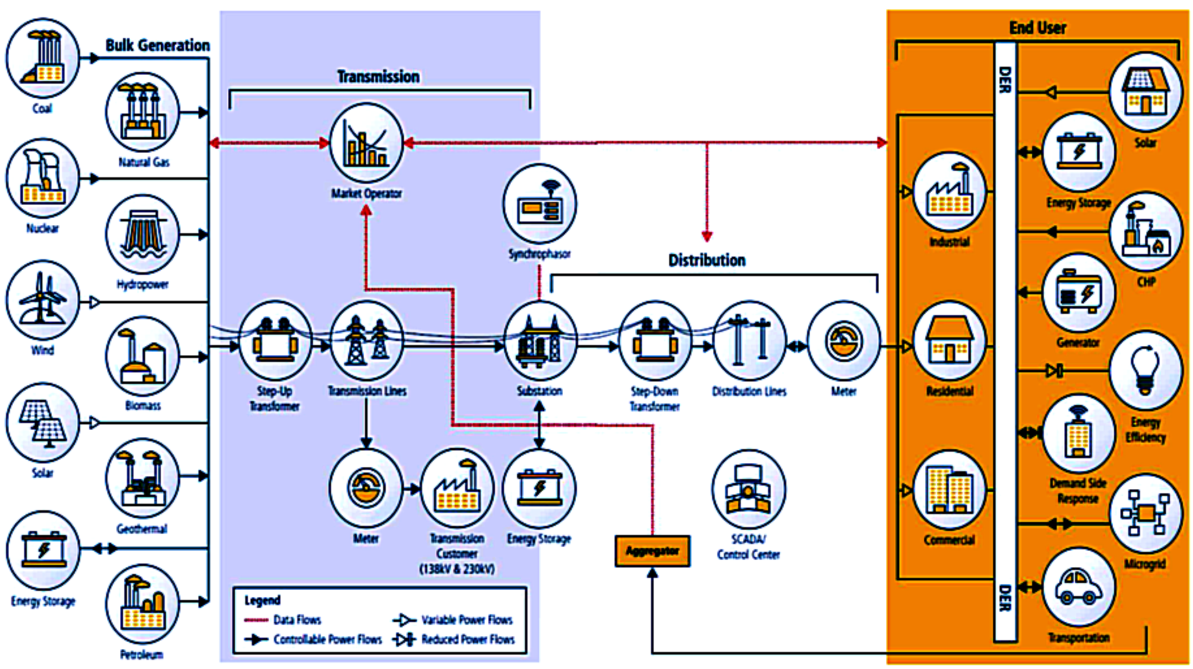


**Figure 54**. Schematic representation of the U.S. electric power system. (Adapted from DOE 2017).

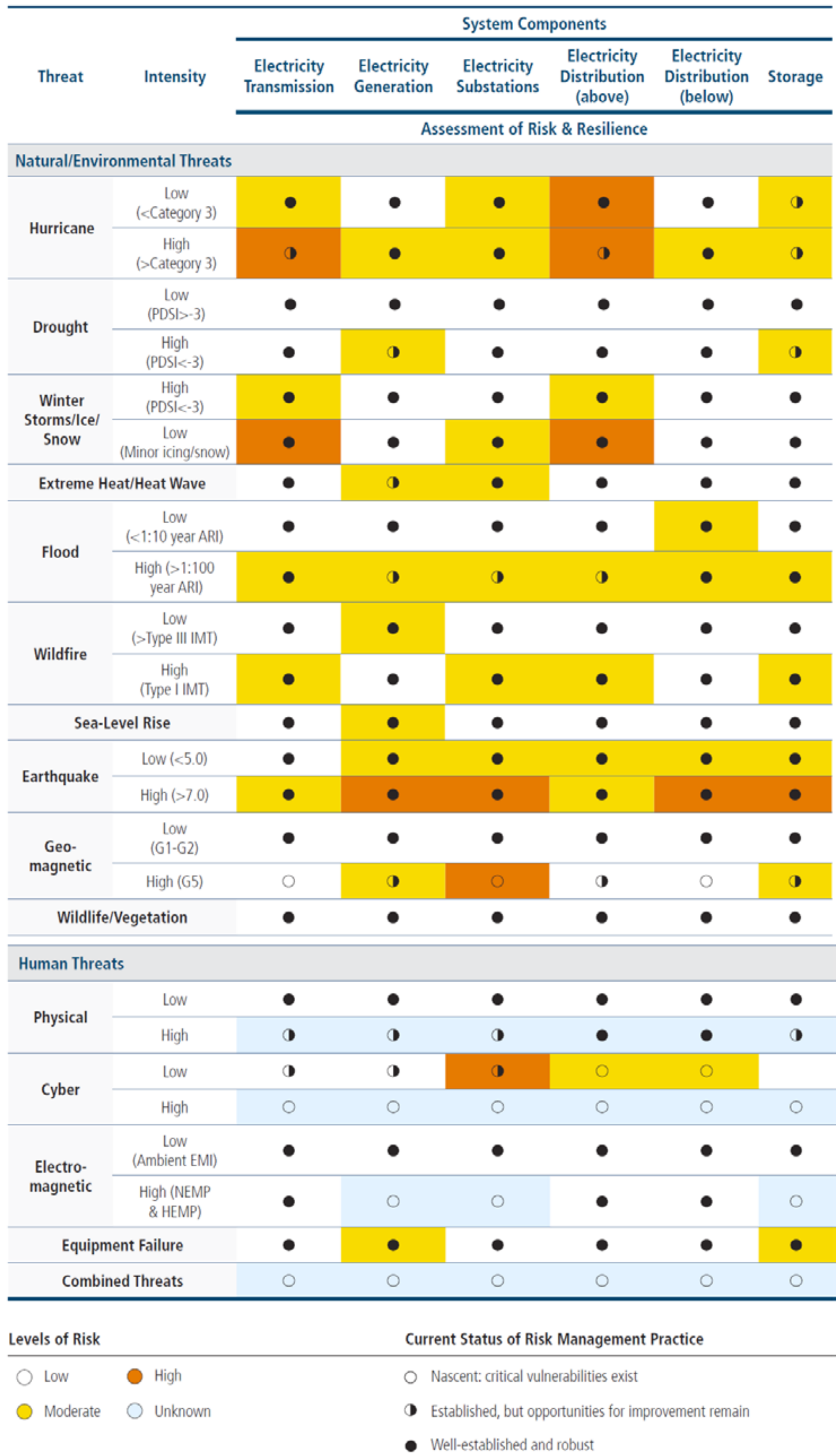


**Figure 55**. Risks to electricity sector resilience from current threats (DOE 2017).

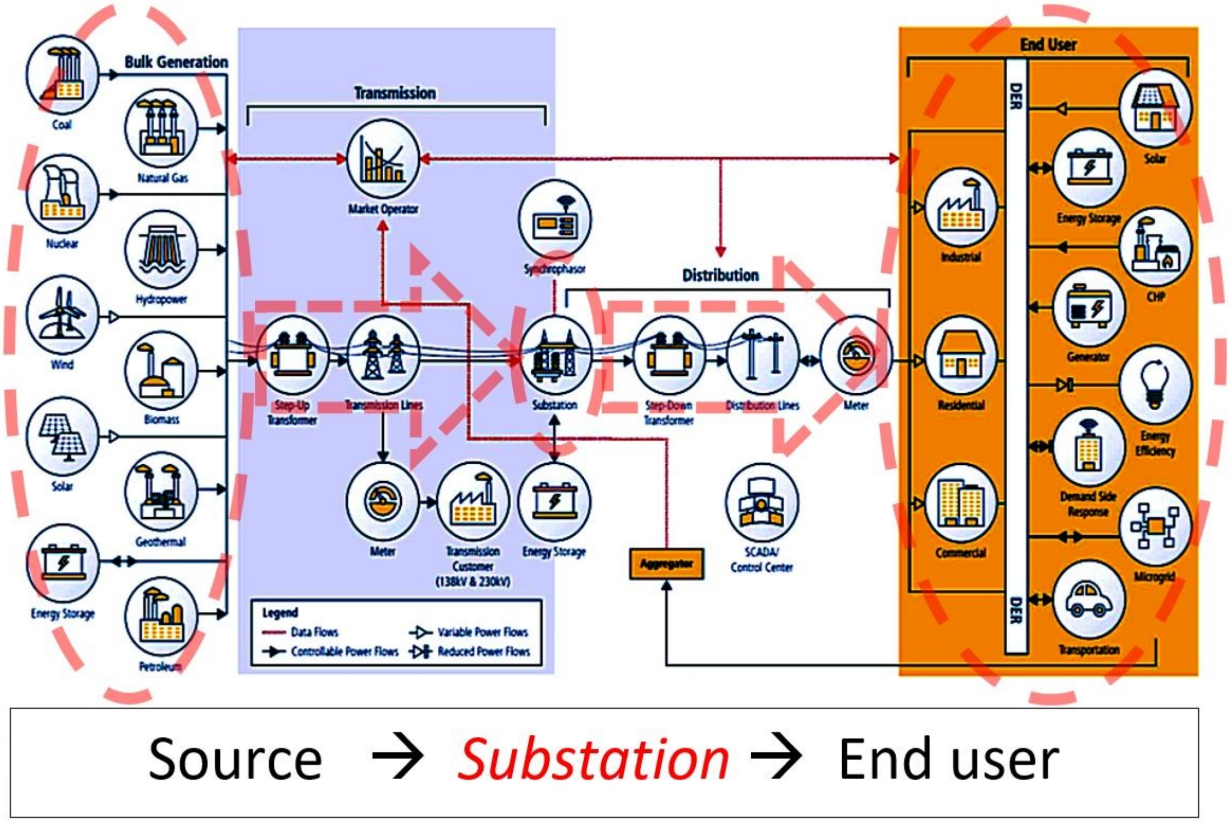


**Figure 56.** Schematic representation of the U.S. electric power system showing EHV substations as a critical link. (Adapted from DOE 2017).

Electric power systems, and substations in particular, are vulnerable to earthquakes. Examples of the impacts of earthquakes on electric power systems are given in Romero et al. (2015):

- On January 17, 1994, the Northridge Earthquake struck the city of Los Angeles and surrounding areas; 2.5 million customers lost power. (Dong et al. 2004)
- On January 17, 1995, the Great Hanshin Earthquake occurred, affecting the city of Kobe, Japan, where 20 fossil-fired power generation units, six 275-kV substations, and two 154-kV substations were damaged; approximately 2.6 million customers were affected by outages. (Noda 2001)
- On May 18, 2008, the Wenchuan Earthquake caused extensive damage to local power transmission and distribution systems in Sinchuan Province, China; approximately 900 substations and 270 transmission lines of the State Power Grid were damaged. (Eidinger 2009)
- Immediately following the February 27, 2010, 8.8-MW Chilean Earthquake, 90% of Chileans did not have electricity, which caused the largest power transmission company in Chile to have direct losses of approximately U.S. $6.5 billion. (Long 2010)
- On March 11, 2011, the devastating Tohoku Chiho–Taiheiyo-Oki Earthquake damaged 14 power plants, 70 transformers, and 42 transmission towers, and caused other failures. Outages affected 4.6 million residences, and the April 7 aftershock affected an additional 4 million. (Shumuta 2011)

Regarding seismic vulnerability of electric substations, there is extensive literature on the performance of substation components (ASCE 1999, Fujisaki 2009, Hosseini 2009, Hosseini et al. 2009, Knight and Kempner 2009) and several guidelines and standards for seismic design (ASCE 1999, IEEE 693 2005). Retrofitting also has been dealt with (Knight and Kempner 2009, Romero et al. 2015, Oikonomou et al. 2016), with some investigations of benefits (Neudorf et al. 1995, Shumuta 2004, Han et al. 2007), but costs of retrofitting substations do not explicitly appear in the literature and there is little to no quantification of BCRs (e.g., Neudorf et al. 1995, who seek the minimum cost alternative, not the BCR).

Given the above knowledge gaps, the focus of this study then was the benefit versus cost of reducing the vulnerability of electric substations and the impact of this vulnerability on service outage. The project team examined the hazard of earthquake, with two conditions: substations with standard (i.e. non-seismically designed) components, versus a substation with seismically designed components. Benefits are the decrease of direct damage and costs of service outage, given seismically designed components. Cost is the financial burden of retrofitting substation components.

## 7.2 Electric Power Grid and Substations Vulnerability

High voltage (HV), 138 kV and greater, and extra high voltage (EHV), 345 kV and greater, electric transmission lines are shown in Figure 57 overlaid on NERC regions, with substations overlaid on Core-Based Statistical Areas (CBSA, greater than 100,000 population) in Figure 58. Reviewing these two figures, it can be seen that major power imports to urban areas pass through a number of large substations, failure of which would disrupt service to major population centers. Analysis of this data shows that in urban areas, high voltage substations on average serve 30,000 customers, with a substation spacing of about 7 km.

HV and EHV substations serve two basic purposes: switching (i.e., opening and closing circuits) and transforming voltage (e.g., from higher to lower voltage). Switching is inherently required in transmission and distribution of electric power via networks, while voltage is transformed at the generator to higher voltage for transmission, and then must be reduced (or stepped down) close to load centers for use at lower voltages. Within the fence of a substation is typically a network of overhead bus (rigid or flexible), which connects switches, circuit breakers, transformers, and other equipment, and sometimes a small building housing monitoring and control equipment. See Figure 59. Switches are required for routing electricity, as well as isolating equipment to protect against overload as well as for maintenance. HV and EHV transformers are typically large, heavy (100 tons and more) equipment that historically are supported on a concrete pad without sufficient attachment for earthquake lateral loading (Kempner Jr. 2008). Large ceramic bushings on the transformers are also vulnerable to seismic loading. Retrofitting of substations typically involves providing sufficient anchorage for transformers and other equipment (occasionally, base isolation is employed), use of more seismically resistant bushings, and allowance for differential movement of bus and equipment under lateral loading. Control buildings, if present, are strengthened. Of these measures, perhaps the most crucial, as well as a cost driver, is the anchorage of transformers (Romero et al. 2015).

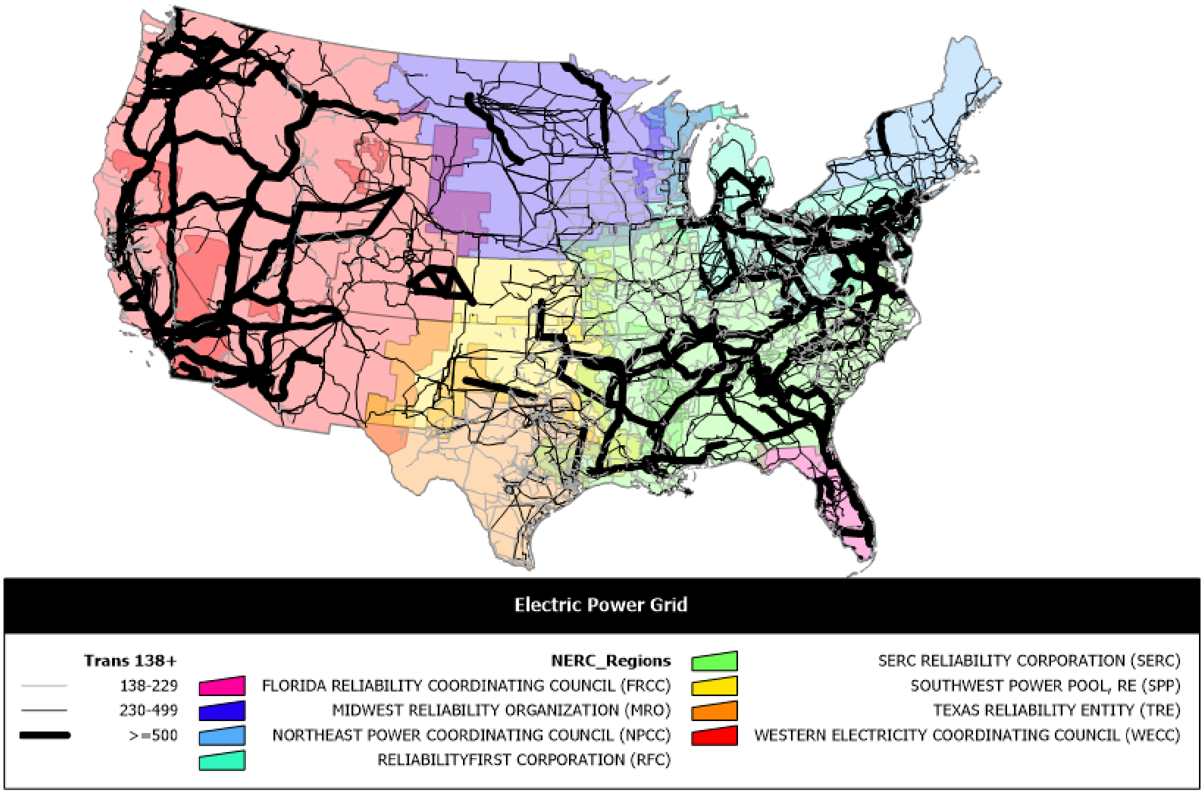


**Figure 57.** Electric transmission (138 kV and greater) overlaid on NERC regions.

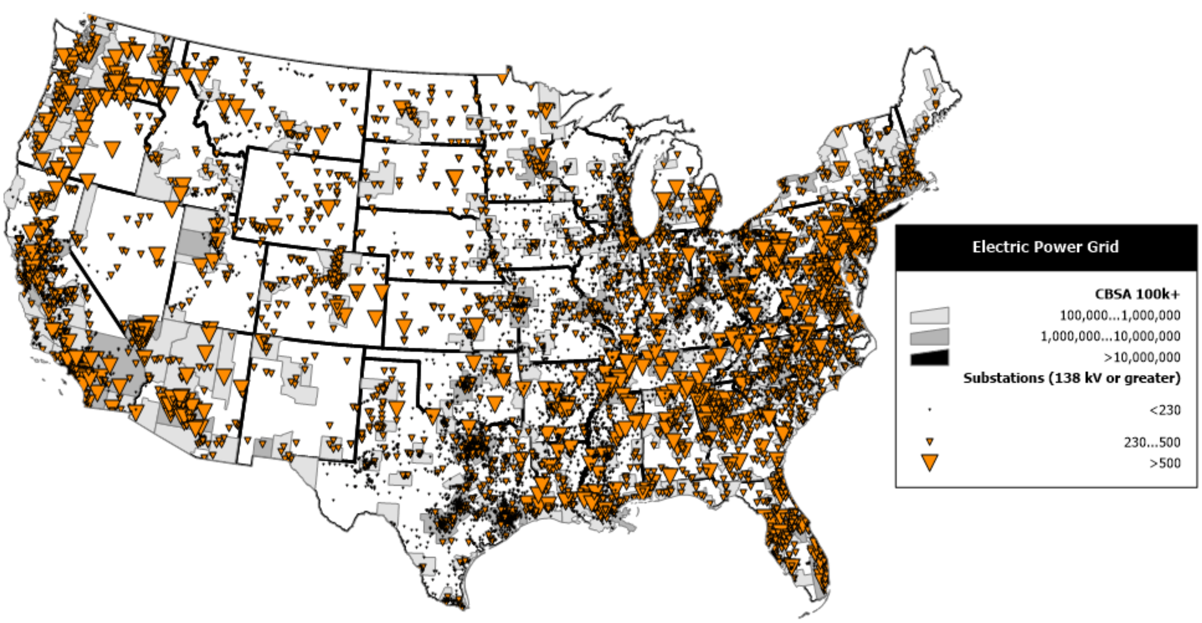


**Figure 58.** Substations (138 kV and larger voltage) overlaid on Core-Based Statistical Areas (CBSA), greater than 100,000 population.

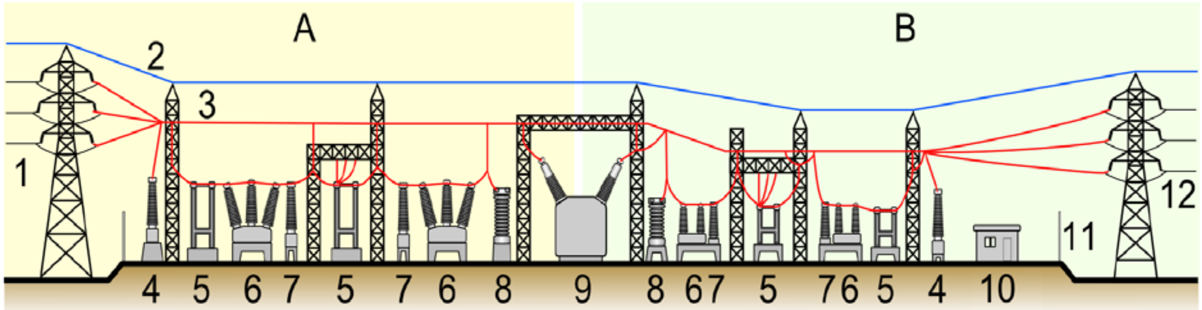


A: Primary power side; B: Secondary power side; 1. Primary power lines; 2. Ground wire; 3. Overhead lines; 4. Transformer for measurement of electric voltage; 5. Disconnect switch; 6. Circuit breaker; 7. Current transformer; 8. Lightning arrester; 9. Main transformer; 10. Control building; 11. Security fence; 12. Secondary power lines

**Figure 59.** Substation schematic.

Figure 60 shows the threat to major urban substations in California by overlaying their locations on a map of a 2% in 50 years probability of PGA exceedance. It can be seen that many substations are subject to a very high seismic hazard. Values for vulnerability of substations are available from various sources (Anagnos and Ostrom 2000, DHS 2003, FEMA 2003, Kempner Jr. 2008, Fujisaki 2009, Kempner Jr. 2009, Knight and Kempner 2009). In this study, the project team used substation fragility and outage duration data from FEMA (2003). Figure 61, for example, shows the probability of a substation being in the complete damage state for a substation with (U) unanchored equipment, with anchorage designed for a PGA of 0.47g and for a PGA of 1g. Complete damage is defined by FEMA (2003) as the "failure of all disconnect switches, all circuit breakers, all transformers, or all current transformers, or by the building being in complete damage state." Other damage states are minor, moderate, and extensive. Table 33 presents the Hazus estimate of the parameters of substation fragility and restoration time for each damage state.

| Damage state | Unanchored | | | | Anchored | | | |
|---|---|---|---|---|---|---|---|---|
| | Min | Mod | Ext | Compl | Min | Mod | Ext | Compl |
| Median PGA (g) | 0.09 | 0.13 | 0.17 | 0.38 | 0.1 | 0.15 | 0.2 | 0.47 |
| Standard deviation of the natural logarithm of capacity, β | 0.5 | 0.4 | 0.35 | 0.35 | 0.5 | 0.45 | 0.35 | 0.4 |
| Median duration outage (days) | 1 | 3 | 7 | 30 | 1 | 3 | 7 | 30 |

**Table 33.** Fragility and median duration of outage, high voltage substations (FEMA 2003).

Using this data, a substation subjected to 0.2g PGA and having unanchored equipment will on average be out of service for about 6.1 days, while if anchored to a design PGA of 0.47g, the outage will be about 4.8 days, or a net benefit of the anchoring of about a 1.3 days' reduction in outage. If the anchorage is designed for a PGA of 1g, the outage is approximately half a day and the net benefit about a 5.6 days' reduction in outage.

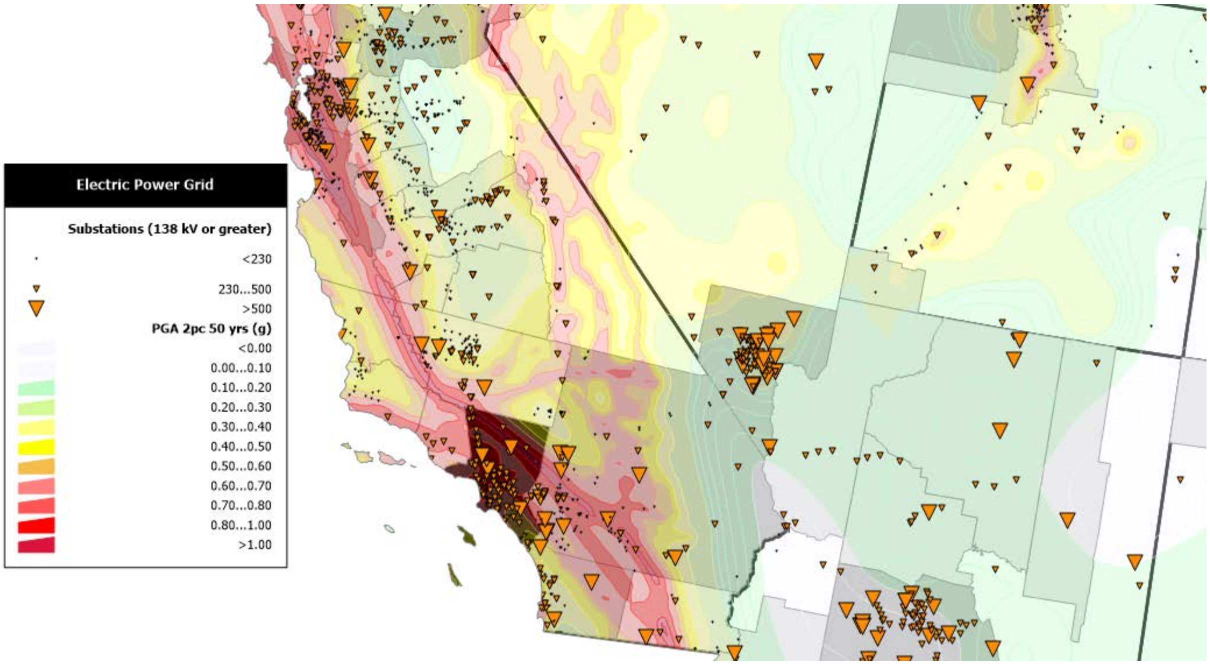


**Figure 60.** Substations (138 kV and larger voltage) overlaid on CBSA and peak ground acceleration (PGA, 2% probability of exceedance in 50 years), Southwestern United States.

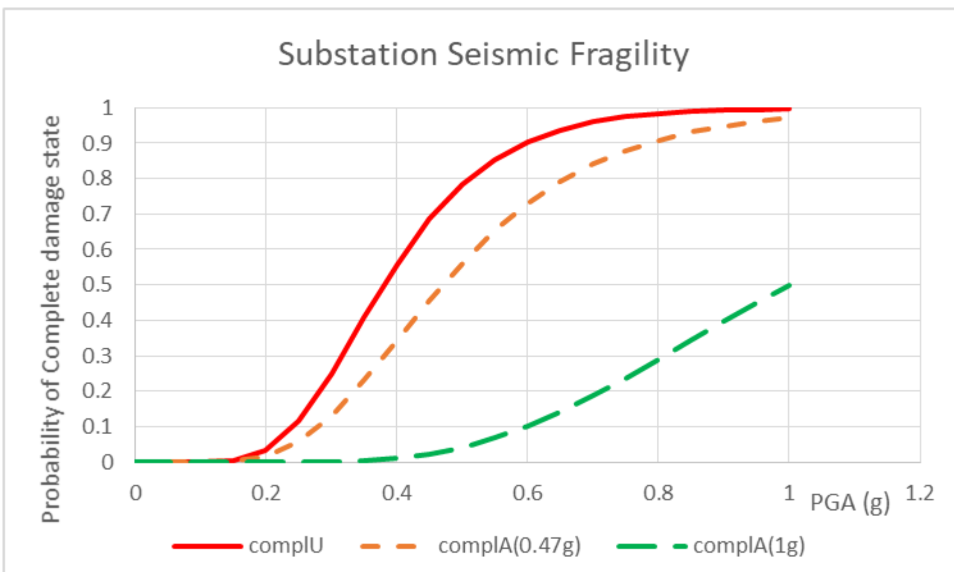


**Figure 61.** Substation seismic fragility – probability of complete damage state if unanchored (U), anchored (A) to 0.47g design, and anchored to 1.0g design.

## 7.3 Impacts of Loss of Electric Power

The difference in electric power outage is a measure of the benefit of the resilient grid, which can more specifically be quantified in terms of reduced losses in several categories.

### 7.3.1 Substation Repair and Retrofitting Costs

Assuming no ground failure, substation repair costs are dominated by damage to large equipment items, particularly large transformers. High voltage transformers typically cost between $5 and $10 million each (DOE 2012) and a typical substation will have a minimum of three such transformers, so that a minimum value of a substation with all associated equipment will be on the order of $20 to $ 50 million (replacement value of equipment only). Using an average HV substation equipment replacement value of $40 million and Hazus vulnerability data, a substation subjected to 0.2g PGA and having unanchored equipment will on average sustain repair costs equivalent to about 56% of replacement value or $22 million, while if anchored to a design PGA of 0.47g, the loss is about $18 million, or a net benefit of the anchoring of about $4 million. If the anchorage and equipment are designed for a PGA of 1g, the loss is about $1 million and the net benefit about $21 million.

Data on the costs to provide this anchorage are sparse. Based on review of proprietary utility data, as well as some limited data available from this study's review of the FEMA database, a value of $5 million per substation is assumed for seismic retrofit.

### 7.3.2 Economic Losses Resulting from Loss of Electric Service

Economic losses resulting from loss of electric service include:

- Direct damage and losses (e.g., food spoilage);
- Direct business interruption due to loss of electric service (e.g., loss of ticket sales at an amusement park); and
- Indirect business interruption losses to the rest of the economy that does business with customers who lose electric service (e.g., loss of parking revenue due to closure of the amusement park).

Numerous studies have been conducted on the economic impacts of blackouts, although almost all address non-disaster caused blackouts of relatively short duration, such as the 2003 Northeast Blackout (Tiedemann and Hydro, LaCommare and Eto 2006, Rose et al. 2007a, Küfeoğlu and Lehtonen 2015, Larsen et al. 2017). The outages addressed in such studies are typically less than a day and more typically an hour, so that they have little direct relevance to this study. An exception is Rose et al. (2007b), from which a current (2018) value of disruption of about $146 per capita per day emerges, for business interruption only. An alternative approach used here is as follows based on a hypothetical outage in California.

Let:

- LTEWA = total weighted average time element loss per day per person who lives in the area affected by loss of power = (1 + Q) × LDTEWA
- Q = indirect time element loss as a factor of direct time element loss, from the *2017 Interim Report* = 0.5
- LDTEWA = weighted average direct time element loss per day per person who lives in the area affected by loss of power = LDBIW × (total number of California firms)/(total California population) + LALER
- LDBIW = loss per day from direct business interruption for workplaces, per workplace = (total California gross state product)/((total number of California firms) × 365)
- LALER = loss per day from additional living expenses for homes, per resident

Using the following data:

- Total California population[10] = 39,536,653
- Total number of California employer establishments[11] = 922,477
- Total number of California non-employer establishments[12] = 3,206,958
- Total number of California firms = total number of California employer establishments + total number of California non-employer establishments =922,477 + 3,206,958 = 4,129,435
- California gross state product[13] = $2,746,873,000,000
- GSA per diem for meals and incidental expenses, not including accommodations[14] = $64

Then LALER = $64, Total number of California firms = 4,129,435, LDBIW = $1,822, LDTEWA = $254, Q = 0.5 and LTEWA = $381. This approach results in an estimate of about 2.6 times that of Rose et al. (2007a). Lacking more accurate data and noting that Rose et al's estimate is for business interruption only, this study uses $300 as the total direct and indirect cost of loss of electric service per day.

### 7.3.3 Deaths, Injuries, and Instances of PTSD Resulting from Loss of Electric Service

Loss of electric service can result in deaths, injuries, and instances of PTSD, for example, due to added traffic accidents in the absence of working traffic signals. While a number of papers in the literature qualitatively discuss this aspect (Beatty et al. 2006, Henneaux et al. 2011, Lin et al. 2011, Matthewman and Byrd 2014), only Anderson and Bell (2012) provide quantitative data, finding about 90 excess deaths occurred in New York City due to the 2003 Northeast Blackout, which had an average duration of about two days. This equates to 0.000005625 deaths per capita per day, which the project team used in this study. The value of a statistical life or cost due to a fatality is $9.4 million, so that the economic cost due to fatalities caused by loss of electrical service is $53 per capita per day.

Regarding injuries, the *2017 Interim Report* included an estimate of the number of earthquake-induced deaths and nonfatal injuries in buildings, as a result of all causes: structural damage, nonstructural damage, and other causes, such as falls and occupant behavior. The analysis found that building occupants face a risk of nonfatal injury on the order of 1,000 times as high as the risk of fatal injuries. The ratio counts injuries requiring treatment by medical professionals or paraprofessionals (emergency medical services), not injuries for which people would not typically seek aid. These include four degrees of nonfatal injury severity, from generally most to least severe and from generally least to most common: hospitalized trauma cases, hospitalized non-trauma cases, people treated and released in an emergency department, and those treated outside of a hospital.

As a check of this purely analytically derived ratio of 1,000 nonfatal injuries per death, researchers can compare it with the ratio of nonfatal injuries to fatal injuries in the 1994

---

[10] Per https://www.census.gov/quickfacts/CA.
[11] See note 8.
[12] See note 8.
[13] Per http://www.dof.ca.gov/Forecasting/Economics/Indicators/Gross_State_Product/.
[14] Per https://www.gsa.gov/travel/plan-book/per-diem-rates/per-diem-rates-lookup/?action=perdiems_report&state=CA&fiscal_year=2018&zip=&city=, using Los Angeles as typical value.

Northridge Earthquake. As reported by several studies and compiled in Porter et al. (2006) for each fatal injury, at least 750 people experienced nonfatal injuries. The phrase “at least” refers to the fact that the Northridge researchers counted households rather than individual people for the last two categories of nonfatal injury. Since more than one person could have been injured in households reporting at least one injury, the ratio of people injured to people killed in the 1994 Northridge Earthquake could have been higher than 750. However, the 1994 Northridge Earthquake injured no more than about 1% of the population to the degree that they required medical treatment, so the conditional probability that two people in a household given that one was injured seems low, probably between 1% and 10%. (The conditional probability, asserted here to be between 1% and 10%, is probably higher than the marginal probability—the 1% figure just mentioned—because of correlation resulting from common causes.) Therefore, assume 1.05 persons injured per household with at least one nonfatal injury, suggesting that the Northridge Earthquake injured on the order of 800 people per fatality. Take an average of the two figures—analytical and empirical—as the best estimate for normal, building-related injuries, and use a ratio of 900 nonfatal injuries per fatal injury.

Naturally, this raises questions about the applicability of the 900 to 1 figure in the case of disrupted electric power. Is injury epidemiology from loss of electric power similar to injury epidemiology caused by other earthquake-related causes? The answer matters as to whether the ratio of 900 to 1, which reflects building damage, is actually applicable to electric power. Anderson and Bell (2012) found that most excess deaths during an August 2003 power outage in New York had disease-related causes, as opposed to falls in the dark and other trauma injuries that seem to dominate earthquake-related injuries.

Medicare data show 180 hospital discharges, including deaths, per 1,000 Medicare enrollees nationwide in 2014 (Dartmouth Institute 2018), and 45 deaths per year per 1,000 Medicare enrollees (Krumholz et al. 2015), suggesting 3 nonfatal injuries per fatal injury for disease-related hospitalization.

Determining which ratio to use, 900 to 1 or 3 to 1, impacts the overall BCR. The former is mostly from trauma: impacts by structural and nonstructural objects, falls that seem associated with ground and building movement, and unsafe behavior caused by panic. The latter is purely related to disease, but would exclude some uniquely earthquake-related non-trauma injuries such as dehydration from prolonged entrapment in elevators. A best estimate might lie somewhere between the two figures. The project team used a figure closer to the 3 to 1 ratio than the 900 to 1 ratio, both to err on the low side and because the causes of the 3 to 1 ratio seem more similar to the ones at issue here. The project team therefore used the geometric mean of the two figures, 52 to 1, for the present analysis. Using a value of a statistical injury, or cost due to an injury of \$0.55 million (MMC 2018) is $52 \times \$53 \times (0.55/9.4) = \$161$ per capita per day.

Lacking data, at present no costs are ascribed to PTSD due to loss of electric service.

Therefore, the total cost per capita per day due to the loss of electric service is the sum of the economic costs plus mortality plus morbidity, or \$300 + \$53 + \$161 = \$514 per capita per day.

The total costs of loss of electric service is this value plus direct damage to electric substations. The possibility of damage to generation equipment due to a blackout exists, but is not accounted for in this analysis.

## 7.4 Benefit-Cost Analysis

The benefit of a resilient grid is calculated as the present value of the reduction in losses, accounting for the frequency of shaking that causes those losses. The project team examined four case studies, for substations located in the Los Angeles, San Francisco, Portland, and Seattle regions. As discussed, the cost of retrofit of a substation is $5 million.

Annual frequency of PGA is inversely correlated and varies by location in the United States, as illustrated in Figure 62. Given the hazard and the expected damage under unanchored and anchored conditions, researchers can numerically integrate to determine the benefit per annum, $B_{pa}$, attributable to a retrofitted substation:

$$B_{pa} = \sum_{PGA=0}^{1.5} B(PGA) f(PGA) \Delta PGA$$

(Equation 17)

where *B(PGA)* is the benefit as a function of *PGA*, *f(PGA*) is the annual frequency of *PGA*, and $\Delta PGA$ is the *PGA* interval employed in the numerical summation.

The present value of all future benefits *PV(B)* is then:

$$PV(B) = \int_0^T B_{pa} e^{-It} dt$$

(Equation 18)

where *I* is the cost-of-borrowing discount rate per annum (2.2%), and *T*, the time horizon of interest, was taken as 100 years.

Using these values and integrating benefits and annual frequency of occurrence of *PGA*, the present value of all future benefits for the several West Coast cities is determined. Dividing the present value of all future benefits by the retrofit cost of a substation determines the benefit cost ratio, *BCR*:

$$BCR = PV(B) / \text{replacement cost}$$

(Equation 19)

For San Francisco, the present value of all future losses due to an unanchored substation is found to be $167 million. If the substation is seismically anchored for a design PGA of 0.47g (the default value in Hazus), this value reduces to $129 million, or a reduction of $38.3 million, which has been achieved at a retrofit cost of $5 million – in other words, a BCR of 7.7.

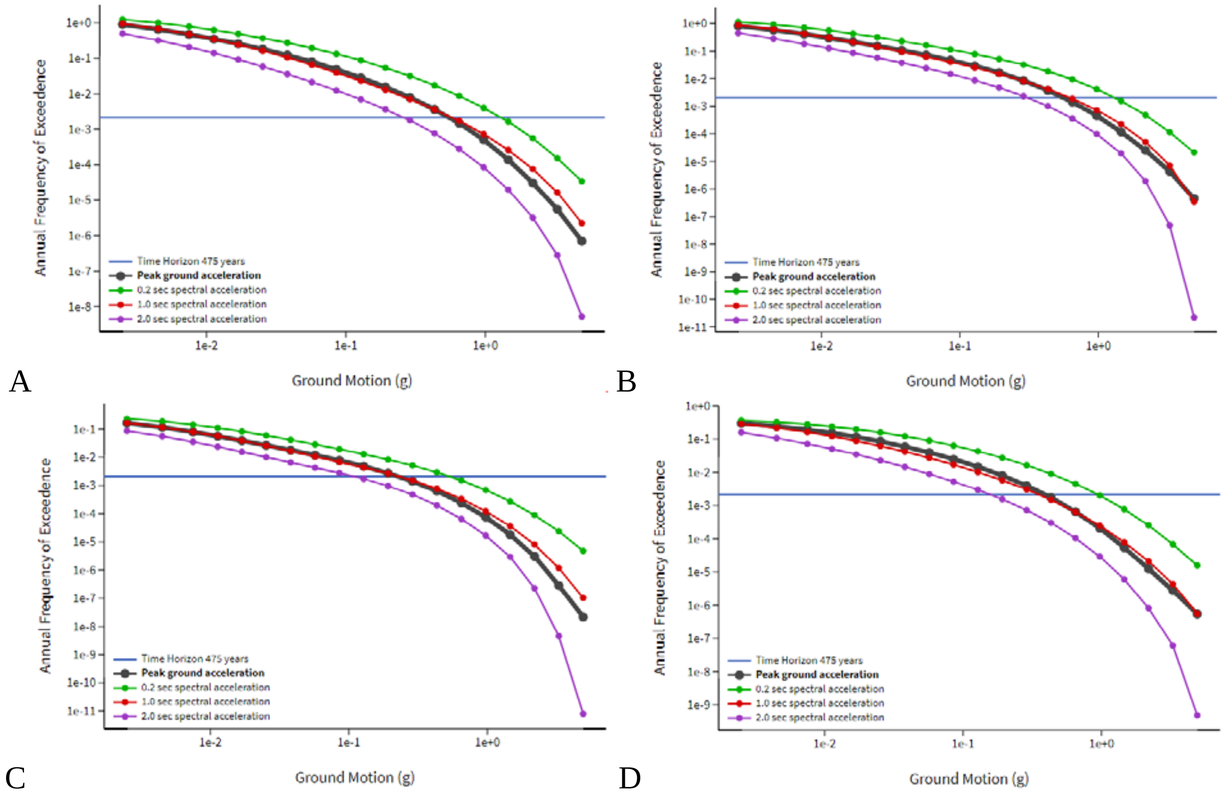


Note: assuming average shearwave velocity in the upper 30 meters of soil to be Vs30 = 360 m/sec.
Source: https://earthquake.usgs.gov/hazards/interactive/.

**Figure 62.** Annual frequency of PGA for (A) Los Angeles, (B) San Francisco, (C) Portland, and (D) Seattle.

However, given that the 0.47g PGA in San Francisco has about a 10% probability of being exceeded in a 50 year period, it would probably be cost-beneficial to anchor the substation equipment for a higher PGA. For an anchorage design value of 1g, which has a negligible added cost, the anchored substation present value of all future losses is $19 million, or a reduction in losses of $148 million; in other words, a BCR of 29.6. This clearly demonstrates the cost effectiveness of mitigating critical infrastructure.

# 8 Benefit-Cost Analysis of Highway Bridge Mitigation for Earthquake

## 8.1 Background

Between the early 1970s and the early 1990s, a series of earthquakes resulted in freeway bridge collapses in urban areas. Notably, 43 people died as a result of a bridge failure following the 1989 Loma Prieta Earthquake in San Francisco. Caltrans identified bridges throughout the state that needed to be retrofitted to meet seismic safety standards (known as a Phase 1). Following the 1994 Northridge Earthquake, additional bridges were identified for a Phase 2. The Phase 1 and Phase 2 Seismic Retrofit Program involved strengthening the columns of existing bridges by encircling certain columns with a steel casing or, in a few instances, an advanced woven fiber casing. In addition to the column casing, some bridge footings were made bigger and given more support by placing additional pilings in the ground, or by using steel tie-down rods to better anchor the footings to the ground.

Quantifying the benefits of retrofitting bridges requires consideration of secondary impacts, which in many cases are far greater than the direct impacts. The delays from traffic disruption during reconstruction requires an assessment of traffic demand and freeway capacity, tools typically used to assess road construction and maintenance rather than loss estimation. The Reference Engineering Data Automated Retrieval System (REDARS) is a software program developed to quantify the primary and secondary impacts of earthquake damage to the transportation network with the specific purpose of evaluating state Department of Transportation bridge retrofit programs. REDARS has been peer reviewed and has been available as a framework for analysis for over 15 years. The software is designed to provide end users with a method to evaluate strategies to reduce post-event congestion by mitigating, repairing and reopening damaged highways.

## 8.2 REDARS Technical Specifications

Figure 63 illustrates the REDARS methodology. Seismicity is provided through a library of earthquake scenarios that can be run probabilistically. For each event, REDARS calculates probable bridge damage, the repair cost of direct damages, and estimated reconstruction time. REDARS includes a transportation network analysis that incorporates surveyed origin-destination data from local metropolitan planning organizations. Traffic disruption is quantified at various time frames following an event: 7 days, 60 days, 150 days, and 221 days. The value of traffic disruption is assessed by evaluating the additional duration that passengers and commercial freight drivers spend traveling. Given road closures, before-event transportation throughput and travel times are compared with after-event transportation throughput and travel times to quantify disruption.

REDARS includes a library of equiprobable earthquakes (Taylor et al., 2001; Werner et al., 2006). It estimates ground motion at bridge and tunnel locations Silva’s (2002) ground motion prediction equation for central U.S. earthquakes, and Abrahamson and Silva (1997) for western states. Soil classification is based on National Earthquake Hazard Reduction Program (NEHRP) site classifications. Damage to highway system components (bridges, pavements, approach fills, tunnels, and embankments) affects the extent of the repairs that are required and the duration of downtime. Bridge damage due to ground shaking is estimated from a version of the Hazus damage functions (FEMA 2008; Dutta and Mander 1998; Mander and Basoz 1999) adjusted to improve comparisons between its bridge-damage predictions and observed damage from the Northridge Earthquake (Appendix K, Werner et al., 2006). The benefits of Caltrans Phase 1 and 2 retrofits were captured by incorporating damage functions from Shinozuka (2004) that were commissioned by Caltrans expressly for this purpose.

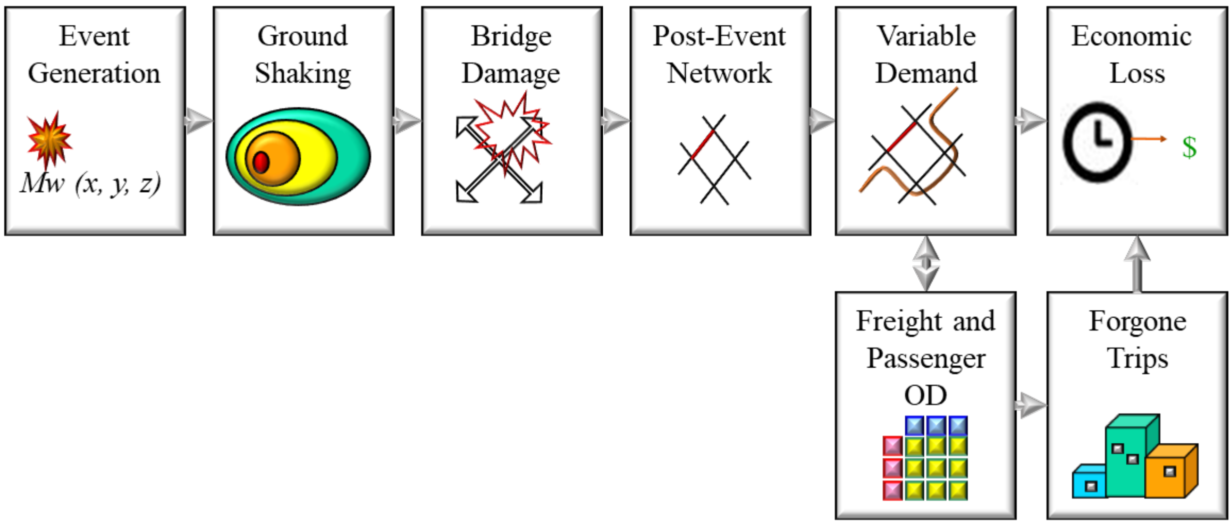


**Figure 63.** REDARS methodology flowchart.

## 8.3 Benefit-Cost Analyses

REDARS requires an evaluation of a study region, and given system limitations, networks that are over 1,000 segments tend to fail. The project team selected a study region roughly corresponding to the Los Angeles metropolitan area. The team obtained a Caltrans bridge database identifying bridge retrofits throughout the region. These were loaded onto the Highway Performance Monitoring System (HPMS) National Highway Planning Network (NHPN), which provides the geospatial component of the NHPN[15] The NHPN provided the locations of 597 retrofitted bridges in the study area. Caltrans identified that a total of 656 bridges have been retrofitted in Southern California, for a total cost of $485 million. These numbers were used to scale an estimated cost of retrofit to $441 million for the 597 bridges in the study area.

The project team incorporated casualty rates by examining fatalities due to bridge collapses in major California earthquakes since 1970, see Table 34). A total of 47 fatalities were sustained from 14 bridge collapses in 4 events, or a fatality rate of 3.35 deaths per bridge collapse. Although Loma Prieta may appear as a statistical outlier given the number of deaths per bridge collapse, it is worth noting that the Northridge Earthquake occurred at 4:30 a.m. and the San Fernando Earthquake occurred at 6:00 a.m., so given a larger sample of events, the number of fatalities per bridge collapse could be substantially higher. Each fatality avoided is valued at $9,500,000. A lifespan of 70 years is assumed for a retrofitted bridge, and future benefits from avoided traffic delays are discounted using a discount rate of 2.2%. Passenger delays are valued

[15] See https://catalog.data.gov/dataset/highway-performance-monitoring-system-hpms-national.

at $21.38 per hour, taken from the report, *California Transportation by the Numbers* (TRIP 2016), and freight is valued at $71.05, a default value within REDARS based on traffic-congestion statistics from the Rand Corporation (Werner et al., 2006).

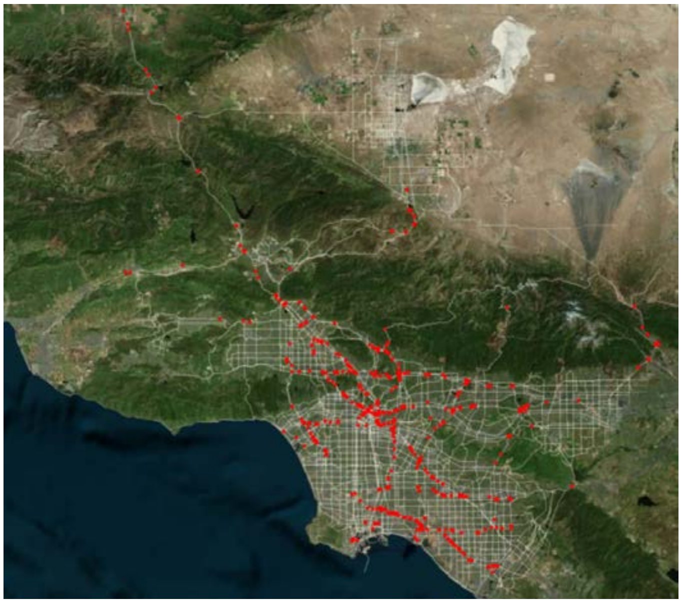

**Figure 64.** Los Angeles study region.

| | Collapsed | Deaths |
|---|---|---|
| San Fernando | 5 | 3 |
| Northridge | 6 | 1 |
| Whittier Narrows | - | - |
| Loma Prieta | 3 | 43 |
| Total | 14 | 47 |

**Table 34**. Fatalities in California due to bridge collapse between 1970 and 2018.

## 8.4 BCR Results

Based on a 3,000-year walkthrough of potential earthquakes effecting the transportation network, with and without bridge retrofits, there is a benefit of $22 million avoided annually attributed to reduced reconstruction and traffic delays, with a $166 baseline EAL in the case of no retrofitting, and $144 million EALconsidering the Caltrans bridge retrofits. Accrued over 70 years at a discount rate of 2.2%, this equates to a benefit of $795 million. The annual probability of collapse before retrofit is estimated at 0.044% before retrofit, and 0.0028% after retrofit, equating to an annual benefit of $548 million. Total benefit is estimated at $1,344 million. Compared to the initial mitigation expenditure of $441 million, the BCR equates to 3.0.

# 9 References

ALA (2001). *Seismic Fragility Formulations For Water Systems, Part 1 - Guidelines*. Pp. 104: American Lifelines Alliance.

Anagnos, T., and D. Ostrom (2000). Electrical Substation Equipment Damage Database for Updating Fragility Estimates. *Proc. 12th World Conference on Earthquake Engineering,* Auckland, New Zealand Paper No. 2262.

Anderson, G. B., and M. L. Bell. (2012). Lights out: impact of the August 2003 power outage on mortality in New York, NY. *Epidemiology* (Cambridge, Mass.) 23:189.

(ASCE) American Society of Civil Engineers (1999). *Guide to Improved Earthquake Performance of Electric Power Systems*. Prepared by Electric Power and Communications Committee, Anshel J. Schiff (ed.), Technical Council on Lifeline Earthquake Engineering, American Society of Civil Engineers, Reston, VA.

(ASCE) American Society of Civil Engineers (2018). ASCE 7 Hazard Tool, https://asce7hazardtool.online/

(ATC) Applied Technology Council (2010). *Here Today—Here Tomorrow: The Road to Earthquake Resilience in San Francisco, Potential Earthquake Impacts*. ATC-52-1 San Francisco: Prepared for the Department of Building Inspection, City and County of San Francisco, under the Community Action Plan for Seismic Safety (CAPSS) Project by the Applied Technology Council.

Association for the Advancement of Automotive Medicine (2001). *Abbreviated Injury Scale* (AIS) 1990 - Update 98, Barrington, IL, 68 pp.

Beatty, M. E., S. Phelps, and Rohner, C. (2006). Blackout of 2003: Public Health Effects and Emergency Response. *Public Health Reports* 12:36-44.

Cornell University (2008) *GIRAFFE User's Manual, Version 4.2*. Ithaca: Cornell University.

Dartmouth Institute for Health Policy and Clinical Practice (2018). *The Dartmouth Atlas of Health Care*, Dartmouth College, Lebanon, NH, http://www.dartmouthatlas.org/.

Darestani, Y.M., Shafieezadeh, A., and DesRoches, R. (2017). Effects of adjacent spans and correlated failure events on system-level hurricane reliability of power distribution lines. *IEEE Transactions on Power Delivery* 33 (5): 2305-2314.

Davis, C.A. (2017). Developing a seismic resilient pipe network using performance based seismic design procedures. Pp. 406-418 in *The 10th JWWA/WRF/CTWWA Water System Seismic Conference*, edited by Nan-Tzer Hu and Shyh-Jiann Hwang. Tainan, Taiwan: National Center for Research on Earthquake Engineering.

DHS (2003). *Multi-Hazard Loss Estimation Methodology, Earthquake Model, Hazus-Mh Mr3 Technical Manual*. 699 pp. Washington, D.C.: Developed by: Department of Homeland Security, Emergency Preparedness and Response Directorate, FEMA Mitigation Division, Washington, D.C. Under a contract with: National Institute of Building Sciences.

DOE (2012). *Large power transformers and the US electric grid*. Page 55 in Department of Energy, editor. Office of Electricity Delivery and Energy Reliability, Washington, D.C.

DOE (2017). *Quadrennial Energy Review Second Installment - Transforming The Nation's Electricity System.* Page 512. Office of Electricity Delivery and Energy Reliability, Department of Energy, Washington, D.C.

Duddu, P. (2015). The 10 worst blackouts of the last 50 years. *Power Technology*. https://www.power-technology.com/features/featurethe-10-worst-blackouts-in-the-last-50-years-4486990/.

Dunn, S., Wilkinson, S., Alderson, D., Fowler, H., and Galasso, C. (2018). Fragility curves for assessing the resilience of electricity networks constructed from an extensive fault database. *Natural Hazards Review*, 19 (1).

Dutta, A. and Mander, J.B. (1998). Seismic fragility analysis of highway bridges. *In Proceedings of the INCEDE-MCEER Center-to-Center Project Workshop on Earthquake Engineering Frontiers in Transportation Systems*, pp. 22-23.

FEMA (2003). *HAZUS-MH MR3 Technical Manual - Earthquake Model.* Federal Emergency Management Agency.

FEMA (2003). *Ice Storm of 2002: Four Rural Electric Cooperatives in Kansas*, EMW-2000-CO-0247 HMTAP Task Order 230.

FEMA (2003). *Multi-Hazard Loss Estimation Methodology, Earthquake Model, Hazus-Mh Mr4 Technical Manual.* Developed by: Department of Homeland Security, Federal Emergency Management Agency, Mitigation Division, Under a contract with: National Institute of Building Sciences, Washington, D.C.

FEMA (2008). *Electrical Transmission and Distribution Mitigation: Loss Avoidance Study - Nebraska and Kansas*. FEMA-1674-DR-KS and FEMA-1675-DR-NE.

Field, E.H., N. Gupta, V. Gupta, M. Blanpied, P. Maechling, and T.H Jordan, 2005. Hazard calculations for the WGCEP-2002 forecast using OpenSHA and distributed object technologies. *Seismological Research Letters* 76, 161-167

Fujisaki, E. (2009). Seismic Design Standards For Electric Substation Equipment. *Proceedings of the 2009 Technical Council on Lifeline Earthquake Engineering Conference.* American Society of Civil Engineers, Oakland, California.

Han, T.-x., L.-h. LI, and Y.-h. YU (2007). *Economy evaluation for 500 kV substation retrofits by using LCC* [J]. East China electric power 8:004.

Henneaux, P., P.-E. Labeau, and Maun, J.-C. (2011). Towards an integrated probabilistic analysis of the blackout risk in transmission power systems. Pages 1149-1160 in *Proc. ANS PSA 2011 Int. Topical Meeting on Probabilistic Safety Assessment and Analysis*.

Hines, P., J. Apt, and Talukdar, S. (2008). Trends in the history of large blackouts in the United States. Pages 1-8 in *Power and Energy Society General Meeting-Conversion and Delivery of Electrical Energy in the 21st Century*, 2008. IEEE.

Hosseini, A. H. K. a. M. (2009). Seismic Performance Of Electrical Substations' Equipment In Bam Earthquake (Iran ). *Proceedings of the 2009 Technical Council On Lifeline Earthquake Engineering Conference*. American Society of Civil Engineers, Oakland, California.

Hosseini, M., A. Raoufi, A. H. Khalvati, and Soroor, A. (2009). A Seismic Risk Management Model For Electric Power Distribution Networks in Large Cities by Concentration on Low-Voltage Substations. *Proceedings of the 2009 Technical Council On Lifeline Earthquake Engineering Conference*. American Society of Civil Engineers, Oakland, California.

Housner, G.W. (1994). *The Continuing Challenge: The Northridge Earthquake of January 17, 1994.* Report to the Director, California Department of Transportation, by the Seismic Advisory Board.

IEEE 693 (2005). *Recommended Practice for Seismic Design of Substations*. IEEE Power Engineering Society Sponsored by the Substations Committee, New York.

Jennings, P.C. and Wood, J.H. (1971). *Earthquake Damage to Freeway Structures, Engineering Features of the San Fernando Earthquake of February 9, 1971*. California Institute of Technology, pp. 366–385.

Jones, L.M., Bernknopf, R., Cox, D., Goltz, J., Hudnut, K., Mileti, D., Perry, S., Ponti, D., Porter, K., Reichle, M., Seligson, H., Shoaf, K., Treiman, J., and Wein, A. (2008). *The Shakeout Scenario*. 312 pp. Reston, VA,: USGS Open File Report 2008-1150, U.S. Geologic Survey.

Kempner Jr., L. (2008). *Substation structure design guide.* American Society of Civil Engineers, Oakland, California.

Kempner Jr., L. (2009). ASCE Guide for Design of Substation Structures. *Proceedings of the 2009 Technical Council on Lifeline Earthquake Engineering Conference.* American Society of Civil Engineers, Oakland, California.

Kenny, J.F., and Juracek,K.E. (2012). *Description of 2005-2010 Domestic Water Use for Selected U.S. Cities and Guidance for Estimating Domestic Water Use*. 31 pp. U.S. Geological Survey.

Knight, B. T., and Kempner, L. (2009). Seismic Vulnerabilities and Retrofit of High-Voltage Electrical Substation Facilities. *Proceedings of the 2009 Technical Council On Lifeline Earthquake Engineering Conference*. American Society of Civil Engineers, Oakland, California.

Krumholz, H.M., Nuti, S.V., Downing, N.S., Normand, S.-L.T., and Wang, Y. (2015). Mortality, hospitalizations, and expenditures for the Medicare population age 65 and older, 1999–2013. *Journal of the American Medical Association*, 314(4), 355–365. http://doi.org/10.1001/jama.2015.8035

Küfeoğlu, S., and Lehtonen, M. (2015). Interruption costs of service sector electricity customers, a hybrid approach. *International Journal of Electrical Power & Energy Systems* 64:588-595.

LaCommare, K. H., and Eto, J. H. (2006). Cost of power interruptions to electricity consumers in the United States (US). *Energy* 31:1845-1855.

Lajoie, K., and Keefer, D. (1981). *Investigations of the 8 November 1980 Earthquake in Humboldt County, California (No. 81-397)*. U.S. Geological Survey.

Larsen, P. H., Boehlert, B., Eto, J., Hamachi-LaCommare, K., Martinich, J. and Rennels, L. (2017). Projecting Future Costs to US Electric Utility Customers from Power Interruptions. *Energy*.

Lew, H.S. (Ed.). (1990). *Performance of Structures during the Loma Prieta Earthquake of October 17, 1989 (Vol. 778)*. U.S. Dept. of Commerce, National Institute of Standards and Technology.

Lew, H.S. (1987). *The Whittier Narrows Earthquake of October 1, 1987: A Reconnaissance Report.* U.S. National Bureau of Standards.

Lin, S., Fletcher, B. A., Luo, M., Chinery, R., and Hwang, S.-A. (2011). Health Impact in New York City during the Northeastern Blackout of 2003. *Public Health Reports* 126 384-393.

Mander, J.B. and Basoz, N. (1999). Seismic fragility curves for highway bridges. optimizing post-earthquake lifeline system reliability. *Proceedings of the 5th U.S. National Conference on Lifeline Earthquake Engineering.* Technical Council on Lifeline Earthquake Engineering Monograph No. 16, pp 31-40.

Matthewman, S., and Byrd, H. (2014). Blackouts: A Sociology of Electrical Power Failure. *Social Space*: 1-25.

(MMC) Multihazard Mitigation Council (2018). *Natural Hazard Mitigation Saves: 2017 Interim Report: An Independent Study.* 330 p. Washington: National Institute of Building Sciences. Principal Investigator: Porter, K.; co-Principal Investigators Scawthorn, C.; Dash, N.; Santos, J.; Schneider, P., Director, MMC.

National Park Service (2018). *NPS Annual Visits Report 2008-2017*. https://irma.nps.gov.

Neudorf, E. G., Kiguel, D. L., Hamoud, G. A. , Porretta, B., Stephenson, W. M., Sparks, R., Logan, D., Bhavaraju, M., Billinton, R., and Garrison, D. (1995). Cost-benefit analysis of power system reliability: two utility case studies. *IEEE Transactions on Power Systems* 10:1667-1675.

NOAA (2018) National Oceanographic and Atmospheric Administration National Centers for Environmental Information (NCEI) *U.S. Billion-Dollar Weather and Climate Disasters* (2018). https://www.ncdc.noaa.gov/billions/

Nowak, A.S. (Ed.). (2012). *Bridge Evaluation, Repair and Rehabilitation* (Vol. 187). Springer Science & Business Media.

Oakeshott, G. B. (1975). *San Fernando, California, Earthquake of 9 February 1971* (Vol. 196). California Division of Mines and Geology.

Oikonomou, K., Constantinou, M.C., Reinhorn, A.M., and Kempner Jr., L. (2016). Seismic isolation of high voltage electrical power transformers. *Technical report MCEER-16-0010*, Multidisciplinary Center for Earthquake Engineering Research, University at Buffalo, Buffalo, NY, Google Scholar.

O'Rourke, M., and Liu, X. (2012). *Seismic Design of Buried and Offshore Pipe*. Buffalo, NY: MCEER.

O'Rourke, T.D., Scawthorn, C.R., Blackburn, F.T., and Dickerman, T.S. (1990). Response of the San Francisco water supply system during the 1989 Loma Prieta earthquake. *Putting the Pieces Together*. San Francisco, CA.

Porter, K., Shoaf, K., and Seligson, H. (2006). Value of Injuries in the Northridge Earthquake. *Earthquake Spectra* 22 (2): 555-563.

Porter, K.A. (2018). A new model of water-network resilience, with application to the HayWired scenario. *The HayWired Earthquake Scenario—Engineering Implications*: chap. N edited by Detweiler, S.T. and Wein, A.M.: U.S. Geological Survey Scientific Investigations Report 2017–5013–I–Q.

Romero, N., Nozick, L.K., Dobson, I., Xu, N., and Jones, D. A. (2015). Seismic retrofit for electric power systems. *Earthquake Spectra* 31 (2): 1157-1176.

Rose, A., Oladosu, G. and Liao, S.Y. (2007a). Business interruption impacts of a terrorist attack on the electric power system of Los Angeles: customer resilience to a total blackout. *Risk Analysis* 27 (3): 513-531.

Rose, A., Porter, K., Dash, N., Bouabid, J., Huyck, C., Whitehead, J., Shaw, D., Eguchi, R., Taylor, C., and McLane, T. (2007b). Benefit-cost analysis of FEMA hazard mitigation grants. *Natural Hazards Review* 8 (4): 97-111.

Rossman, L.A. (2000). *Epanet User Manual*. 200 p. Cincinnatti: Water Supply and Water Resources Division, National Risk Management Research Laboratory, Environmental Protection Agency.

RSMeans (2016). *Building Construction Costs with RSMeans Data*. Rockland, MA: Gordian RSMeans Data.

Scawthorn, C. (2018). Fire following the HayWired scenario mainshock. *The HayWired Earthquake Scenario—Engineering Implications*: chap. P edited by Detweiler, S.T. and Wein, A.M. Washington: U.S. Geological Survey Scientific Investigations Report 2017–5013–I–Q.

Scawthorn, C., Myerson, D., York, D., and Ling, E. (2017). Determining water distribution system pipe replacement given random defects – case study of San Francisco's auxiliary water supply system. *Water System Seismic Conference, Joint Conference of the American Water Works Association, Japan Water Works Association and the Chinese Taiwan Water Works Association.* Tainan, Taiwan.

Scawthorn, C.R. (2011). Fire following earthquake aspects of the Southern San Andreas Fault Mw 7.8 earthquake scenario. *Earthquake Spectra* 27 (2): 419-41.

Scawthorn, C., Ballantyne, D.B., and Blackburn, F. (2000). Emergency water supply needs lessons from recent disasters. *Water Supply* 18 (3): 69-81.

Schlake, B., Barkan, C., and Edwards, J. (2011). Train delay and economic impact of in-service failures of railroad rolling stock. *Transportation Research Record: Journal of the Transportation Research Board*, (2261), 124-133.

Shafieezadeh, A., Onyewuchi, U.R., Begovic, M.M. and DesRoches, R., (2014). Age-dependent fragility models of utility wood poles in power distribution networks against extreme wind hazards. *IEEE Transactions on Power Delivery*, 29 (1): 131-139.

(Sea Grant) Sea Grant North Carolina and Duke Nicholas Institute for Environmental Policy Solutions (2017). *North Carolina's Ocean Economy A First Assessment and Transitioning to a Blue Economy*, 29 p. https://ncseagrant.ncsu.edu/ncseagrant_docs/products/2010s/NC_Ocean_Economy_White_Paper.pdf

Shafieezadeh, A., Onyewuchi, U.P., Begovic, M.M., and DesRoches, R. (2014). Age-dependent fragility models of utility wood poles in power distribution networks against extreme wind hazards. *IEEE Transactions on Power Delivery*, 29 (1), February 2014.

Shinozuka, M., Zhou, Y., Kim, S.H., Murachi, Y., Banerjee, S., Cho, S., and Chung, H. (2005). Socio-economic effect of seismic retrofit implemented on bridges in the Los Angeles highway network. *Final Report to the California Department of Transportation*.

Shumuta, Y. (2004). Benefit cost analysis for renewal planning of existing electric power equipment. *Modeling Spatial and Economic Impacts of Disasters*. Springer, p. 257-287.

SPA Risk LLC (2009). *Enhancements in Hazus-Mh Fire following Earthquake, Task 3: Updated Ignition Equation*. 74 pp. San Francisco: SPA Risk LLC, Berkeley, CA. Principal Investigator C. Scawthorn. Prepared for PBS&J and the National Institute of Building Sciences.

Spence, R.J.S., So, E., and Scawthorn, C. (2011). *Human Casualties in Earthquakes: Progress in Modelling and Mitigation*. New York: Springer.

Stanley Consultants (2011). *Facility Plan for Expansion of South Wastewater Treatment Plant, City of Iowa City, Iowa*. Stanley Consultants, Inc., Muscatine, Iowa, 132 p.

Sutliff, K. (2011). *Memorandum-Quarterly Non-Toll Seismic Safety Retrofit Report.* Prepared for The State of California Department of Transportation. CTC Meeting March 23-24, 2011.

Sveikauskas, L., Rowe, S., and Mildenburger, J.D. (2018). Measuring productivity growth in construction. *Monthly Labor Review.* January 2018. U.S. Bureau of Labor Statistics.

TCLEE (Ed.) (2005). *Fire Following Earthquake.* Reston, VA: American Society of Civil Engineers, Technical Council for Lifeline Earthquake Engineering, Scawthorn et al. (eds).

Tiedemann, K., and Hydro, B.C. (2015). Modelling the value of reliability for residential electricity customers. *Proc., Software Engineering and Applications/831: Advances in Power and Energy Systems (SEA 2015*), October 26-27, 2015, Marina del Rey, California.

Todd, D.R., Carino, N.J., Chung, R.M., Lew, H.S., Taylor, A.W., and Walton, W.D. (1994). *1994 Northridge Earthquake: Performance of Structures, Lifelines and Fire Protection Systems*. NIST Interagency/Internal Report (NISTIR)-5396.

TRIP (2016). California Transportation by the Numbers. Washington, D.C., 23 p. https://mtc.ca.gov/sites/default/files/CA_Transportation_by_the_Numbers_TRIP_Report_2016.pdf

U.S. Census Bureau (2018). *Population Division Annual Estimates of the Resident Population for Incorporated Places of 50,000 or More, Ranked by July 1, 2017 Population: April 1, 2010 to July 1, 2017*.

USFA (2018). Residential and Nonresidential Building Fire and Fire Loss Estimates by Property Use and Cause (2003-2015). U.S. Fire Administration, https://www.usfa.fema.gov/data/statistics/order_download_data.html#download, accessed 27 April 2018.

Wald, D.J., Quitorano, V., Heaton, T., and Kanamori, H. (1999). Relationships between peak ground acceleration, peak ground velocity, and modified Mercalli intensity in California. *Earthquake Spectra* 15 (3): 557-564.

Werner, S.D., Cho, S., Taylor, C.E., Lavoie, J.P., Huyck, C.K., Chung, H., and Eguchi, R.T. (2006). *Technical Manual: REDARS™ 2 Methodology and Software for Seismic Risk Analysis of Highway Systems*. Report MCEER-06-SP08, Buffalo, NY: Multidisciplinary Center for Earthquake Engineering Research.

Whitehead, J.C., Haab, T.C., and Huang, J.C. (2000). Measuring recreation benefits of quality improvements with revealed and stated behavior data. *Resource and Energy Economics* 22, 339-354.

# 10 Project Participants

The MMC Board wishes to acknowledge the efforts of its subcontractor, SPA Risk LLC, and the project participants, as follows.

**MMC BOARD OF DIRECTION**

*Chair*: Kevin Mickey, Polis Center, Indianapolis, IN
*Vice-Chair*: Bryan Koon, National Emergency Management Association, Lexington, KY
*Secretary*: Keith Porter, SPA Risk LLC, Denver, CO
*At-Large*: Nancy McNabb, McNabb & Associates, Alexandria, VA
*At-Large*: Sara Yerkes, International Code Council, Washington, DC
*Past Chair*: Neil Blais, Blais & Associates, Little Elm, TX

**PROJECT TEAM**

*Principal Investigators*
Keith Porter, SPA Risk LLC, Denver, CO, Principal Investigator
Charles Scawthorn, SPA Risk LLC, Berkeley, CA, Co-Principal Investigator
Nicole Dash, University of North Texas, Denton, TX, Co-Principal Investigator
Joost Santos, George Washington University, Washington, DC, Co-Principal Investigator

*Riverine Flooding*
Kevin Mickey, Polis Center, Indianapolis, IN, Investigator
Tarek Rashed, Polis Center, Indianapolis, IN, Investigator

*Coastal Flooding/Wind*
Charles Huyck, Imagecat, Inc., Long Beach, CA, Investigator
Michael Eguchi, Imagecat, Inc., Long Beach, CA, Investigator

*Earthquake*
Keith Porter, SPA Risk LLC, Denver, CO, Principal Investigator
Moad Isteita, University of Colorado Boulder, Investigator
Sannidhye Ghosh, University of Colorado Boulder, Investigator

*Fire at the Wildland-Urban Interface*
Charles Scawthorn, SPA Risk LLC, Berkeley, CA, Co-Principal Investigator

*Economics*
Joost Santos, George Washington University, Washington, DC, Co-Principal Investigator

*Social Issues*
Nicole Dash, University of North Texas, Denton, TX, Co-Principal Investigator

**PROJECT MANAGEMENT**

*National Institute of Building Sciences, Washington, DC*

Philip Schneider, Director, Multihazard Mitigation Council
Jiqiu Yuan, Project Manager

*Economic Development Administration (EDA), Washington, DC*
Ryan Smith, EDA HQ
Bernadette Grafton, EDA HQ

**OVERSIGHT COMMITTEE**

*Water Supply*
Craig Davis, Los Angeles Department of Water and Power, Los Angeles, CA

*Electricity*
Wally Mealiea, Edison Electric Institute, Washington, DC
Sandor Williams, Exelon, Oakbrook Terrace IL

National Institute of
BUILDING SCIENCES

1090 Vermont Avenue, NW
Suite 700
Washington, D.C. 20005
(202) 289-7800
www.nibs.org